

**Bedload Transport and Large Organic Debris  
in Steep Mountain Streams in Forested Watersheds  
on the Olympic Peninsula, Washington**

**Final Report**

By

Matthew O'Connor and R. Dennis Harr



October 1994

BEDLOAD TRANSPORT AND LARGE ORGANIC DEBRIS  
IN STEEP MOUNTAIN STREAMS  
IN FORESTED WATERSHEDS ON THE  
OLYMPIC PENINSULA, WASHINGTON

**FINAL REPORT**

Submitted by

Matthew O'Connor  
College of Forest Resources, AR-10  
University of Washington  
Seattle, WA 98195

and

R. Dennis Harr  
Research Hydrologist  
USDA Forest Service  
Pacific Northwest Research Station  
and  
Professor, College of Forest Resources  
University of Washington  
Seattle, WA 98195

to

Timber/Fish/Wildlife  
Sediment, Hydrology and Mass Wasting Steering Committee

and

State of Washington  
Department of Natural Resources

October 31, 1994

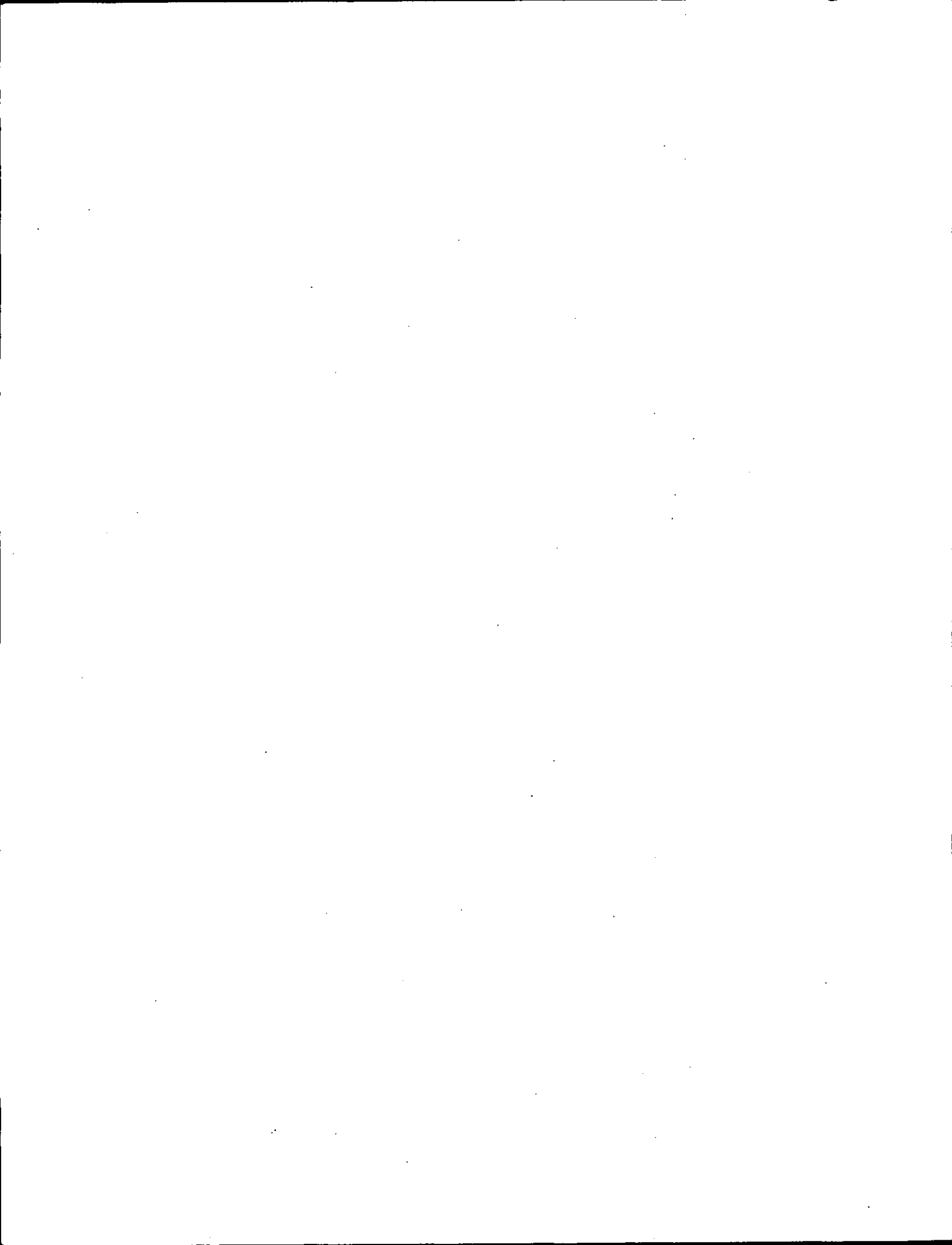


## TABLE OF CONTENTS

LIST OF FIGURES	iv
LIST OF TABLES	vi
ACKNOWLEDGEMENTS	vii
OVERVIEW	1
INTRODUCTION	2
BACKGROUND	3
Sediment Routing in Low-Order Channels	3
Timber/Fish/Wildlife Literature Review of Sediment Dynamics in Low-order Streams	5
Conceptual Model of Bedload Routing	6
Effects of Timber Harvest on LOD Accumulation Rates	8
MONITORING SEDIMENT TRANSPORT IN LOW-ORDER CHANNELS	11
Monitoring Objectives	11
Field Sites for Monitoring Program	12
BEDLOAD TRANSPORT MODEL	16
Model Overview	16
Stochastic Model Outputs from Predictive Relationships	17
24-Hour Precipitation	17
Synthesis of Frequency of Threshold 24-Hour Precipitation	18
Peak Discharge as a Function of 24-Hour Precipitation	21
Excess Unit Stream Power as a Function of Peak Discharge	28
Mean Scour Depth as a Function of Excess Unit Stream Power	30
Mean Bedload Velocity as a Function of Excess Unit Stream Power	32
Active Bed Width	36
Calculating Bedload Transport	36
SEDIMENT ROUTING MODEL	38
Model Overview	38
Conceptual Model of Fluvial Sediment Transport for Low-order Streams	40
Key Model Elements	40

Sediment Reservoir Definition	40
Sediment Reservoir Geometry	41
Interaction of Sediment Reservoirs	45
Dynamics of LOD Dams	45
Hillslope Sediment Inputs to the Fluvial System	46
Sediment Sorting	47
Bedload Transport	47
Components of the Routing Model	49
Channel and Reservoir Geometry	49
Sediment Inputs by Soil Creep Processes	52
Sorting of Sediment Inputs by Fluvial Processes	53
Attrition of Bedload	53
Random Variation of Bedload Transport Capacity	54
Initial Density of LOD Dams	56
Annual Variation of Density of LOD Dams	59
Steady-State Scenario	61
Increasing-Decreasing Scenario	61
Decreasing Scenario	63
Logical Rules for Sediment Routing	63
Computations of the Routing Model	64
RESULTS	75
Bedload Model	75
Routing Model	78
Comparison of Scenarios	79
Relationship Between Dam Changes and Bedload Yield	89
Residence Time	98
Suspended Sediment Yield	102
DISCUSSION	103
Suspended Sediment	104
Ratio of Bedload to Total Sediment Load	106
Sediment-Supply-Limitations on Yield of Bedload	107
Potential Transport of Bedload in First-Order Channels	108

Sediment Routing by Debris Flow	112
Influence of Timber Harvest on Creep Rates	115
Residence Time	116
Management Implications	117
REFERENCES	123

## LIST OF FIGURES

Figure 1: Location Map	14
Figure 2: Observations of 24-Hour Rainfall, 1991-1992	20
Figure 3: Frequency and Magnitude of 24-Hour Precipitation Totals Greater Than 2.6 Inches, Forks, Washington, 1931-1991	22
Figure 4: Annual Frequency of Number of Days per Year with at Least 2.6 Inches of Precipitation, Forks, Washington, 1931-1991	23
Figure 5: Peak Discharge as a Function of 24-Hour Precipitation, Eight-ten Creek	25
Figure 6: Peak Discharge as a Function of 24-Hour Precipitation, Ramp Creek	26
Figure 7: Synthetic Peak Discharge as a Function of 24-Hour Precipitation, Sister Creek	27
Figure 8: Mean Channel Bed Scour as a Function of Excess Unit Stream Power	31
Figure 9: Mean Tracer Travel Distance as a Function of Excess Unit Stream Power	33
Figure 10: Hypothetical Channel Network for Sediment Routing Model	39
Figure 11: Hypothetical Two-dimensional Geometry of LOD Dam Sediment Reservoirs	42
Figure 12: Frequency Distribution of Height of LOD Dams, Olympic Peninsula	51
Figure 13: Frequency Distribution of Density of LOD Dams from 16 Streams	57
Figure 14: Probability of LOD Dam Formation in Model Streams	62
Figure 15: Cumulative Frequency Distributions of Bedload Transport Capacity	76
Figure 16a: Reservoir Change and Bedload, Steady-State Scenario	80
Figure 16b: Reservoir Change and Bedload, Increasing-Decreasing Scenario	81
Figure 16c: Reservoir Change and Bedload, Decreasing Scenario	82
Figure 17: Predicted Annual Bedload Yield for Each Channel Segment and Each Scenario	84

Figure 18: Percent Change in Average Bedload Yield and LOD Dams Relative to Steady-State Scenario for 60-Year Model Cycles	85
Figure 19a: Cumulative Frequency Distribution of Mean Annual Bedload Yield, High Initial Debris Dam Density	87
Figure 19b: Cumulative Frequency Distribution of Mean Annual Bedload Yield, Average Initial Debris Dam Density	88
Figure 20: Yield of Bedload From Retention Storage Reservoirs in Modelled Channel Network in Comparison with Total Bedload Yield from Modelled Third-Order Channels	90
Figure 21a: Mean Annual Bedload vs. Number of Debris Dams, High Initial Density, Steady-State Scenario	92
Figure 21b: Mean Annual Bedload vs. Number of Debris Dams, High Initial Density, Increasing-Decreasing Scenario	93
Figure 21c: Mean Annual Bedload vs. Number of Debris Dams, High Initial Density, Decreasing Scenario	94
Figure 21d: Mean Annual Bedload vs. Number of Debris Dams, Average Initial Density, Steady-State Scenario	95
Figure 21e: Mean Annual Bedload vs. Number of Debris Dams, Average Initial Density, Increasing-Decreasing Scenario	96
Figure 21f: Mean Annual Bedload vs. Number of Debris Dams, Average Initial Density, Decreasing Scenario	97
Figure 22: Average Median Bedload Residence Time	101
Figure 23: Average Bedload Yield and Transport Capacity for a 60-Year Model Cycle, High Initial Density of LOD Dams, Steady-State Scenario	109
Figure 24: Bedload Transport Capacity and Bedload Yield as a Function of Drainage Area	111

## LIST OF TABLES

Table 1: Monitoring Site Characteristics	15
Table 2: Bedload Transport Model Regression Coefficients and Statistics	19
Table 3: Bedload Transport Thresholds	29
Table 4: Observed Bankfull Channel and Active Bed Width	36
Table 5: Geometry of Hypothetical Channels in Routing Model	50
Table 6: Calculation of Bedload Attrition Rates	55
Table 7: Debris Dam Density Observations, Pacific Northwest	58
Table 8: Observed LOD Dam Dynamics, 1991-1993	60
Table 9: Predicted Bedload Transport Capacity of Selected Recurrence Intervals	77
Table 10: Changes in LOD Dams	99
Table 11: Bedload Residence Time	100
Table 12: Ratio of Bedload Transport Capacity to Bedload Yield	108

## ACKNOWLEDGEMENTS

Many individuals and organizations provided invaluable assistance in the completion of this project. The Soleduck Ranger District, Olympic National Forest, provided considerable logistical support in the form of overnight facilities and radio communications at field sites. Individual Forest Service employees on the Soleduck Ranger District who assisted at various times and in various ways were Molly Erickson, Steve Allison, Don Coburn, Pat VanEimeren and Cathy Leer. Local field assistants were Dave Ayres and Ron Darrow. Joni Sasich, Watershed Officer at the Olympic National Forest Supervisors Office, also provided assistance in coordinating efforts with the Soleduck Ranger District. Tom Koler, Olympic National Forest, Geotechnical Section, provided early assistance in locating field sites and obtaining topographic maps. Additional laboratory assistance at the University of Washington was provided by Bob Salazar. Additional field assistance was provided by Dave Parks, Brian Sugden, and Steve Liu. Professor Terrance Cundy, University of Washington, gave generously of his time checking the logic of the model. Dr. Kate Sullivan, Weyerhaeuser Co., provided help in developing the initial project proposal to TFW/SHAMW. Funding for this research project was provided by the State of Washington, Department of Natural Resources, Cooperative Monitoring, Evaluation and Research Committee contract FY92-008 and by the U.S.D.A. Forest Service under Cooperative Agreement Supplement PNW90-338.

## OVERVIEW

The objectives of this report are to summarize the key elements of a model of sediment transport in Type 4 streams, to present results from model runs, and discuss the management implications of our findings. Two stochastic models have been developed. The first estimates bedload transport capacity as a function of flow intensity. The second model, which utilizes a frequency distribution of annual bedload transport rates produced by the transport model, routes sediment through a 1 km-long network of second- and third-order channels according to a simple mass balance scheme. The routing model is used to assess the sensitivity of bedload yield from low-order channels to changes in the abundance of large organic debris (LOD) dams in stream channels. Insights regarding sediment routing in low-order stream channel networks and potential cumulative effects of forest management activities are discussed.

Field observations over two winters in three disturbed Type 4 streams in the western Olympic Mountains indicate that bedload transport events occur frequently, often more than once each year. Virtually all sediment in these channels up to at least 128 mm diameter is mobile. Observed mean annual transport distance for individual bedload sediment grains are equivalent to between 2 and 20 channel widths. Channel bed scour ranged up to 0.35 m; mean scour depths ranged from 0.03 to 0.10 m.

The simulation model of sediment routing indicates that these stream types are capable of transporting most of the sediment delivered to them by soil creep processes and bank erosion. Sediment transport and channel morphology in these streams can be considered to be supply-limited with respect sediment input via creep processes and fluvial transport processes. Storage of sediment subject to fluvial transport in these channels is due largely to LOD dams. In contrast, large, rapid inputs of sediment to these channels from mass wasting often results in large increases in long-term sediment storage, despite high fluvial sediment transport capacity.

The model suggests that if LOD inputs to the stream channel are not maintained over time, sediment in storage behind LOD dams will be released downstream over a period of a few decades. The simulation model predicted increases of about 40 to 130 percent in the bedload yield from low-order watersheds over a 60-year period resulting from a gradual decline in inputs of LOD to channels. In-channel sediment storage might be maintained if sources of LOD for recruitment to channels are preserved.

### **INTRODUCTION**

The subject of bedload transport in low-order streams in forested watersheds is an important one to forest and aquatic ecosystem managers. Low-order channels are the primary link between steep, sediment-producing hillslopes in headwater areas and the higher-order channels downstream which contain spawning and rearing habitats for salmonid fishes. Sediment production, whether in excess or deficit, in these higher-order channels may affect the quality and quantity of habitat for various life-stages and species of salmonid.

Although mass wasting in headwater areas is likely to be the dominant source and routing mechanism of sediment found in higher-order channels, fluvial sediment transport is a determinant of sediment storage and, consequently, sediment routing by debris flow (Benda 1994). In addition, fluvial sediment transport from low-order channels determines the sediment supply to higher-order, fish-bearing streams in the absence of episodic delivery of sediment by debris flow. Hence, fluvial sediment transport in low-order streams is one of the major processes determining the sediment characteristics in spawning and rearing habitats of salmonids.

This report presents scientific background of the subject, methods, model structures, model results, and discussion. First, we will discuss some previous efforts to quantify fluvial sediment transport in low-order channels to illustrate why it is

an important question to managers of forest and aquatic ecosystems. Second, we describe our conceptual model of the fluvial sediment transport process in low-order channels. Third, we describe our monitoring program and the field data used to construct the models. Fourth, we describe the models and the different scenarios used in the sensitivity analysis. Fifth, we present model results. Finally, we discuss the model results in the context of ecosystem management.

#### **BACKGROUND**

Quantifying transport rates of fluvial sediment in low-order channels is a necessary step for quantitatively predicting sediment yield from mountain drainage basins. The low-order channels of interest are first-, second- and third-order streams with slopes sufficient to sustain debris flows. In the absence of debris flow, sediment enters streams from hillslopes by creep processes including bank erosion, tree-throw, burrowing by rodents, and small streamside slope-failures (Reid 1981). Creep processes are generally slow and pervasive over watersheds, causing a relatively small, steady supply of sediment to enter low-order stream channels over a wide area.

LOD also enters channels gradually over a wide area (Lienkaemper and Swanson 1987). In forested mountain watersheds, streams contain abundant tree boles, branches, and rootwads, collectively referred to as large organic debris (LOD). LOD is frequently incorporated in stream channels, forming flow obstructions called LOD dams (Bilby 1981, O'Connor 1986). The sediment-storage capacity of LOD dams and their role in sediment routing in forested drainage basins is of particular interest and has not been well-quantified (MacDonald and Ritland 1989).

Sediment Routing in Low-Order Channels. Episodic debris flows in low order channels either deposit sediment in these channels or scour much or all of the accumulated sediment and LOD and transport it downstream. The frequency of channel-scouring

debris flow in second-order channels is on the order of several centuries in the Oregon Coast Range as reported by Benda (1990). In other mountain landscapes, the frequency of channel-scouring debris flow may differ, but few comparable data exist. Benda (1990) estimates that in an 52-square km watershed in the Oregon Coast Range where logging has occurred, approximately 68 percent of sediment supplied to third- through fifth-order streams has been delivered by debris flow. This suggests that debris flow is the dominant long-term sediment transport process.

Benda's (1990) figure for the proportion of sediment delivered by debris flow to third- through fifth-order streams is derived from a sediment budget. In his sediment budget, he estimates that 20 percent of the sediment entering first- and second-order channels is transported downstream by fluvial processes. This fluvial transport rate for first- and second-order channels also determines the transport rate by debris flow because sediment entering these channel must be transported by either by debris flow or by fluvial transport. Hence, the accuracy of estimates of long-term sediment transport by debris flow is limited by uncertainty regarding the actual fluvial transport rate.

The uncertainty regarding fluvial sediment transport rates reflects the lack of previous research on fluvial transport processes in low-order streams and sparse monitoring data. The following statements (Benda 1990) give the most reasonable description of fluvial sediment transport processes, given the scarcity of data:

There are several reasons why sediment delivered to first- and second-order channels resists fluvial erosion and accumulates...Instantaneous delivery of thick wedges of sediments to narrow channels reduces the opportunity for streamflow to erode and transport sediments...headwater channels have large boulders and both live and dead large woody material on surfaces of deposits which increase roughness and reduces gradients

thereby reducing sediment transport. Fluvial sediment transport is minimal also because water velocities in streams are insufficient to transport the coarse armor layer that protects the underlying sediment from stream erosion. (p. 460)

Fluvial export of sediment from headwater basins depends upon availability of mobile sediment which is controlled by time since last debris flow and the occurrence of landslides and floods in the basin. (pp. 462-3)

In the absence of data on fluvial transport processes and rates, it may be reasoned that deposition of sediment entering low-order channels, rather than transport, is the dominant sediment routing characteristic of these channels. With respect to long-term rates of sediment transport, fluvial processes in low-order channels appear to be of secondary importance compared to debris flow processes.

Timber/Fish/Wildlife Literature Review of Sediment Dynamics in Low-Order Streams. A literature review of sediment dynamics in steep low-order streams in the Pacific Northwest by MacDonald and Ritland (1989) found that fluvial sediment transport in low-order streams is significant, but is difficult to reliably quantify. They found no published data from direct field studies of sediment transport rates. MacDonald and Ritland concluded that:

Calculation of long-term sediment yield by fluvial erosion in headwater channels will require some form of simulation modeling...to account for the stochastic nature of sediment supply and the required magnitudes of streamflow...this...will require a better understanding of fluvial sediment transport mechanics in small channels than is currently available (p. 24).

In coming to this conclusion, MacDonald and Ritland offer a review of existing data and a conceptual model for the interactions between sediment supply, sediment storage, and streamflow that determine sediment transport. Their main findings are summarized below.

MacDonald and Ritland conclude that fluvial sediment transport is rapid for fine materials (that which is transported as suspended sediment load) and episodic for coarser material (bedload). Citing studies from California, Oregon and Idaho, they found that bedload ranged from 36 to 70 percent of total fluvial sediment load in low-order streams.

MacDonald and Ritland identify three fundamental channel types based on published descriptions. These are bedrock channels with few obstructions and little sediment storage, step-pool channels which have rhythmically-spaced obstructions formed by boulders and cobbles, and stepped-bed channels with frequent, randomly spaced obstructions dominated by LOD. Although we recognize that all three of these channel types occur in forested headwater basins, often in the same stream, we will focus on stepped-bed morphology because of its sediment storage capacity and potential effects of timber harvest on LOD accumulation rates.

Erosion and deposition patterns in stepped-bed channels are governed by obstructions (LOD dams) that act as local base levels. Upstream of the obstruction, channel slope and therefore stream power is reduced and downstream, turbulence dissipates energy in a plunge pool and maintains the suspension of relatively coarse particles. Significant storage of sediment upstream of LOD and other obstructions has been observed in field surveys. Where sediment yield has been monitored in conjunction with channel storage in undisturbed watersheds, annual sediment yield ranges from 3 to 30 percent of in-channel storage.

MacDonald and Ritland suggest that bedload entering a channel is not necessarily immobilized upstream of obstructions. Citing research by Tally (1980), who found that surface sediment upstream of LOD obstructions to be more mobile than riffle gravel, MacDonald and Ritland hypothesize that LOD-dam-stored sediment is stratified into a basal layer in semi-permanent

storage and a more easily mobilized surface layer. Other studies have suggested that bedload is transported downstream after LOD dams were eroded (Mosely 1981, Sidle 1988).

Conceptual Model of Bedload Routing. MacDonald and Ritland offer a conceptual model for the interactions between sediment supply, sediment storage, and streamflow that control sediment transport in stepped-bed channels. First, sediment is either eroded from the channel bed by streamflows exceeding some critical discharge or is supplied by bank erosion and/or in-channel landslide deposits and/or failure of channel obstructions. When streamflow exceeds the critical discharge, fluvial transport occurs.

Entrained sediment may be deposited in areas of low transport capacity. Many of these deposition zones are pools upstream of channel obstructions. Such pools may fill quickly; MacDonald (unpublished) calculated that an  $50 \text{ m}^3$  storage compartment upstream of an obstruction in a third-order stream could be filled by bedload after 10 to 20 hours of bankfull flow.

Successive storage compartments continue to be filled until streamflow drops below the transport threshold or all available storage space is filled. If streamflow remains competent to transport sediment when all storage space is filled, the bedload transport rate is expected to rapidly increase. Transportable sediment and competent streamflow must both be available for transport to occur.

MacDonald and Ritland's conceptual model of the sediment transport process in low-order channels with obstructions identifies sources of sediment, postulates a threshold of stream discharge for sediment transport, and describes interactions of fluvial sediment with storage reservoirs in the channel. Their model captures many essential elements of a sediment routing model, but it lacks a detailed description of the interaction between sediment storage reservoirs and fluvial sediment

transport processes. Moreover, data are presently unavailable to validate or quantify such a process model.

The implication of MacDonald and Ritland's model is that the transport rate of sediment depends largely on the status of sediment storage sites. Their conceptual model asserts that sediment transport rates are low until sediment reservoirs are filled. Once filled, the net transport rate increases rapidly. A corollary to this conceptualization is that when the storage reservoirs are full, fluvial sediment transport proceeds as if in a steady-state condition controlled by flow competence. In the context of the reservoir-theory-approach to sediment routing, MacDonald and Ritland's model suggests that when the reservoirs are full there is no change in sediment storage and sediment output therefore equals sediment input.

Although they allude to the possibility of re-entrainment of sediment from storage sites in their literature review, MacDonald and Ritland's conceptual model does not take this process into account. Whether the sediment storage sites are viewed as static (once filled, remaining filled), or dynamic (subject to scour and fill), has significant ramifications in a sediment routing model. In particular, the interaction of sediment in fluvial transport with storage reservoirs is minimal if the filled storage reservoirs are considered static, but the interaction is significant if the storage reservoirs are dynamic. The degree of interaction between sediment in transport and sediment in reservoirs should have significant effects on long-term rates of bedload transport and residence times.

Effects of Timber Harvest on LOD Accumulation Rates. When timber stands adjacent to stream channels are harvested, the source of future inputs of LOD to stream channels is altered. In coastal watersheds of the Pacific Northwest, it has been demonstrated that inputs of coniferous LOD from second-growth riparian stands begins about 60 years after harvest (Grette 1985,

Andrus et al. 1988). Inputs of LOD from deciduous trees (typically alder) become significant about 30 to 60 years after harvest. In larger, low-gradient streams, deciduous LOD constitutes the majority of LOD inputs from the second-growth forest. In small, steep tributaries, however, coniferous LOD from second-growth stands is more abundant than deciduous LOD (Andrus et al. 1988). Thus, it is likely that LOD accumulation rates will decline steeply over a 60 year period following timber harvest, particularly in steep tributary streams where deciduous LOD inputs are relatively small.

Logging operations may also increase the LOD load in stream channels. Froehlich (1973) found a two-fold increase in LOD load in, above and adjacent to tributary streams in the western Cascades of Oregon immediately following clearcut harvest and yarding with no riparian buffers. Swanson et al. (1984) found a three-fold increase in LOD load in southeast Alaska streams immediately following clear-cut logging. These short-term increases in LOD load resulted from inadvertent deposition of LOD near the stream channel. Such LOD is often relatively short in length, and therefore has a greater propensity to enter stream channels and to be mobilized during peak flow events.

The pattern of formation and failure of LOD dams may also be expected to change following timber harvest. Hedin et al. (1988) found that density of LOD dams in the Hubbard Brook Experimental Forest in New Hampshire decreased about 80 percent following timber harvest. They also found that sediment yield measured in sedimentation basins correlated with the decline in density of LOD dams and suggested that the increased sediment yield may reflect removal of sediment from storage behind LOD dams.

O'Connor (1986) also found a decline in LOD dams following timber harvest and a significant quantity of sediment storage upstream of LOD dams. Several other studies have found decreases in LOD load following timber harvest, including one at Carnation

Creek in British Columbia (Toews and Moore 1982) and one in Alaska (Bryant 1980).

The foregoing studies, together with the observations at Hubbard Brook, led Hedin et al. (1988) to propose a general model of long-term changes in density of LOD dams and sediment yield. In their model, density of LOD dams declines rapidly over a period of decades, then increases gradually until an asymptote is reached equivalent to initial density of LOD dams.

Sediment yield is coupled to the net change in density of LOD dams. Sediment export occurs during the period of declining density of LOD dams. During the period of increasing density of LOD dams, sediment export is zero, reflecting the increasing sediment storage capacity of LOD dams. When density of LOD dams reaches its maximum value, sediment export becomes possible because no new storage capacity is available, and new sediment entering the system can be routed downstream.

Given the preceding evidence regarding changes in LOD inputs following timber harvest, decreases in density of LOD dams following timber harvest, and the hypothesized role of LOD dams in sediment routing, it is reasonable to hypothesize that timber harvest may have a significant influence on density of LOD dams and sediment routing. The potential influence of LOD dams on sediment routing is a primary issue motivating our research.

We seek to progress toward a better-constrained estimate of long-term fluvial sediment transport in low-order channels by directly observing fluvial sediment transport processes in relation to streamflow rate. Given reasonably accurate estimates of long-term sediment transport capacity (that is, potential sediment transport regardless of sediment supply), it is possible to assess the influence of changes in the dynamics of LOD dams on long-term sediment yield.

## MONITORING SEDIMENT TRANSPORT IN LOW-ORDER CHANNELS

Monitoring Objectives. The primary objectives of our monitoring program were to determine the annual rate of bedload transport in low-order channels and to determine the approximate grain-size of sediment transported in suspension. Secondary objectives were to determine the density of LOD dams and to determine the approximate annual rates of LOD dam failure and establishment.

Annual bedload transport rates have rarely been measured in low-order stream channels (e.g. Sidle 1988, Grant and Wolfe 1991). The scarcity of such data reflects the difficulty of data collection. Traditional techniques include collection of transported sediment either in large sedimentation basins on an annual basis or with a Helley-Smith sampler during individual transport events. These methods were not feasible for this study.

Recent research suggests that bedload tracers can serve as a means to estimate bedload transport rates (Hassan et al. 1992). A simple expression for bedload transport ( $Q_b$ ) is

$$Q_b = V_b S W_{ab} (1-P) \quad (1)$$

where  $V_b$  is the mean bedload velocity,  $S$  is mean scour depth,  $W_{ab}$  is mean active channel width, and  $P$  is porosity of the bed material. Bedload tracers composed of natural stream gravels tagged with ceramic magnets can be used to estimate  $V_b$ .  $S$  can be estimated using scour chains and by examining recovery depth of tracers.  $W$  can be estimated from channel cross-section surveys and from post-event observations of active channel dimensions.

Hassan et al. (1992) found that peak unit stream power in excess of threshold unit stream power is a good predictor of  $V_b$ . This suggests that by determining predictive relationships between excess stream power and  $V_b$ ,  $S$  and  $W_{ab}$ , as well as

developing a means of simulating long-term distributions of peak stream flow (and therefore stream power), it is possible to simulate long-term rates of bedload transport. This is precisely what we have done in developing the transport model.

Simulation of long-term peak streamflow was based on two predictive relationships. The first relationship was between 24-hour rainfall at the field sites and peak stream discharge. The second relationship was between 24-hour rainfall at the field sites and 24-hour rainfall at a nearby recording station with a 61-year period of record.

Another objective was to determine the grain sizes that are transported in suspension. This allows the routing model to sort sediment entering the channel via creep processes.

Hence, the specific objectives of our monitoring program were to determine the following:

- threshold of entrainment of bed sediment in terms of unit stream power and stream discharge,
- mean bedload velocity for transport events as a function of peak unit stream power in excess of threshold unit stream power,
- mean depth of bed scour for transport events as a function of excess unit stream power,
- mean width of the active channel as a function of excess unit stream power,
- peak stream discharge as a function of 24-hour precipitation, and
- representative sediment grain sizes transported in suspension.

A detailed description of the monitoring program will be available in the dissertation or other publications. The relationships developed from monitoring data are presented later in this report.

Field Sites for Monitoring Program. Site selection for sediment transport monitoring was guided by the following criteria in order of importance: reasonable winter access, high

sediment supply in the stream channel, and a range of contributing drainage areas.

Abundant in-channel sediment supply was required because we wanted to monitor bedload transport in locations where transport would not be supply-limited. A range of contributing drainage areas was desired to ensure that data were collected from a range of stream sizes and flow intensities representative of headwater channel networks.

Three streams located in the northwestern Olympic Mountains (Figure 1) meeting these criteria were selected (Table 1). Monitoring was conducted during the winters of 1991/92 and 1992/93.

Each stream has had a history of disturbance. Debris flows in the winter of 1990/91 entered Eight-ten Creek and Ramp Creek. These debris flows did not scour the study reaches, but they deposited abundant sediment (O'Connor and Harr 1991). In addition, large portions of the drainage areas in Ramp Creek and virtually all of the Eight-ten Creek drainage were logged within the past 20 years, including forest stands in the riparian-zone. Sister Creek was affected by an intense wildfire in 1951 and subsequent road-building and salvage logging. Abundant woody debris and frequent small-scale streamside landslides and bank erosion have created a sediment-rich stream channel in Sister Creek.

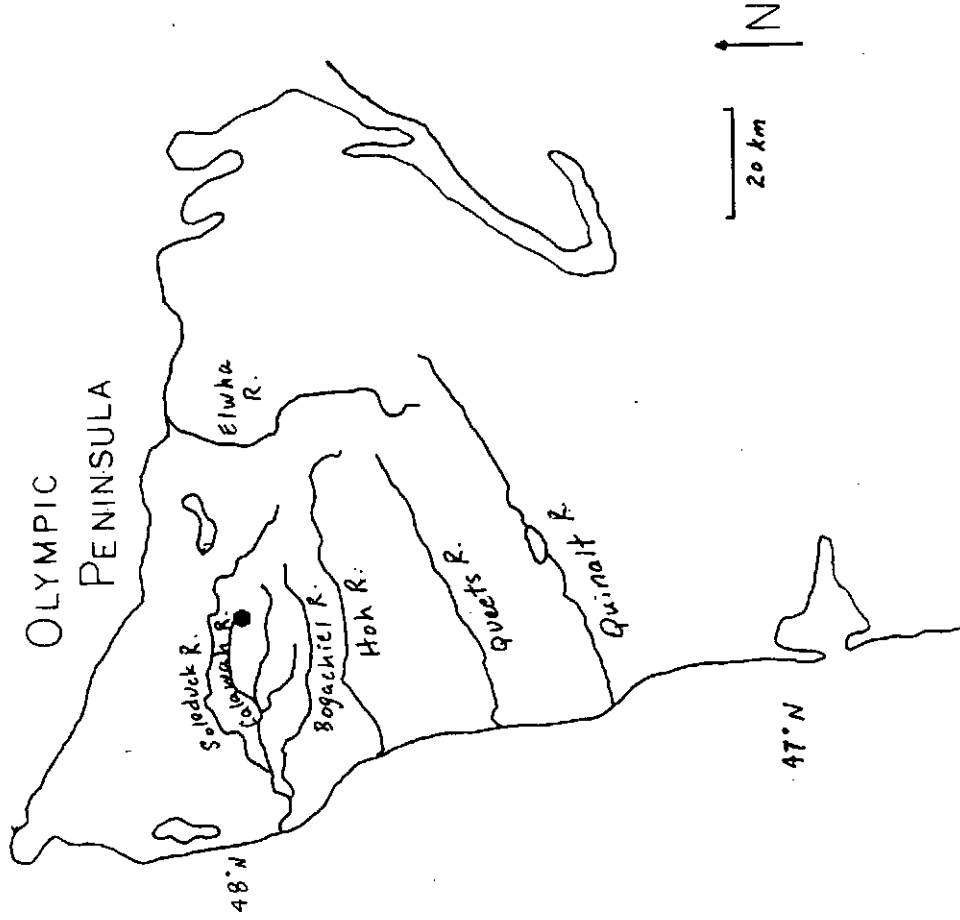
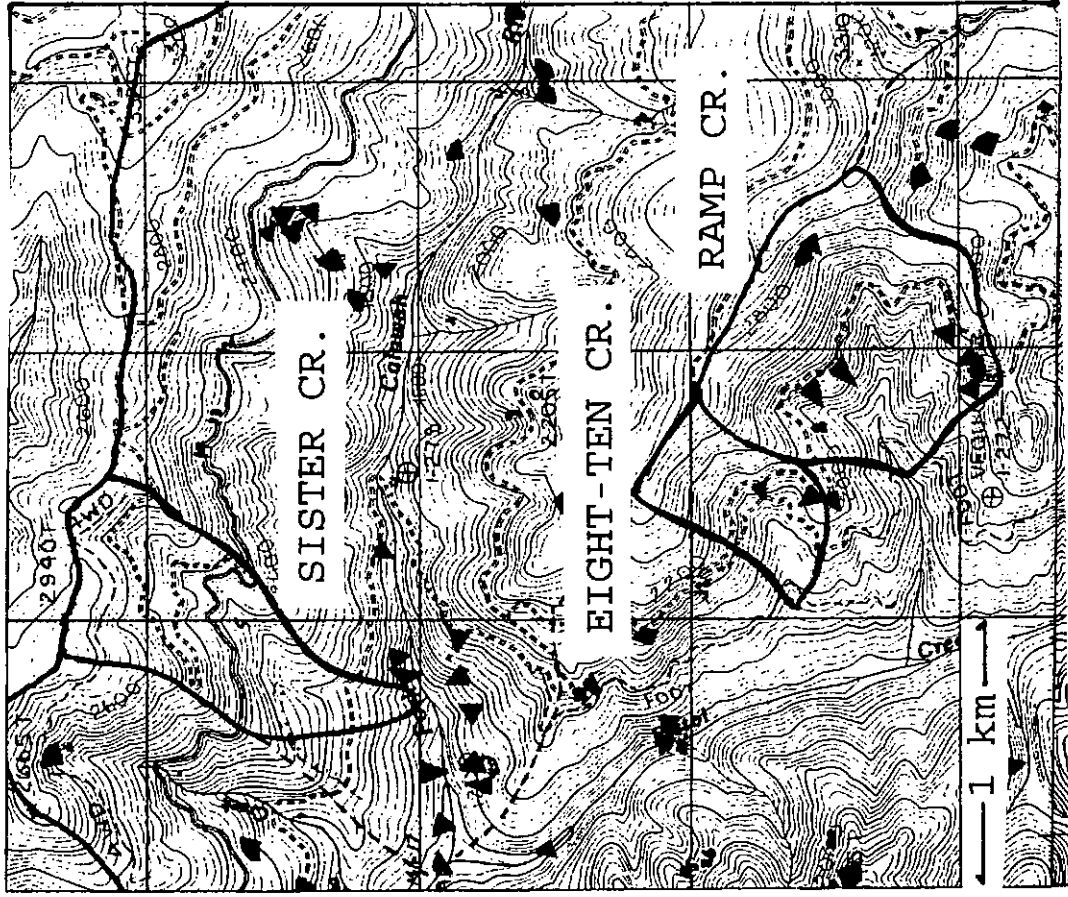


FIGURE 1: LOCATION MAP

Table 1: Monitoring Site Characteristics

Stream	Drainage Area (km <sup>2</sup> )	Mean Slope	Median Slope	Mean Width (m)	Surface d84 (mm)	Surface d50 (mm)	Subsurf. d50 (mm)
Eight-ten	0.31	0.16	0.11	3.3	114	50	23
Sister	0.53	0.14	0.07	2.8	64	30	14
Ramp	1.12	0.14	0.12	4.1	120	70	17

## BEDLOAD TRANSPORT MODEL

The bedload transport model produced a frequency distribution of annual bedload transport events based on data from each of the three monitored streams. These frequency distributions were subsequently employed in the routing model to determine the bedload transport potential in each annual time step. The bedload transport model is described below beginning with a brief overview of the model structure. The predictive relationships used in the model are subsequently described in greater detail. It should be noted at the outset that each predictive relationship was extrapolated beyond the range of data used to determine the relationships.

Model Overview. The transport model was used to predict annual bedload transport in three channels with drainage areas of about 0.3 km<sup>2</sup>, 0.5 km<sup>2</sup>, and 1.1 km<sup>2</sup>. These three channel-sizes represent the upper, middle, and lower portions of the model channel network used in the routing model. The transport model employed a Monte Carlo scheme that explicitly incorporated the random scatter in each predictive relationship in the model output.

The driving independent variable in the transport model was 24-hour precipitation ( $P_{24}$ ). For any given value of  $P_{24}$ , there was an infinite number of potential bedload transport capacities. A frequency distribution of annual bedload transport capacity was generated by running the model over a simulated period of 5000 years. The frequency distribution gives the modelled probability of occurrence and recurrence interval of any magnitude of bedload transport in a single year. The probability distribution also expresses the extreme values and the central tendency of annual bedload transport capacity.

The model consists of a sequence of predictive relationships. The independent driving variable,  $P_{24}$ , was randomly selected for each storm event by a method described in

detail below. In turn,  $P_{24}$  became an independent variable predicting peak instantaneous discharge ( $Q_{pk}$ ). If  $Q_{pk}$  did not exceed the bedload transport threshold, the bedload transport for that storm event was zero. If  $Q_{pk}$  did exceed the threshold,  $Q_{pk}$  was transformed into excess unit stream power ( $\omega_e$ ).  $\omega_e$  then became the independent variable predicting mean bed scour ( $S$ ) and mean bedload velocity ( $V_b$ ). Mean active bed width  $W_{ab}$  was a constant derived from field observations. Finally,  $Q_b$  for the storm event was calculated according to Eqn. 1. This sequence was iterated for each simulated storm event in each simulated year (see below) and the predicted bedload transport capacity for each storm event was summed to yield the predicted annual bedload transport capacity ( $Q_{ba}$ ).

Stochastic Model Outputs From Predictive Relationships. For each predictive relationship, the mean predicted value of the dependent variable and a random deviation from the predicted mean value were calculated. The random deviation was selected from a normal distribution of random errors about the mean calculated for each value of the independent variable. The range of deviates was constrained within the 95 percent confidence limits for prediction of each dependent variable. The mean predicted value of the dependent variable and the random normal deviation were summed to determine the "Monte Carlo" value for the dependent variable. This value was subsequently used as the independent variable in the next predictive relationship, and the Monte Carlo procedure was repeated. This procedure introduces random variability contributing to the stochastic character of the model.

24-Hour Precipitation. The master driving variable  $P_{24}$  was the key to extrapolating a 2-year record of bedload transport data to a prediction of long-term bedload transport capacity.  $P_{24}$  at our monitoring sites could be predicted from  $P_{24}$  at a recording station in the community of Forks 20 km to the west

(denoted as station Forks 1 E in the NOAA climate data base) by simple linear regression. This relationship allowed us to synthesize a long-term distribution of  $P_{24}$  at the monitoring sites based on the 61-year period of record at Forks.

A scatter-plot of the data for the winter of 1991/92 is shown in Figure 2. Precipitation data from 1992/93 were scant, and all gages failed during the single significant storm event, so data from only the winter of 1991/92 were used. Regression equations and statistics are presented in Table 2.

Differences in precipitation totals less than 10 percent were noted among the three sites, with higher totals occurring at higher elevations. For the purposes of this modelling exercise, and given the magnitude of random scatter (Figure 2), we selected the most conservative predictive relationship, that between  $P_{24}$  at Forks and  $P_{24}$  at Sister Creek. Moreover, Sister Creek had the most complete precipitation record; the other two stations had significant gaps in the data, including some large storm events.

#### Synthesis of Frequency of Threshold 24-Hour Precipitation.

We found that a  $P_{24}$  of about 4.1 inches (104 mm) at our monitoring sites was necessary to generate a streamflow peak large enough to entrain streambed pavement (the exception to this precipitation-runoff threshold is discussed in the following subsection). This precipitation threshold could be related to  $P_{24}$  at Forks, giving us the opportunity to greatly reduce our requirements for long-term precipitation data.

Rather than analyzing daily records over a 61-year period (a total of 22,280 days), we abstracted only those precipitation records likely to trigger a bedload-transport discharge peak at our monitoring sites. We used the lower bound of the 95 percent confidence interval of the Forks-monitoring site precipitation regression to determine the minimum  $P_{24}$  at Forks that would be likely to exceed the threshold  $P_{24}$  for bedload transport at the monitoring sites. All 304 records (1.34 percent of the total) of

**Table 2: Bedload Transport Model Regression Coefficients and Statistics**

<u>Stream Order</u>	<u>Dependent Variable</u>	<u>Independent Variable</u>	<u>Regression Coefficient</u>	<u>Regression Constant</u>	<u>n</u>	<u>r-squared</u>	<u>p</u>
--	24-Hr. PPt.	24-Hr. Ppt.-Forks	1.08	0	112	0.71	<0.001
2-Upper	Peak Discharge	(24-Hr. PPt)^2	0.0130	0	10	0.95	<0.001
2-Lower	Peak Discharge	(24-Hr. PPt)^2	0.0187 (a)	0	--	--	--
3	Peak Discharge	(24-Hr. PPt)^2	0.0347	0	12	0.91	<0.001
2-Upper	Mean Bed Scour	Excess Stream Power	0.0404 (b)	0	--	--	--
2-Lower	Mean Bed Scour	Excess Stream Power	0.0807	0	7	0.89	<0.001
3	Mean Bed Scour	Excess Stream Power					
All Data	Mean Bedload Travel	Excess Stream Power	1.78 (c)	0.00637 (d)	11	0.75	<0.001

**NOTES**

- a. For the lower second order channel, the relationship between 24-hour precipitation and peak stream discharge was synthesized (see text).
- b. Mean bed scour in the upper second order channel was fit by eye as half that for the two larger channels.
- c. Exponent to which independent variable is raised; regression coefficient in simple linear regression using log-transformed data.
- d. Multiplicative coefficient of the quantity of the independent variable raised to the exponent 1.78; regression constant in simple linear regression using log-transformed data.

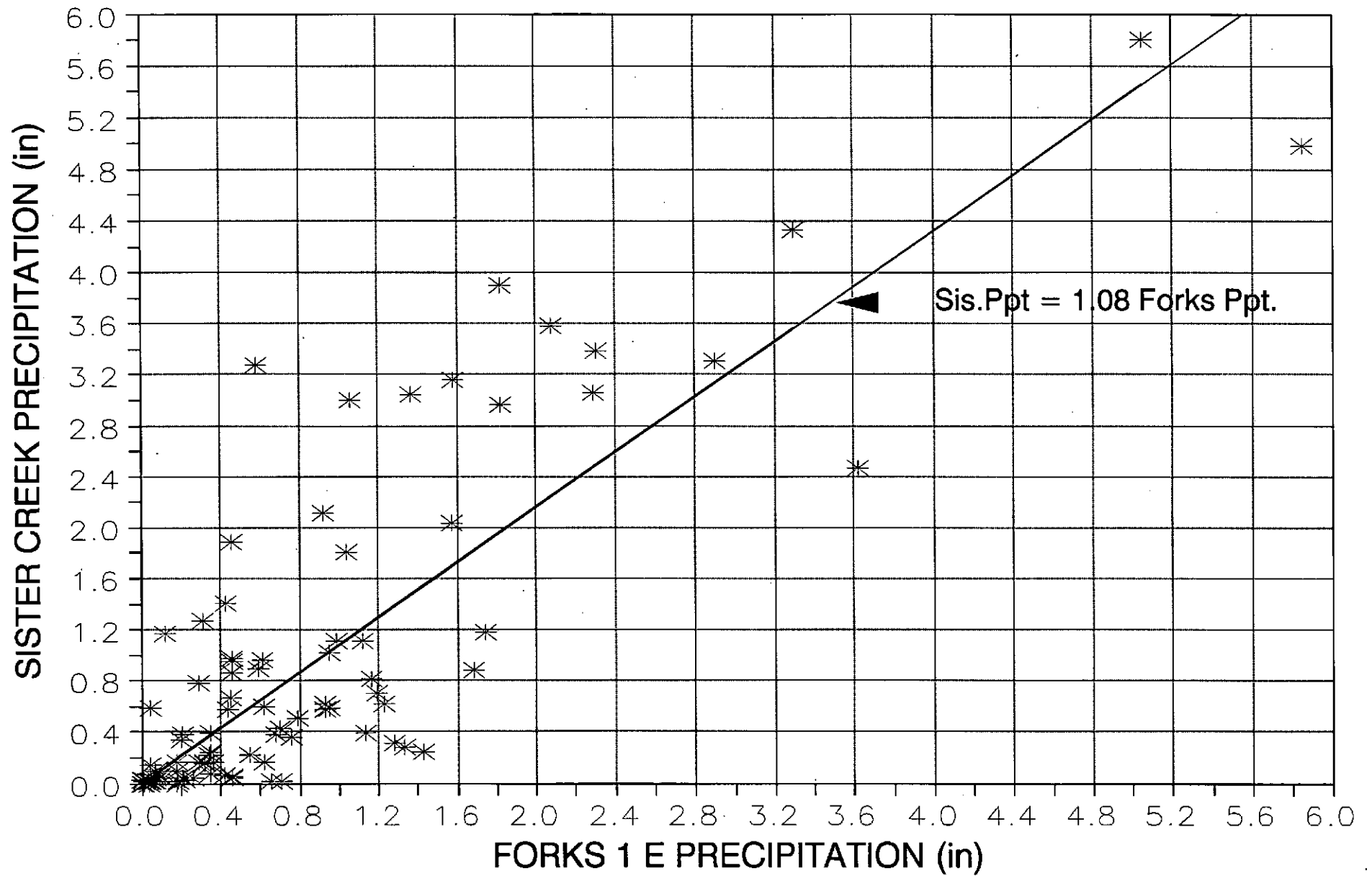


Figure 2: Observations of 24-Hour Rainfall, 1991-1992

$P_{24} \geq 2.6$  inches (66 mm) were abstracted from the 61-year record. The distribution of these data is shown in Figure 3. The number of  $P_{24}$  events greater than or equal to 2.6 inches in each year was also determined. The distribution of these data is shown in Figure 4.

To generate the values of  $P_{24}$  used to drive the bedload model, the following procedure was employed. A random number between 0 and 1 was drawn from a uniform distribution. This number was then used as the point in a cumulative frequency distribution (based on Figure 4) in that year determining the number of potential threshold  $P_{24}$  events occurring in that model year.  $Q_b$  for that number of events, ranging from 0 to 12 per year, were subsequently modeled. Once the number of events was determined, a uniform random number was drawn for each model event. Each random number represents a point in the cumulative frequency distribution of magnitudes of  $P_{24}$  (Figure 3), and a  $P_{24}$  value for Forks is selected for each storm. The frequency distribution was divided into increments of 0.1 inch for this purpose.  $P_{24}$  becomes the independent driving variable predicting the peak discharge associated with each storm event. The foregoing procedure is the second element of random variation that is responsible for the stochastic character of the model.

#### Peak Discharge as a Function of 24-Hour Precipitation.

Simultaneous stream gaging and precipitation records were collected at each of the three monitoring sites. At Eight-ten Creek and Ramp Creek,  $Q_{pk}$  could be predicted by simple linear regression as a function of the square of  $P_{24}$  (Table 2).

At Sister Creek, however, antecedent precipitation had much more influence. We found that the three-day precipitation total was the best predictor of  $Q_{pk}$ . We attribute this difference to deeper soils and different bedrock geology found in the Sister Creek drainage.

The different form of this rainfall-runoff relationship

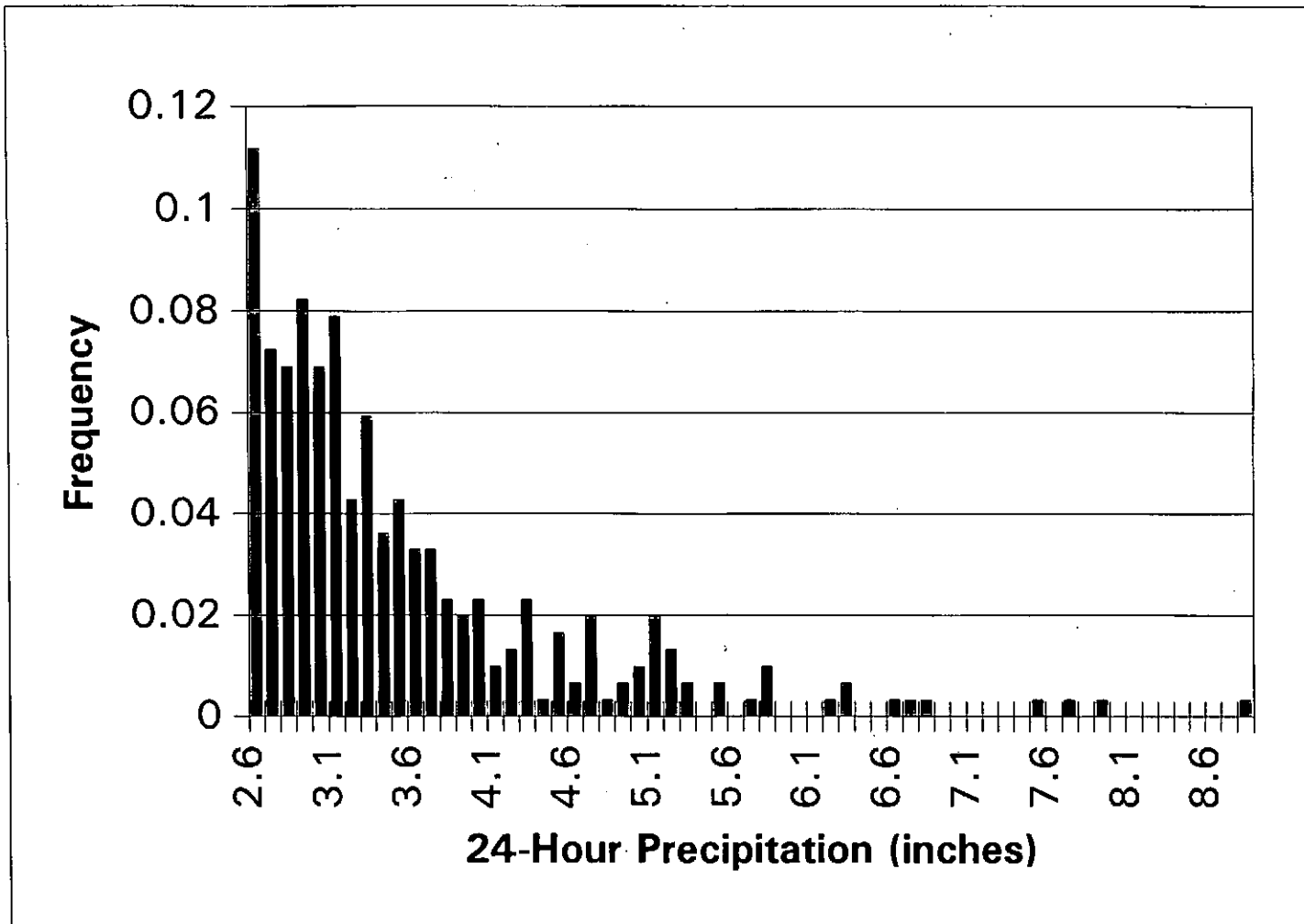


Figure 3: Frequency and Magnitude of 24-Hour Precipitation Totals Greater Than or Equal to 2.6 Inches, Forks, Washington, 1931-1991

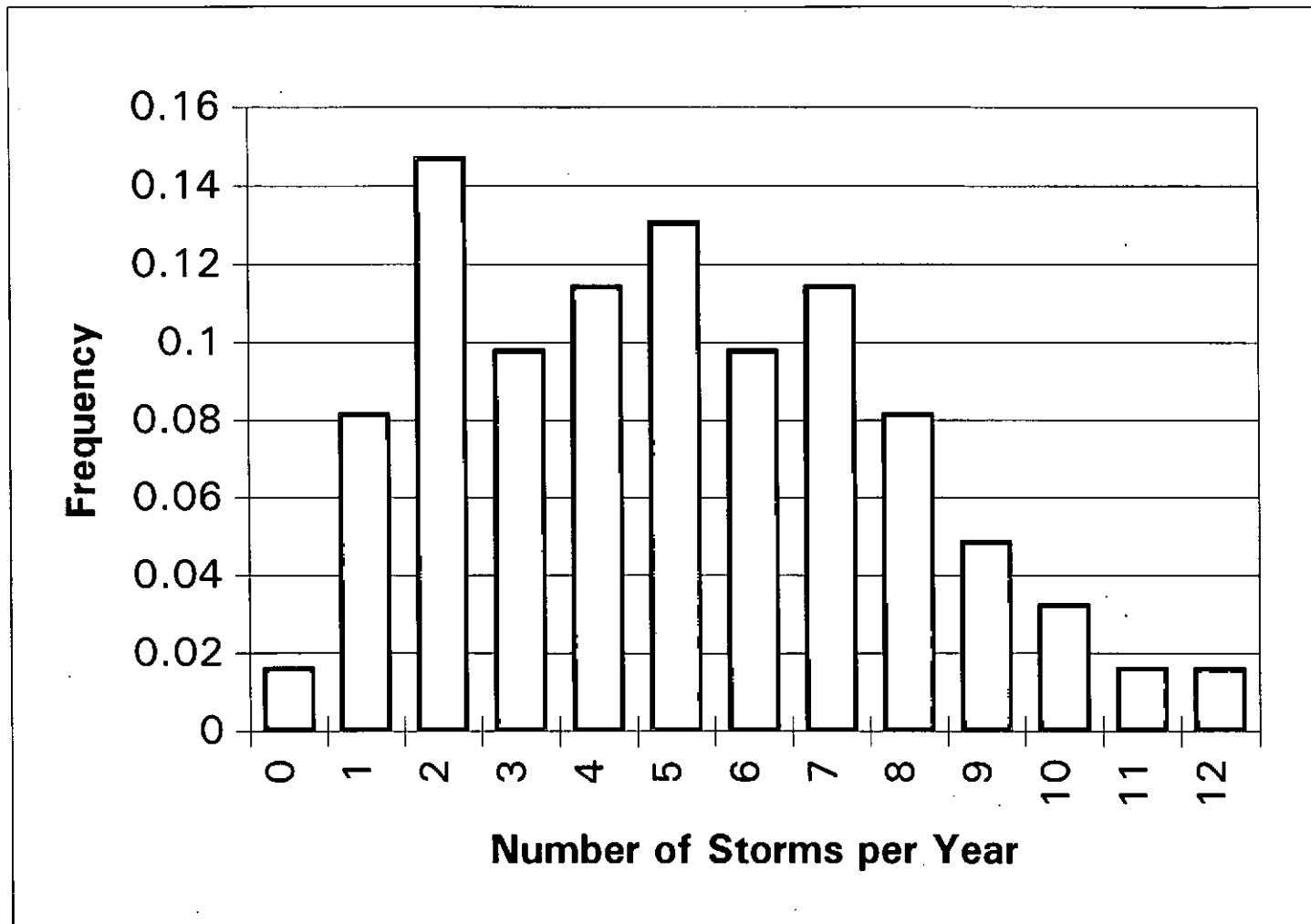


Figure 4: Annual Frequency of Number of Days per Year with at Least 2.6 Inches Precipitation, Forks, Washington, 1931-1991

presented a serious difficulty for the routing model in that the bedload transport data derived from Sister Creek was to be used for the middle portion of the model channel network, and each portion of the model network would need to have similar rainfall-runoff relationships. We overcame this obstacle by synthesizing a relationship between  $P_{24}$  and  $Q_{pk}$  for the middle-portion of the channel network.

The relationship between  $P_{24}$  and  $Q_{pk}$  for the mid-network channel was synthesized based on the relationships for Eight-ten Creek, representing the upper network channel, and Ramp Creek, representing the lower network channel. The regression coefficient was synthesized by assuming that the regression coefficients would plot as a straight line on a log-log plot of coefficients versus drainage area. This is similar to plotting stream discharge versus drainage area on a log-log plot, a relationship which typically forms a straight line with positive slope. A line was drawn between points plotted for Eight-ten Creek and Ramp Creek; the coefficient value was determined by the point where the line intersected the drainage area value for Sister Creek.

It was also necessary to synthesize the random variation of  $Q_{pk}$  around the regression line relating  $P_{24}$  and  $Q_{pk}$ . This was accomplished by averaging the variances for the regression relationships for Ramp Creek and Eight-ten Creek for each value of  $P_{24}$  from 2.6 inches to 12.4 inches in 0.1 inch increments. Plots of the data, regression lines and 95 percent confidence prediction intervals for Eight-ten Creek and Ramp Creek are shown in Figures 5 and 6, respectively. The synthesized regression line and 95 percent confidence prediction intervals for the mid-network channel segment is shown in Figure 7. The synthetic predicted mean  $Q_{pk}$  and the synthetic variance were then used in the Monte Carlo procedure which determines the predicted value of  $Q_{pk}$  for that storm event.

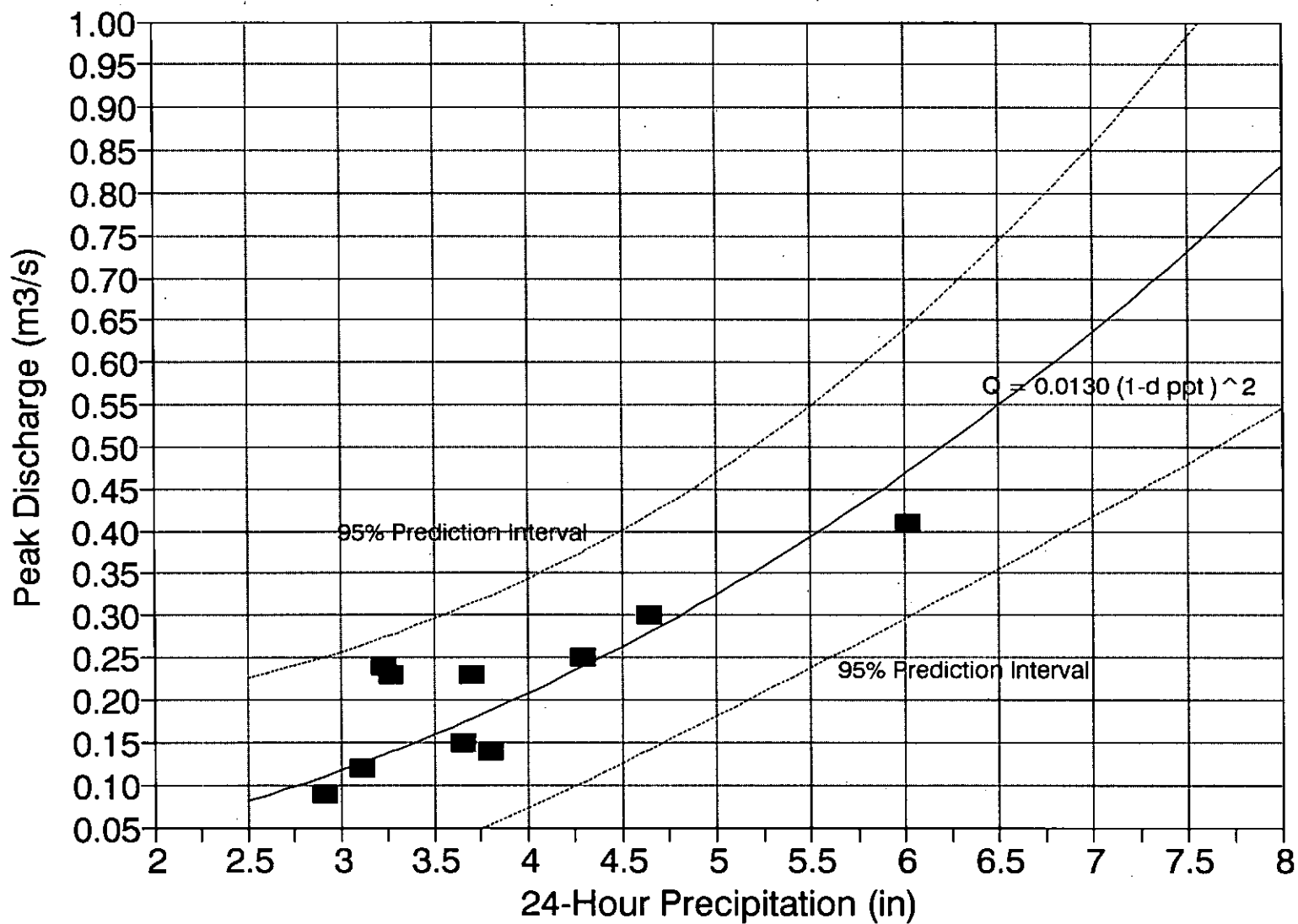


Figure 5: Peak Discharge as a Function of 24-Hour Precipitation, Eight-ten Creek

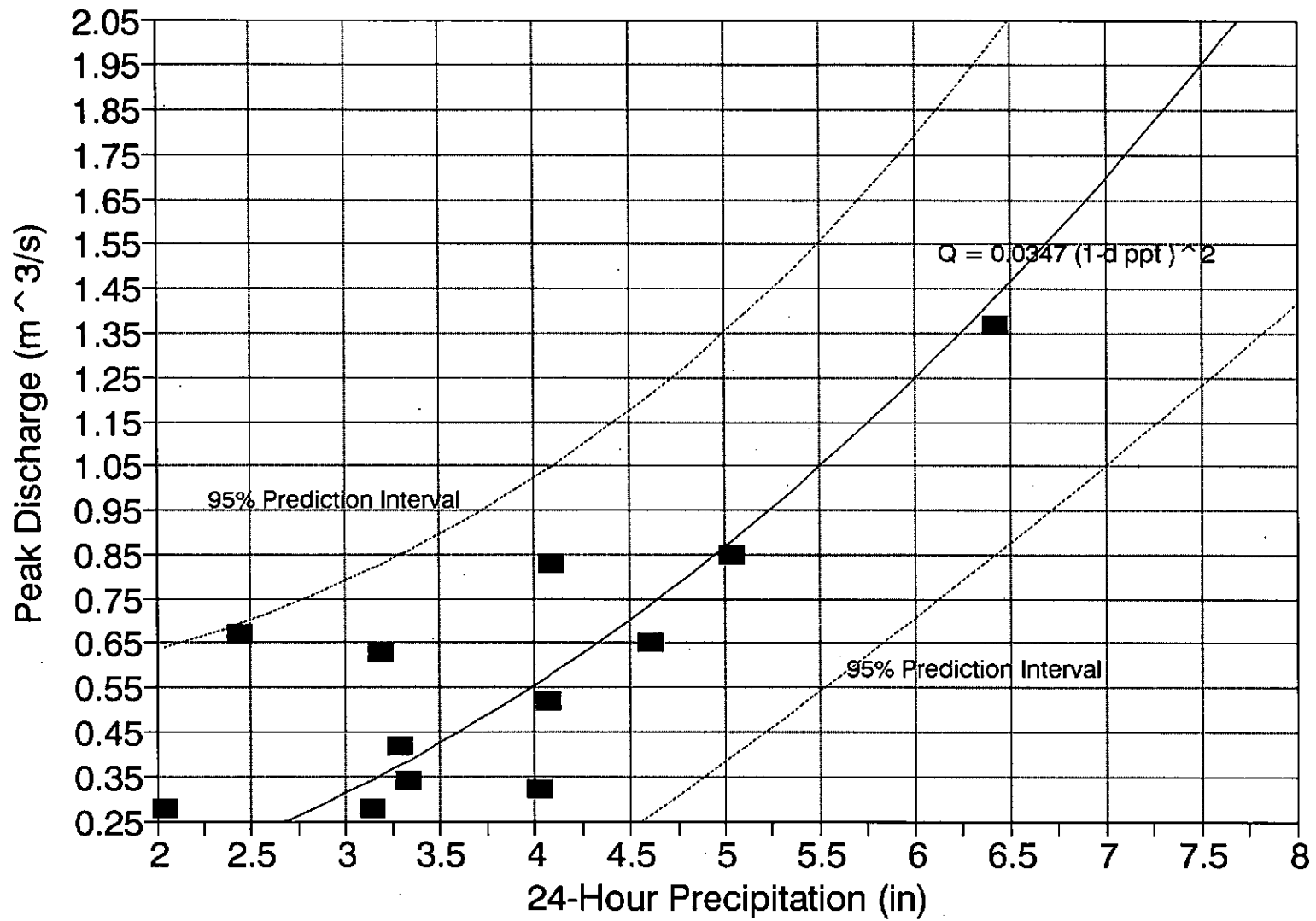


Figure 6: Peak Discharge as a Function of 24-Hour Precipitation, Ramp Creek

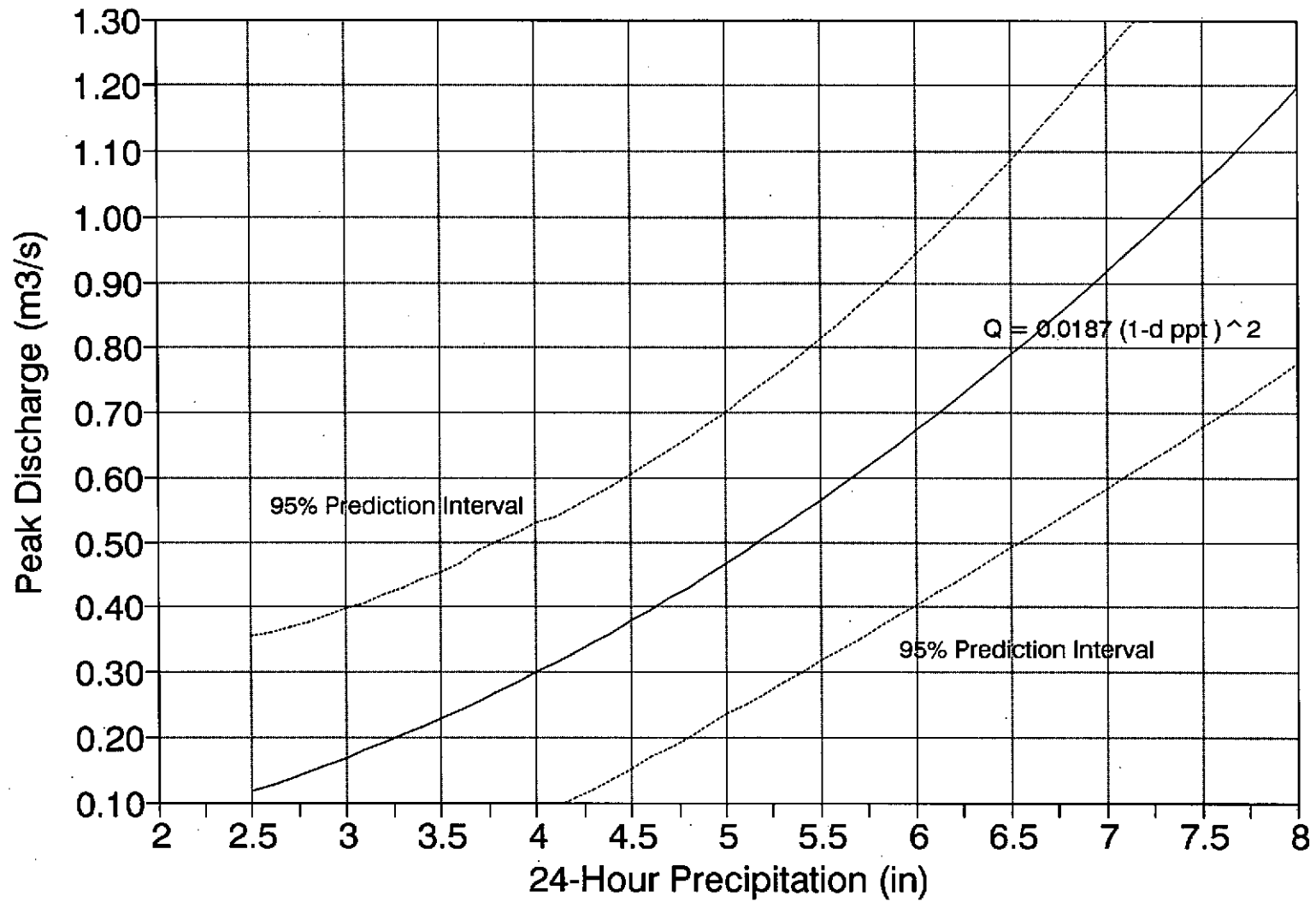


Figure 7: Synthetic Peak Discharge as a Function of 24-Hour Precipitation, Sister Creek

Excess Unit Stream Power ( $\omega_e$ ) as a Function of Peak Discharge. The next independent variable used in the bedload model,  $\omega_e$ , is calculated as:

$$\omega_e = (\omega - \omega_o) \quad (2)$$

where  $\omega$  is unit stream power and  $\omega_o$  is threshold unit stream power. Unit stream power ( $\omega$ ) can be calculated as

$$\omega = \rho g Q s w^{-1} \quad (3)$$

where  $\rho$  is the density of water,  $g$  is gravitational acceleration,  $Q$  is stream discharge,  $s$  is slope and  $w$  is channel width. If SI units are used, Eqn. 3 yields stream power in watts per unit channel area ( $W/m^2$ ). For streamflow below the threshold of bed entrainment, Eqn. 2 yields a value less than or equal to zero.

We used an unconventional definition of bed slope. In lower-gradient streams, the mean bed slope is a good predictor of the central tendency of slope. In steep, low-gradient streams, the stair-step profile creates a wide range of local slopes. Much of the elevation drop is consumed as the stream flows over obstructions. Much of the intervening riffle-like portions of stream have relatively low gradients compared to the mean slope gradient. We selected the median slope of length-weighted channel units as most representative of the central tendency of channel slope; median channel slope is used in Eqn. 3.

The thresholds of bedload transport in terms of discharge and threshold unit stream power ( $\omega_o$ ) were determined by observations of gravel tracers, scour chains, and discharge peaks which did and did not transport tracers and scour the streambed (O'Connor 1993). These data made it possible to bracket the threshold value of discharge for bed entrainment with values somewhat below and above the threshold. The resulting range of values within which the threshold lay was bisected, yielding the estimated threshold values. The values of  $\omega_o$  used in the model are listed in Table 3.

**Table 3: Bedload Transport Thresholds**

Stream	Maximum Incompetent Discharge (m <sup>3</sup> /s)	Minimum Competent Discharge (m <sup>3</sup> /s)	Mid-point (Threshold) (m <sup>3</sup> /s)	Threshold Unit Power $\omega_o$ (W/m <sup>2</sup> )
Eight-ten	0.15	0.24	0.195	62
Sister	0.26	0.31	0.285	70
Ramp	0.52	0.66	0.59	165

Mean Scour Depth as a Function of Excess Unit Stream Power.

For each bedload-transporting event observed during the monitoring period, the mean of scour depths recorded by scour monitors was calculated for each stream. These scour data were regressed against the independent variable  $\omega_e$  (Table 2) and plotted (Figure 8). Given the paucity of data, we decided that the most representative predictive relationship was that from the aggregate data from all three streams. This regression relationship was used to predict  $S$  in Eqn. 1 for the middle and lower portions of the channel network.

For the upper portion of the channel network, we used a predictive relationship based on the aggregate data, but with a significant downward adjustment. For a given value of  $\omega_e$ , the predicted value of  $S$  was half of that predicted based on the aggregate data. This adjustment was justified in part by the position of the data points from Eight-ten Creek below the regression line in Figure 8.

Further justification for a downward adjustment to predicted scour depth for the upper portion of the channel network was drawn from the patchy spatial distribution of scour recorded by scour monitors and the depth of burial of tracers. Sixty-three percent of scour monitors in Eight-ten Creek recorded zero scour. In contrast, 41 and 14 percent of scour monitors recorded zero scour in Sister and Ramp Creeks, respectively. The percentage of recovered gravel tracers found on the surface of the streambed was much higher in Eight-ten Creek than in the other two sites. Seventy-one percent of tracers were found on the surface in Eight-ten Creek. Only 25 and 40 percent of tracers were found on the surface in Sister and Ramp Creeks, respectively. Finally, the mean tracer burial depth in Eight-ten Creek was 0.022 m. In Sister Creek, mean burial depth was 0.094 m; in Ramp Creek, 0.066 m. Collectively, these data strongly suggest that the depth of scour in Eight-ten Creek was significantly less than in the other

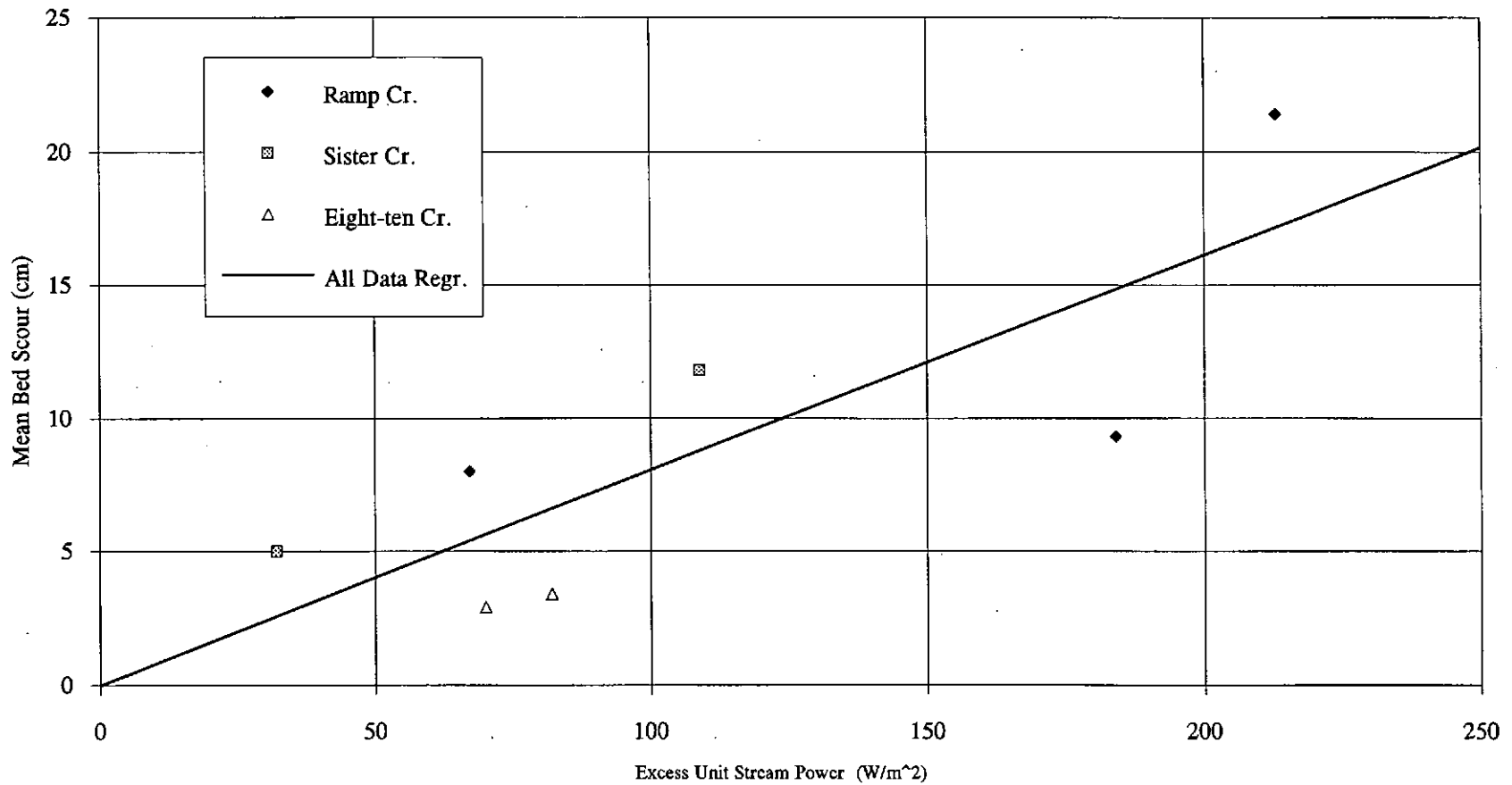


Figure 8: Mean Channel Bed Scour as a Function of Excess Unit Stream Power

two monitored sites.

No formal procedure was used to determine the magnitude of the adjustment. The stochastically-predicted value of  $S$  was reduced by half in the model for the upper portion of the model channel network. This adjustment was based on an alternate, fit-by-eye regression line projected from the origin through the Eight-ten Creek data points in Figure 8. Given such limited data, a more refined adjustment is not justifiable.

The relationships used to predict mean bed scour ( $S$ ) are conservative. Because the data points from Eight-ten Creek decrease the slope of the regression line, the predictive relationship used for the middle and lower portions of the channel network may tend to underestimate  $S$ . In addition, the Monte Carlo procedure produces a substantial number of instances where the predicted value of  $S$  is negative. In these cases,  $S$  is assigned a value of 1 cm. This model "rule" preserves the integrity of the bedload transport threshold of the model by ensuring that  $S$  has a positive value when  $\omega$  is greater than  $\omega_0$ .

Mean Bedload Velocity as a Function of Excess Unit Stream Power. Magnetically-tagged gravel tracers were placed on the surface of the streambed at the beginning of each monitoring season and after streamflow peaks that transported bedload tracers. At the conclusion of each monitoring season, a magnetic-field detector was used to relocate tracers. Groups of tracers (tracer cohorts) placed on the bed at the same time were exposed to the same pattern of streamflows. The travel distance and burial depth of each tracer was determined.

The logarithm of mean travel distance of each cohort was calculated and plotted (Figure 9) against the logarithm of cumulative excess unit stream power ( $\Sigma\omega_e$ ), that is, the sum of peak  $\omega_e$  for all bedload-transporting flow events that occurred while each tracer cohort was in the channel. Tracers that did not move were excluded from calculations of mean travel distance.

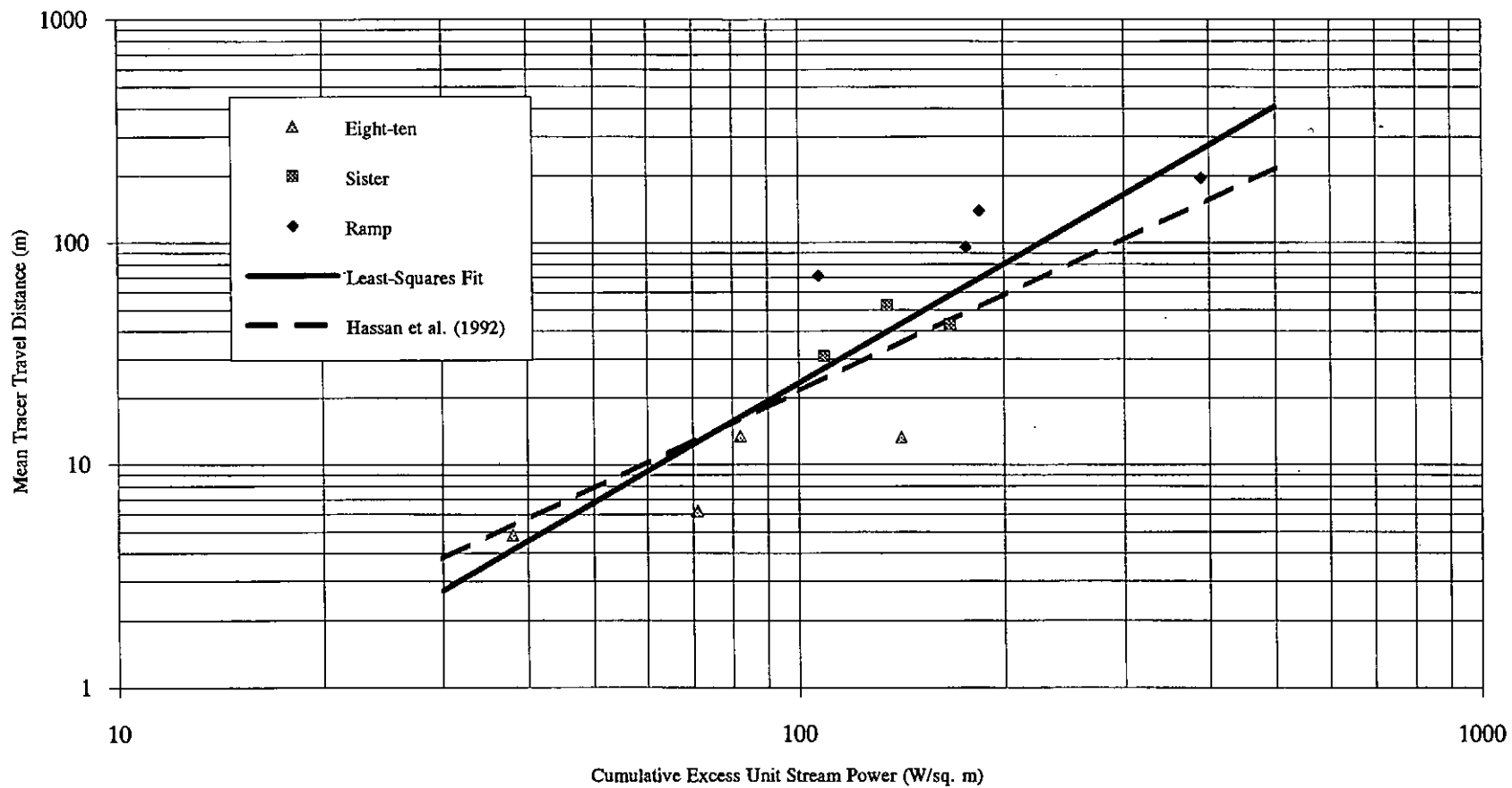


Figure 9: Mean Tracer Travel Distance as a Function of Excess Unit Stream Power

Tracers which did not move comprise fewer than five percent of the total. Unmoved tracers could be categorized into two groups. The first group of unmoved tracers were placed at the margin of the active channel bed, and therefore were not entrained. The second group of unmoved tracers were relatively large-diameter tracers (90 mm or greater).

The latter group reflects the influence of grain size on travel distance and entrainment. Hassan et al. (1992) present evidence that the transport distance of individual sediment grains is only weakly size-dependent and is inversely related to grain size. O'Connor (1993) found that for sediment grains greater than a minimum size, ranging from about 180 to 340 mm diameter depending on stream size, individual sediment grains were likely to be either immobile or weakly-mobile. Hence, although gravel and cobble grains tend to be transported comparable distances, larger particles should have a greater tendency to move short distances or remain immobile, and a few tracers may be expected to remain unmoved. For these reasons, we believe the exclusion of unmoved tracers is reasonable. In any event, given their small numbers, these data would not be expected to have a significant effect.

The predictive relationship between  $\log \Sigma \omega_e$  and  $\log V_b$  was determined for the aggregate data from all streams and cohorts (Table 2). This relationship can be expressed as

$$V_b = 0.00637 (\Sigma \omega_e)^{1.78} \quad (4).$$

Eqn. 4 was used to calculate  $V_b$  in Eqn. 1. These data plot consistently with several data sets analyzed by Hassan et al. (1992), as shown in Figure 9, suggesting that the behavior of tracers at our study sites is comparable to that observed elsewhere.

Although  $\omega_e$ , the independent variable used in the model, and  $\Sigma \omega_e$ , the independent variable in the predictive relationships derived from the field data, are different variables in the

strictest sense, we believe that they are interchangeable for our purposes. A mixture of single- and multiple-streamflow peak data were used.

There is some evidence that mean tracer travel distance from multiple-peak events plots differently than single-event data. Data points for two cohorts that were exposed to all streamflows during the first monitoring season plotted below the best-fit line. In that monitoring season, there was a large, single-peak streamflow event early in the season, and a large, multi-peak period of streamflow late in the season. The first event had a higher peak discharge. This pattern of streamflow suggests that tracers exposed to the first flow may have had a tendency to be buried at a depth below the scour depth of subsequent events, thereby decreasing the mean travel distance.

On the other hand, mean travel distance data collected in the second monitoring season, resulting from a single streamflow peak, plotted very near the best-fit regression line determined by the combined single- and multiple-peak event data. Overall, the evidence suggests that it is reasonable to derive a predictive relationship from the aggregate data from single- and multiple-streamflow peaks. The presumed effect of tracer burial would be to reduce the predicted mean travel distance, making the predictive relationship conservative.

Experimental evidence regarding the burial of gravel tracers subsequent to transport and a simulation model of the process suggests that over the course of many events, tracers become uniformly distributed throughout the depth of the active bed (Hassan and Church 1994). In other words, the behavior of gravel tracers indicates that the active streambed is a well-mixed sediment reservoir. This supports the presumption of Eqn. 1 that the mean travel distance of tracers accurately represents the mean velocity of sediment in the active bed.

Active Bed Width ( $W_{ab}$ ). To determine appropriate values of  $W_{ab}$ , we resurveyed several cross-sections following bedload transport events and measured the active bed width based on comparisons to previous cross-section surveys. These widths were consistent with our observations of tracer deposition and channel changes in locations where no cross-sections were surveyed.

The observed active bed width was at least 60 percent of the bankfull channel width in each channel over the observed range of streamflow (Table 4). In the two larger channels, the observed active bed width deviated from bankfull channel width by only 10 percent.

TABLE 4: OBSERVED BANKFULL CHANNEL AND ACTIVE BED WIDTH

<u>Stream</u>	<u>Bankfull Width (m)</u>	<u>Active Width (m)</u>	<u>Std. Error (m)</u>
Eight-ten	3.3	2.0	0.1
Sister	2.8	2.5	0.2
Ramp	4.1	4.3	0.4

Active bed width during the largest flows which could occur remains unknown, but is likely to be equal to the channel width. A predictive relationship between active bed width and streamflow could not be defined from available data. The potential variation in active bed width relative to channel width is small relative to potential variation in  $V_b$  and  $S$  in large storms. The observed active bed widths were chosen to represent  $W_{ab}$  in Eqn. 1. For Ramp Creek, where the observed active width was greater than bankfull width, bankfull width was used. Use of observed active width, as opposed to bankfull width, may tend to underestimate  $Q_b$  from Eqn. 1, making the sediment transport model conservative.

Calculating Bedload Transport. As described above, bedload transport for a storm event was calculated according to

$$Q_b = V_b S W_{ab} (1-P) \quad (1).$$

The first two factors in Eqn. 1,  $V_b$  and  $S$ , were calculated, ultimately, as a function of  $P_{24}$ .  $W_{ab}$  was taken as a constant for each channel. The porosity ( $P$ ) of the bed material in the monitored streams was measured in bulk samples and averaged 0.19; we rounded this value to 0.2. Thus, the output of the bedload model was volumetric and adjusted for porosity so that the transport rate could be easily converted to units of mass.

## SEDIMENT ROUTING MODEL

### Model Overview

The routing model characterizes bedload dynamics in an hypothetical channel network composed of two 200-m reaches in the upper portion of second-order channels, one 300-m reach of lower second-order channel, and one 300-m reach of third-order channel (Figure 10). The model channel network thus contains 1 km of channel and drains a watershed of about 1.1 km<sup>2</sup>.

The model is governed by mass balance. Sediment outputs from each model reach become inputs to reaches downstream, adding to creep inputs of sediment. First-order stream channels were not modeled. These intermittent and ephemeral channels would add about 7 km of channel length to the model channel network. The implications of excluding first order channels from the model is discussed later.

The routing model is simple. Bedload transport capacity is determined by random selection of annual bedload from the distributions developed in the transport model. In 60 annual time-steps, the model generates random creep inputs, sorts these sediment inputs into bedload and suspended load, calculates attrition of bedload, generates random formation and failure of LOD dams under two scenarios of initial density of LOD dams and three scenarios of availability of LOD, routes sediment volumes downstream according to sediment availability and transport capacity, and calculates annual sediment yield.

In keeping with the stochastic character of the model, results are presented as probability distributions. Each model run generated 100 60-year routing intervals, each run being driven by a different set of random bedload transport capacities from the transport model. The central tendencies of these output distributions are later used to assess the sensitivity of bedload yield to LOD dam dynamics. Model outputs are calculated for bedload. Changes in the number of LOD dams are also produced.

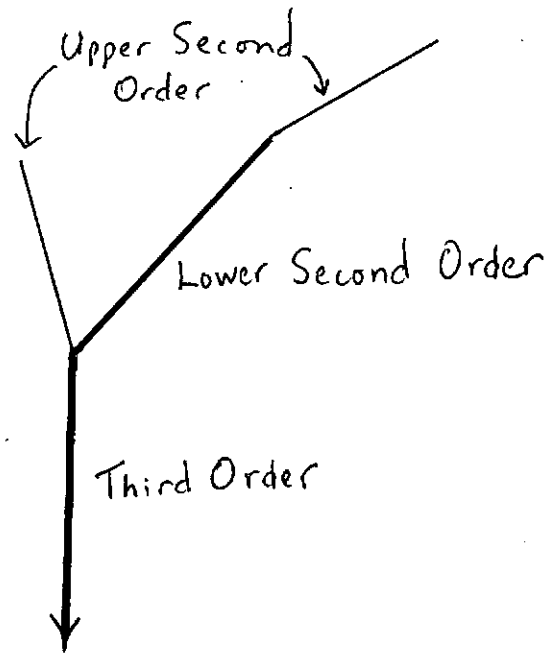


Figure 10: Hypothetical Channel Network for Sediment Routing Model

In the following section, the conceptual model which guided the development of the routing model is discussed first. Second, we discuss the geometry of sediment reservoirs which was used to determine the quantities of bedload potentially in storage. Finally, we describe the routing model in detail.

### Conceptual Model of Fluvial Sediment Transport for Low-Order Streams

The following conceptual model draws on the model described by MacDonald and Ritland (1989), but was more carefully constructed to support a quantitative model for routing of fluvial sediment in low-order channels. The key conceptual elements of the model are described here with additional details described later in the report.

Key Model Elements. Like MacDonald and Ritland, we considered the channel bed as the source of bedload sediment for transport. We also required that stream discharge exceed a threshold for entrainment of bed material as a necessary condition for sediment routing through the channel.

Our model also included sediment input to channels via creep processes and a simple sediment-sorting function to separate bedload from suspended load as it entered the channel from the hillslope. Our model also simulated the decay and creation of LOD dams, enabling us to move sediment between active and semi-active sediment storage sites (i.e. sediment reservoirs) on the channel bed.

Sediment Reservoir Definition. Readily-transportable sediment is stored in the channel bed near the surface, extending to a depth defined by scour of the bed. Given sufficient streamflows the sediment stored in this surface reservoir, which we call the detention reservoir, is entrained and transported.

Conceptually, the detention reservoir is defined by sediment entrainment. Because entrainment is expected to be a function of streamflow, the size of the detention reservoir is expected to

vary with flood magnitude. The lower size-limit of the detention reservoir is conceived as that portion of the channel bed which is entrained during flows just large enough to entrain the coarse surface pavement of the streambed. The upper size-limit of the detention reservoir is conceived as that portion of the channel bed entrained during lower-frequency, higher-magnitude floods large enough to achieve maximum scour of the channel bed.

Sediment storage upstream of channel obstructions, particularly LOD dams, is common. Cobble and boulder obstructions are less effective sediment storage sites. We have chosen to neglect cobble and boulder obstructions in the routing model, focusing instead on LOD dams.

Conceptually, the surface layer of sediment stored upstream of LOD dams is in the detention reservoir. Sediment stored upstream of obstructions at a depth below the zone of scour and fill is in the retention reservoir. Sediment in the retention reservoir cannot be transported by fluvial processes until the channel obstruction erodes, decays or otherwise fails.

Sediment Reservoir Geometry. The two-dimensional geometry of retention and detention reservoirs as conceived above can be defined as a function of valley slope ( $\alpha$ ), channel bed slope ( $\beta$ ), and obstruction height ( $h$ ) (Figure 11). This geometry defined reservoir volumes in the routing model. The length ( $L$ ) of the sediment reservoirs in Figure 10 is needed to derive of the formulae below, but drops from the reduced equations. The values of  $\alpha$  and  $h$  determine  $L$  as

$$L = h / \alpha \quad (5).$$

When slope is expressed as a fraction (i.e. vertical drop divided by horizontal length), the trigonometric function  $\tan \alpha$  equals  $\alpha$ .

The volume per unit width of the detention reservoir ( $D$ ) associated with one obstruction is

$$D = (\beta/2) (h/\alpha)^2 \quad (6)$$

where slope is expressed as a fraction. Eqn. 6 was derived from

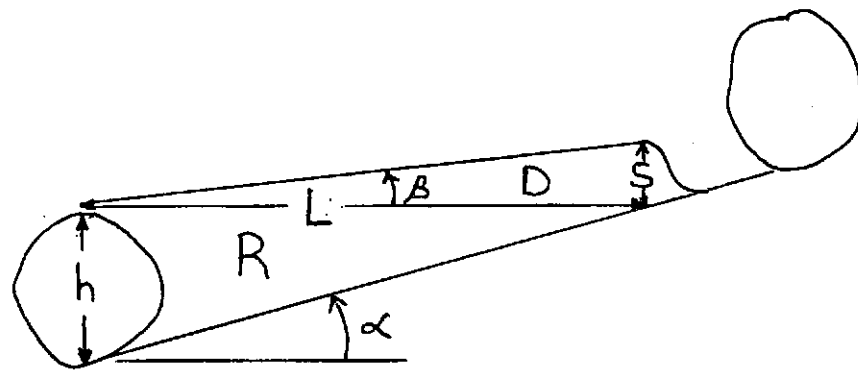


Figure 11: Hypothetical Two-dimensional Geometry of LOD Dam Sediment Reservoirs

the area of the triangle formed by L and S in Figure 11, where

$$S = \beta h / \alpha \quad (7)$$

Equation 7 follows from the fact that S equals L tan  $\beta$  and substitution of Eqn. 5 for L. Reservoir volume was calculated by multiplying unit volume by channel width.

This geometry approximated the scour-dependent variable thickness of the detention reservoir as the difference between the bed surface and a line (L in Figure 11) with zero slope extending upstream from the lip of the obstruction. This approximation was both convenient and reasonable. The level base line represents a slope gradient of zero when the bed surface is congruent with the base line, and implies that no stream energy is available for sediment transport. This condition defines an empty detention reservoir. The level base line also partitions the detention and retention reservoirs.

The zero-slope base line (L in Figure 11) defines the upper boundary of the retention reservoir. The retention reservoir volume (R) is calculated as

$$R = h^2 / 2\alpha \quad (8)$$

for a reservoir of unit width. Eqn. 8 was derived from the formula for the area of the triangle defined by h and L in Figure 10 where Eqn. 5 substitutes for L.

Equations 6 and 8 quantify the potential sediment storage associated with LOD dams. These two equations would suffice if the stream channels in the model contained the maximum density of LOD dams, that is, LOD dams placed at intervals of length L (Figure 11). When LOD density is below the maximum, sediment may be stored in channel segments located downstream of an LOD dam by a distance greater than L from the next LOD dam downstream. Sediment in these inter-dam areas is defined to be in the detention reservoir. The average depth of sediment in these areas is assumed to be one-half S, the same depth defined for detention storage associated with an LOD dam. Because the

average depth of the detention reservoir is uniform, total sediment storage potential per unit width in the detention reservoir is simply the product of reach length and one-half  $S$ .

The model geometry approximates the maximum depth of the detention reservoir as  $S$  (Eqn. 7). Conceptually,  $S$  is equivalent to maximum scour depth. Field data for scour depth are consistent with  $S$  (0.33 m), as defined by Eqn. 7 and the values of  $h$ ,  $\alpha$ , and  $\beta$  selected for use in the routing model (Table 5). Maximum observed scour depth for the three monitoring sites ranged from 0.25 m to 0.35 m. Mean scour depth associated with different peak flows in different streams ranged from less than 0.03 m to greater than 0.21 m. The grand mean scour depth was 0.09 m. The mean depth of the detention reservoir in the model is 0.17 m. These field data suggest that the model of LOD dams and sediment-storage reservoirs is scaled appropriately.

Despite the general agreement between observed scour and the geometrically-determined scour depth, field observations of scour indicate that the model reservoir is a significant simplification. In some locations, scour caused by large roughness elements was observed to extend far below the line dividing the detention and retention reservoirs. If scour extends into the geometrically-defined retention reservoir, the conceptual distinction between the retention and detention reservoirs is lost. In other words, when LOD dams have a height less than or equal to the scour depth, there is no retention reservoir. Sediment stored in the retention reservoir of LOD dams defined by the geometry of Figure 11 would be improperly classified for purposes of sediment routing in the model.

To reduce the potential for overestimating retention reservoir storage in the model according to the reasoning above, LOD dams less than 0.4 m high were ignored. This dam height was selected because maximum observed scour depths were at least 0.35 m and LOD dam heights were measured to the nearest 0.1 m.

Imposing a minimum dam height influenced the interpretation of field data regarding LOD dam density and dynamics by eliminating smaller dams from the data set.

Interaction of Sediment Reservoirs. Sediment in the retention reservoir interacts with sediment in the detention reservoir if a new LOD dam forms, in which case sediment in the detention reservoir is captured by the retention reservoir when a competent streamflow occurs. If an existing LOD dam fails, sediment from the retention reservoir is released to the detention reservoir for subsequent transport. The two sediment reservoirs are treated as the sum of discrete reservoir units distributed throughout a modeled channel reach.

Dynamics of LOD Dams. Three key research findings regarding the dynamics and density of LOD in stream channels influenced the simulation of the dynamics of LOD dams in the routing model. First, logging may significantly affect input rates of LOD to stream channels, in some cases doubling the density of LOD (e.g. Froehlich 1973). Second, a period of 60 years of forest regrowth is required prior to resumption of significant inputs of coniferous LOD to stream channels (e.g. Andrus et al. 1988). Third, the turnover time (i.e., standing crop divided by input rate) for LOD in two stream channels less than 1 km<sup>2</sup> in the Oregon Cascades averaged 59.5 years (Lienkaemper and Swanson 1987).

The average turnover time suggests that in-channel supplies of LOD would be exhausted at about the same time that second-growth conifers begin to contribute LOD to the channel. Therefore, a 60-year modelling period for the simulation of bedload routing is appropriate.

The model simulates, albeit crudely, the influence of input rates of LOD on formation rates of LOD dams. The model assumes that the likelihood of formation of LOD dams is proportional to density of LOD. It is also assumed that steady input rates of

LOD to the channel are required to maintain an approximately constant density of LOD dams.

In one of the three model scenarios simulating dynamics of LOD dams, it was assumed that formation rates of LOD dams increased for 10 years after logging. This scenario simulates potential changes in formation rates of LOD dams in response to a rapid increase in density of LOD.

The model assumes that logging may reduce or eliminate inputs of LOD from riparian zones for a period of at least 60 years, and that formation rates of LOD dams would decline in response to declining inputs of LOD. Formation rates of LOD dams decline gradually in the scenarios simulating the effects of logging. The gradual decline of LOD dams simulates the expectation that LOD already in or near the channel, and LOD entering the channel as the result of logging, would contribute to the formation of new LOD dams. In addition, LOD from dams that fail would remain in the channel and could contribute to the formation of new dams.

Hillslope Sediment Inputs to the Fluvial System. Soil creep processes deliver sediment to the channel. This sediment is sorted as it enters the channel and is routed through the reservoir system. Sediment from small landslides which create thin sediment deposits are processed like soil creep. These sediment input processes are considered in our model. Potential changes in the rate of creep processes caused by logging are not incorporated in the simulation.

Sediment deposited by a landslide or debris flow often overwhelms the local transport capacity of the stream. Sediment in pre-existing detention and retention reservoirs may be buried and placed in a long-term storage reservoir mobilized only by debris flow. When such thick deposits create a new channel surface, the stream erodes and sorts the surface of the new deposit and new detention and retention reservoirs form. These

massive sediment input processes are excluded from our model. As shall be discussed later, the model provides insights regarding fluvial transport of sediment deposited by large mass wasting events.

Sediment Sorting. Fluvial transport processes sort sediment entering the channel into suspended load and bedload according to grain size. Fine sediment, roughly less than 1 mm diameter, is transported in suspension and leaves the channel rapidly. Consequently, storage of sediment less than 1 mm in the detention and retention reservoirs is expected to be negligible.

Data on the grain size distribution of suspended load from monitoring sites suggested that material finer than 1 mm was transported in suspension. Storage of suspended load sediments in the channel bed was small. In nine bulk samples of bed material from the monitoring sites, sediment finer than 1 mm comprised an average of 11.1 percent of the bed material. Typical grain size distributions of soils in the field area indicate that of the sediment entering stream channels via creep processes, roughly 30 percent is finer than 1 mm. These data suggest that fluvial processes are selectively transporting fine-grained sediment. Sediment finer than 1 mm is treated as suspended load in the model and is routed out of the channel system without any intermediate storage. This simplification of the model discounts infiltration of suspended sediment into the channel bed.

Additional suspended load is generated from bedload sediment. When bedload is transported, it is abraded and fragmented, producing fine-grained sediment which adds to the suspended load. Bedload volume is reduced correspondingly.

Bedload Transport. Sediment stored in the detention and retention reservoirs is transported as bedload. The sediment stored in these reservoirs is primarily gravel (2 to 64 mm diameter). In the three monitoring sites, about 70 percent of

the mass of bulk sediment samples was in the gravel size-class. Sand (finer than 2 mm) and cobbles (greater than 64 mm) compose the remainder of sediment in the streambed reservoirs. The model assumes that all bedload sediment moves at the same average velocity, regardless of size.

Although an analysis of travel distance of gravel tracers showed a weak inverse relationship between grain size and travel distance, Hassan and Church (1992) described the effect of grain size on travel distance as a second-order effect that could be ignored for practical purposes. Hassan and Church (1992) present data indicating that a single mean transport rate is representative for tracers between roughly 30 and 100 mm. Grains finer than about 30 mm had a higher mean transport rate, and cobbles coarser than about 100 mm had a lower mean transport rate. In our study, no relationship was found between tracer diameter and travel distance for tracers 25 to 120 mm diameter.

It is likely that mean bedload velocity has been underestimated in this study. The fraction of gravel finer than about 30 mm is likely to have a greater mean velocity than the fraction coarser than 30 mm. Few of the tracers used in this study were less than 30 mm diameter, hence the higher-velocity grains are under-represented in the sample population of bedload from which mean bedload velocity was estimated. The model is therefore conservative with respect to bedload transport rates.

Previous analyses (O'Connor 1993) of the monitoring sites in this study showed that sediment coarser than about 180 mm in the second-order channels and about 340 mm in the third-order channel are weakly-mobile. These large-diameter grains tend to accumulate in bedforms that resist erosion and are unlikely to be routed out of the channel by fluvial processes during the 60-year modelling period. This material is ignored in the model, which addresses routing of sediment by fluvial processes. These sediment sizes were among the coarsest 10 percent of the surface

grain size distributions for these channels, and were not represented in bulk samples. Excluding these size classes from the routing model is not expected to have a significant effect on the accuracy of the model.

Summarizing the sediment sorting function used in the model, there are three grain size classes that manifest the fluvial sediment sorting process. Clay, silt and fine sand less than 1 mm diameter are transported primarily in suspension and are effectively absent from the detention and retention reservoirs. Sand, gravel and cobbles between about 1 and 180 mm diameter are transported as bedload and comprise the mass contained in the detention and retention reservoirs. Boulders and cobbles coarser than about 180 mm diameter are considered immobile.

#### Components of the Routing Model.

Channel and Reservoir Geometry. Five constants determine the quantities of sediment in storage in the model channels. These are the channel length and width, the mean height of LOD dams ( $h$ ), valley slope ( $\alpha$ ), and channel bed surface slope ( $\beta$ ). The values used in the model are given in Table 5.

Representative values of channel length and width were selected based on field observations. LOD dam height was taken as the median of the distribution of observed dam heights  $\geq 0.4$  m in six Olympic Peninsula streams (Figure 12). The slope  $\alpha$  (0.15) was the mean of the three monitored reaches. The slope  $\beta$  (0.07) was the percentile of the distribution of bed slopes upstream of LOD dams in the three monitored reaches at which 90 percent of bed slopes were gentler.

The relatively high value for  $\beta$  was chosen to allow the detention reservoir to accommodate a greater volume of sediment. This would allow sediment to accumulate in the detention reservoir when transport capacity is low without violating the geometrically-defined storage capacity. The choice of  $\beta$  proved

Table 5: Geometry of Hypothetical Channels in Routing Model

Parameter	Upper 2nd Order	Lower 2nd Order	3rd Order
Length (m)	200	300	300
Width (m)	2.5	3.0	4.0
h (m)	0.7	0.7	0.7
$\alpha$	0.15	0.15	0.15
$\beta$	0.07	0.07	0.07
Dam Detention Volume <sup>1</sup> (m <sup>3</sup> )	1.52	1.83	2.44
Dam Retention Volume <sup>2</sup> (m <sup>3</sup> )	3.27	3.92	5.23
Maximum Scour Depth (m)	0.33	0.33	0.33

Notes:

1. Volume of sediment only, calculated as reservoir volume minus 20 percent void space according to Eqn. 6 (see text).
2. Volume of sediment only, calculated as reservoir volume minus 20 percent void space according to Eqn. 8 (see text).

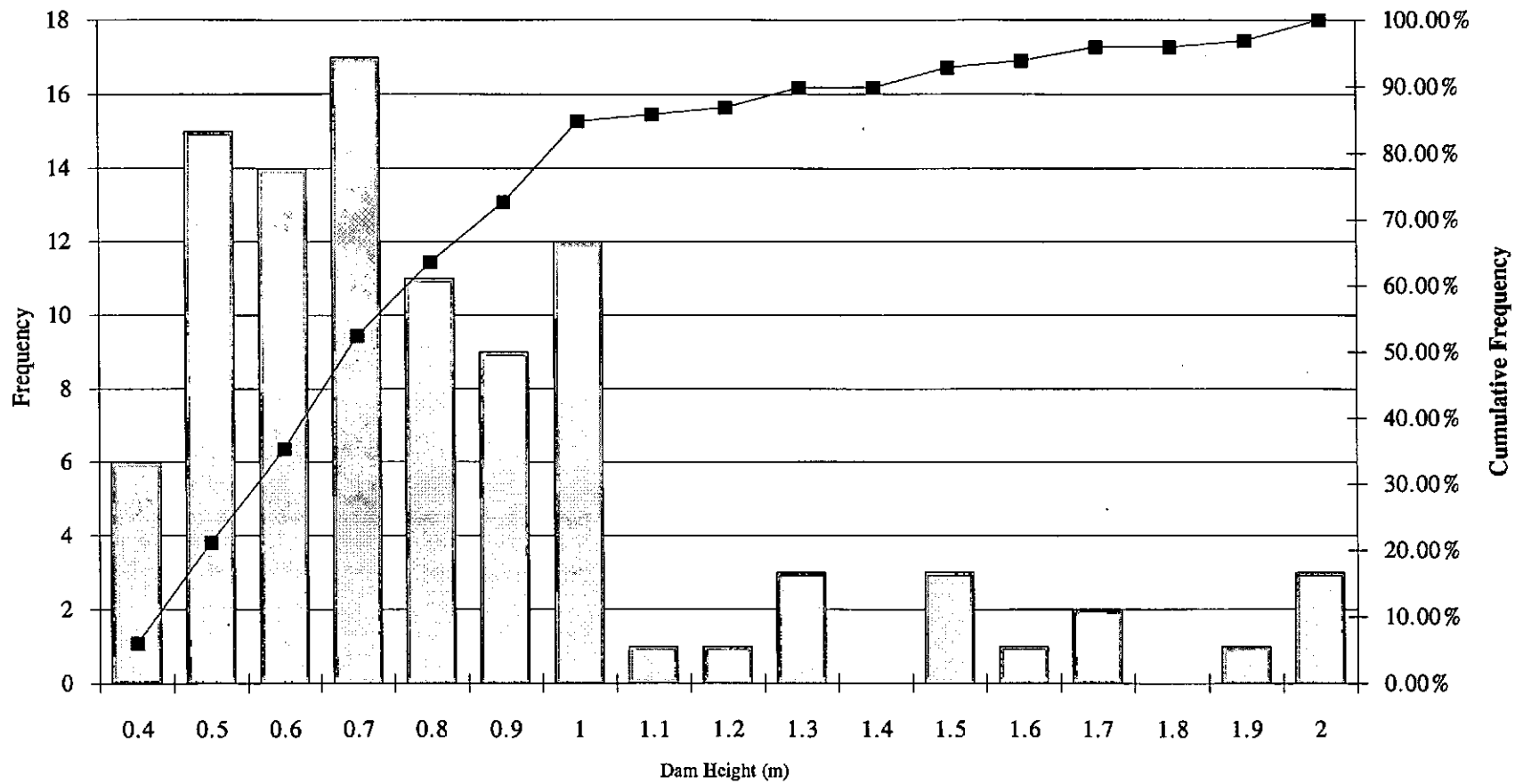


Figure 12: Frequency Distribution of Height of LOD Dams, Olympic Peninsula

to be of little consequence because transport capacity was much greater than detention reservoir storage, and accumulations of sediment determined by mass balance never threatened to exceed the geometrically-defined storage capacity.

Sediment Inputs By Soil Creep Processes. Detailed data on creep rates in undisturbed headwater streams on the western Olympic Peninsula were collected by Reid (1981) in watersheds with annual precipitation and geologic and geomorphic characteristics similar to those of our monitoring sites. Reid's data were collected in drainages where logging had not occurred; they are the best data available for regional creep rates.

We based our model creep rates on Reid's data, despite the fact that our monitoring sites were disturbed by logging and the likelihood that post-logging creep rates would be greater than those she measured. Although creep rates may be underestimated in the model, we reasoned it was better to use conservative, well-founded estimates for creep inputs. Moreover, the main objective was to assess the influence of LOD dams on bedload routing. To achieve this objective, it was necessary only to estimate creep rates to the appropriate order of magnitude.

Reid summarizes her data by giving low, mean, and high range estimates for volumetric creep inputs per kilometer of channel length per year. We used the differences between Reid's low and high range estimates and mean estimate to estimate the standard deviation of her data as  $3.1 \text{ m}^3/\text{channel-km/yr}$ . The mean estimate of creep was  $7.5 \text{ m}^3/\text{channel-km/yr}$ . The mean and standard deviation were used to input random normal annual creep rates to the model stream channels. Although it is likely that annual creep rates are linked to annual climatic variation, we elected to determine random inputs from creep processes independently of the simulated climatic variation that drives sediment transport in the routing model.

Sorting of Sediment Inputs by Fluvial Processes. Inputs of sediment via creep processes were sorted into bedload and suspended load. Typical grain size distributions for the soils in the field area (USDA Soil Conservation Service 1987) indicated that roughly 70 percent of hillslope sediments were coarser than 1 mm. Therefore, 70 percent of sediment inputs were assumed to enter the sediment reservoirs of the channel bed. The remaining 30 percent of sediment input via creep was assumed to be suspended load.

Creep inputs of hillslope sediment were assumed to have a density of 1 tonne/m<sup>3</sup>. As hillslope sediment enters the channel and becomes bed material, a volumetric conversion is made based on bed material density of 2.1 tonnes/m<sup>3</sup>. Accounting for sorting and changes in bulk density, 1 m<sup>3</sup> of creep inputs generates 0.33 m<sup>3</sup> of bed material. Suspended load material routed from the channel system is calculated in units of mass; since this material is never incorporated in the model channel bed, no density conversion is necessary. Each cubic meter of sediment input via creep processes generates 0.3 tonnes of suspended load.

Attrition of Bedload. Abrasion and fragmentation of bedload in transport generates suspended-load sediment, a process called bedload attrition. Tumbling mill experiments (Perkins 1988, Collins and Dunne 1989) have been used to quantify attrition as a function of simulated bedload travel distance. In these studies, it was assumed that grains finer than 0.5 mm were transported in suspension. The reduction of mass of grains coarser than 0.5 mm was measured in these experiments to determine attrition of bedload to suspended load.

In the tributary systems we studied, monitoring data suggested that grains finer than 1 mm were typically transported in suspension. The attrition rates reported by Perkins (1988) and Collins and Dunne (1989) applied to our channel system underestimated bedload attrition because of the discrepancy

between maximum suspended load grain size. The production of suspended load by bedload attrition was somewhat underestimated in our model. This bias is expected to slightly increase the quantity of bedload in the model's sediment storage reservoirs.

We calculated attrition rates for three colluvial materials (Collins and Dunne 1989, Perkins 1988) for travel distances ranging from 0.1 to 0.8 km, and then averaged the attrition rates for the three materials (Table 6). The first 0.1 km of travel reduced bedload-size sediment by 6.6 percent. After 0.8 km of travel, reduction of an additional 1.3 percent of the original material occurred, totalling 7.9 percent. These calculations suggest that most bedload attrition occurs immediately after new hillslope material enters the channel.

For simplicity, we accounted for bedload attrition as material entered the channel by reducing bedload by 7 percent and adding an equivalent quantity to suspended load. Other possible accounting methods would have been complex, difficult to justify, and fruitless given that attrition proved to have a minor influence on sediment yields predicted by the model.

Random Variation in Bedload Transport Capacity. The transport model simulates the stochastic nature of climatic variability and its effect on streamflow and bedload transport capacity. The probability distributions generated by the transport model were critical elements of the routing model. In the routing model, the effect of annual climatic conditions on bedload transport capacity was based on the cumulative frequency distributions of bedload transport from the transport model. A random number between 0 and 1 was drawn from a uniform distribution for each year. The random number between 0 and 1 was compared to the cumulative frequency distributions of bedload transport predicted by the transport model and the annual bedload transport capacity corresponding to the random number was selected. The random number 0.5 was equivalent to a 2-year

Table 6: Calculation of Bedload Attrition Rates

Material	Po	k	P (0.1 km)	P (0.2 km)	P (0.3 km)	P (0.5 km)	P (0.8 km)
Alpine outwash 1	0.905	-0.0143	0.903	0.902	0.900	0.897	0.892
Alpine outwash 2	0.972	-0.0168	0.970	0.968	0.966	0.962	0.956
Basaltic colluvium	0.93	-0.0171	0.928	0.926	0.924	0.920	0.914
<b>Mean</b>	--	--	0.934	0.932	0.930	0.926	0.921

**Notes:**

1.  $P = P_o \exp(kt)$
2. 1 km. travel distance is equivalent to 0.8 hr of travel time
3. After Collins and Dunne, 1989.

recurrence interval, 0.9 was equivalent to a 10-year recurrence interval, 0.95 was equivalent to a 20-year recurrence interval, and so on.

Initial Density of LOD Dams. The initial number of debris dams in each modeled channel was derived from observed density of LOD dams in steep, narrow headwater streams with drainage areas less than 2 km<sup>2</sup> in the western Olympic Peninsula and in northern California (Figure 13, Table 7). LOD dams that appeared to be stable, long-lived stream features were classified separately. The chief classification criteria were whether dams contained unusually large-diameter logs or rootwads, and whether these structural elements were keyed into the streambed or banks.

Stable LOD dams were assumed to be unlikely to fail. In the routing model, the significance of stable LOD dams was that their density served as an estimate of the minimum density likely to remain in a channel after less stable LOD dams failed. The median of observed density of stable LOD dams for the available data was 3.3 per 100 m. We used a density of 3 dams per 100 m as the minimum allowed density. This minimum was a lower limit below which random fluctuations of density of LOD dams was not allowed.

An upper limit to density of LOD dams was also used to constrain the random fluctuation of LOD dams. This maximum density of LOD dams was determined from the model channel geometry (Figure 11). The length of retention reservoirs (L) was calculated and divided into the reach length, giving the maximum number of non-overlapping LOD dam/retention reservoir complexes. This number was used as the maximum number of LOD dams.

Given the range of observed density of LOD dams (Figure 13) and the hypothesized sensitivity of bedload yield to dynamics of LOD dams, two initial LOD dam scenarios were tested. In the "high" density scenario, the initial density was 15 per 100 m of stream channel. The "typical" density scenario used an initial

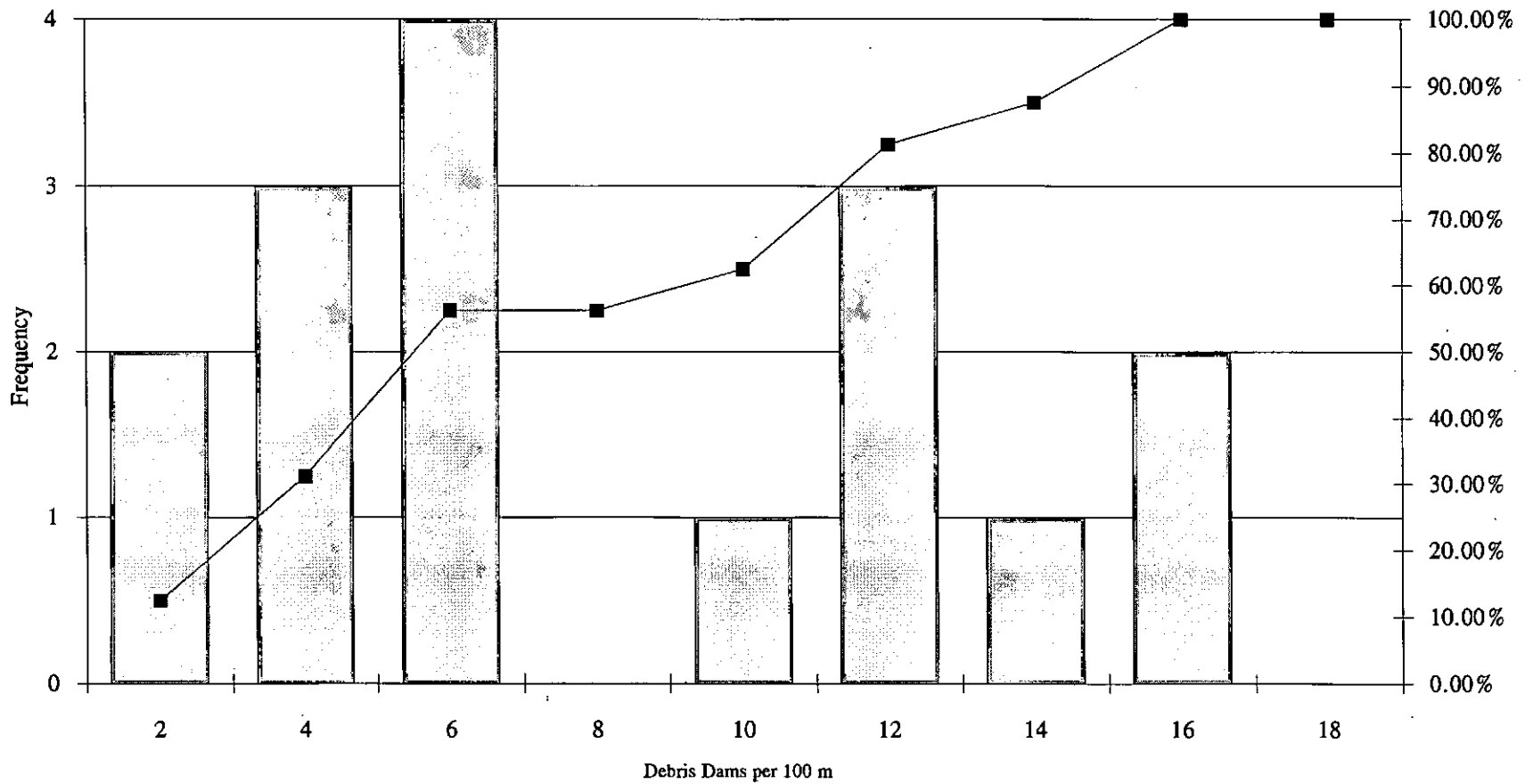


Figure 13: Frequency Distribution of Density of LOD Dams from 16 Streams

Table 7: Debris Dam Density Observations, Western North America

Stream	Region	Known Disturbance	Drainage Area (sq. km)	Bankfull Width (m)	Length Surveyed (m)	Debris Dams per 100 m	Key Debris Dams per 100 m
East Fork Indian	Klamath Mtns.	none	1.2	2.7	200	12.5	7.5
Upper Four Bit	Klamath Mtns.	none	0.7	2.8	200	12.0	7.0
Upper Two Bit	Klamath Mtns.	none	0.7	2.3	180	13.9	4.4
West Fork Indian	Klamath Mtns.	L(6)	1.8	3.2	200	7.0	4.9
Lower Four Bit	Klamath Mtns.	L(13)	1.1	2.7	200	7.5	3.0
Lower Two Bit	Klamath Mtns.	L(13), DF(3?)	1.2	2.0	180	6.7	1.7
New York Trib	Northern Sierra	L(11)	0.9	2.4	200	17.5	9.0
Upper Taylor	Northern Sierra	none	1.2	3.0	200	6.5	1.5
Empire Trib	Northern Sierra	none	0.8	---	200	10.5	---
West Twin	Olympic Peninsula	none	0.6	4.3	355	3.4	1.4
Lower Sister	Olympic Peninsula	F,L (35+)	0.53	2.8	230	17.4	5.7
Upper Sister	Olympic Peninsula	F,L (35+)	0.45	2.3	150	15.3	4
Eight-ten	Olympic Peninsula	L(< 10),DF(1)	0.31	3.3	140	5	3.6
Upper Ramp	Olympic Peninsula	L(< 10),DF(1)	1.12	4.3	230	3.9	2.6
Lower Ramp	Olympic Peninsula	L(< 10),DF(1)	2	6.1	250	1.2	1.2
Two-try	Olympic Peninsula	F,L(35+),DF(30)	0.36	2.9	430	4.7	2.1
Washout	Olympic Peninsula	DF(> 10)	0.47	3.5	250	4.4	2.8

Notes:

1. L = logging
2. DF = debris flow
3. F = wildfire
4. (#) = # years since disturbance

dam density equal to the median of observed density (Figure 13), 8 per 100 m of stream channel. In the "high" scenario, an 80 percent decline in dam density was possible (15 initial dams less three dams minimum, leaving 12 dams). In the "typical" scenario, an 62.5 percent decline was possible.

Annual Variation of Density of LOD Dams. Model variation of density of LOD dams was based on observed short-term variation in three streams (Table 8). Annual changes in the number of dams at least 0.4 m high were recorded on channel maps. Although a two-year record for three streams is rather short to serve as the basis for simulation of long-term dam dynamics, these data were drawn from the field area and were accurate. Moreover, no other accurate data are available. Assuming that a longer monitoring period would include higher peak streamflow, it is possible that the available two-year record underestimates the frequency of dam failure and formation. However, fragmentary data from a series of relatively large storms during the winter of 1990/91 did not appear to produce a much larger number of dam failures.

Based on the data in Table 8, the probability of any single dam failing in any year was estimated to be 0.0356. The complementary probability of any single dam remaining stable in any year was 0.9644. Each model LOD dam must either remain stable or fail in each model year. The preceding probabilities were calculated as the mean of two-year probabilities for each channel weighted by the initial number of dams in each channel.

New LOD dams may also form. This probability was again estimated by the weighted mean for the three monitored channels. The estimated probability of new dam formation, 0.0360, was calculated independently from the fail/stable probability. Probability of dam formation was defined as the fraction of new dams formed relative to existing dams.

In the model, formation of new dams was stochastically simulated. For each existing LOD dam, a new LOD dam formed with

Table 8: Observed LOD Dam Dynamics, 1991-1993

Dam Status	1991-1992		1992-1993		Mean
<u>Eight-ten Cr.</u>					
Stable	7/7 <sup>a</sup>	(1.0) <sup>b</sup>	7/7	(1.0)	(1.0)
Failed	0/7	(0.0)	0/7	(0.0)	(0.0)
New	0/7	(0.0) <sup>c</sup>	0/7	(0.0)	(0.0)
<u>Sister Cr.</u>					
Stable	37/40	(0.925)	39/39	(1.0)	(0.9625)
Failed	3/40	(0.075)	0/39	(0.0)	(0.0375)
New	2/40	(0.05)	1/39	(0.026)	(0.038)
<u>Ramp Cr.</u>					
Stable	8/9	(0.89)	10/10	(1.0)	(0.945)
Failed	1/9	(0.11)	0/10	(0.0)	(0.055)
New	1/9	(0.11)	0/10	(0.0)	(0.055)
<u>Weighted Mean Probability<sup>d</sup></u>					
Stable					(0.9644)
Failed					(0.0356)
New					(0.0360)

Notes:

- a. Fractional representation (e.g. #1/#2) where #1 is final number of dams of that status and #2 is initial number of dams.
- b. Probability of a dam's status at the end of the year; the ratio of #1 to #2.
- c. Proportion of new dams formed relative to the initial number of dams.
- d. Weighting of means was in proportion to the initial number of dams in 1991

a frequency of 0.036. Consequently, the number of new dams formed would tend to increase as the number of dams increases. The converse would also be expected--fewer new dams formed as the number of dams decrease. This probability structure for new dam formation mimics natural LOD dam-forming processes in that LOD entering the channel from the riparian zone or LOD from failed LOD dams moving in the channel when LOD accumulations already exist. In other words, the likelihood of formation of an LOD dam is proportional to density of LOD.

Steady-State Scenario. The probabilities above formed the basis for the "steady-state" scenario for dynamics of LOD dams. In the steady-state scenario, the probabilities were held constant. Since the probability of formation of new LOD dams was slightly greater than the probability of LOD dam failure, an approximate steady-state condition was expected.

Two additional scenarios were tested in the model: "increasing-decreasing" and "decreasing". In all three scenarios, the fail/stable probabilities remain constant throughout the 60-year model runs. Hence, differences between the scenarios was modulated by the probability of LOD dam formation.

Increasing-Decreasing Scenario. In the "increasing-decreasing" scenario, the probability of LOD dam formation is initially doubled, then gradually declines to the nominal probability in year 11 (Figure 14). From year 11 to year 20, the probability remains constant. From year 21 through year 60, the probability gradually declines to 0.005.

The initial decade of a high probability of forming LOD dams simulated the possibility of high rates of LOD recruitment associated with timber harvest (e.g. incidental breakage of felled trees near channels, disposal of slash, etc.) Subsequent decades of diminishing probability of formation of new LOD dams occur through the balance of the period, during which LOD inputs

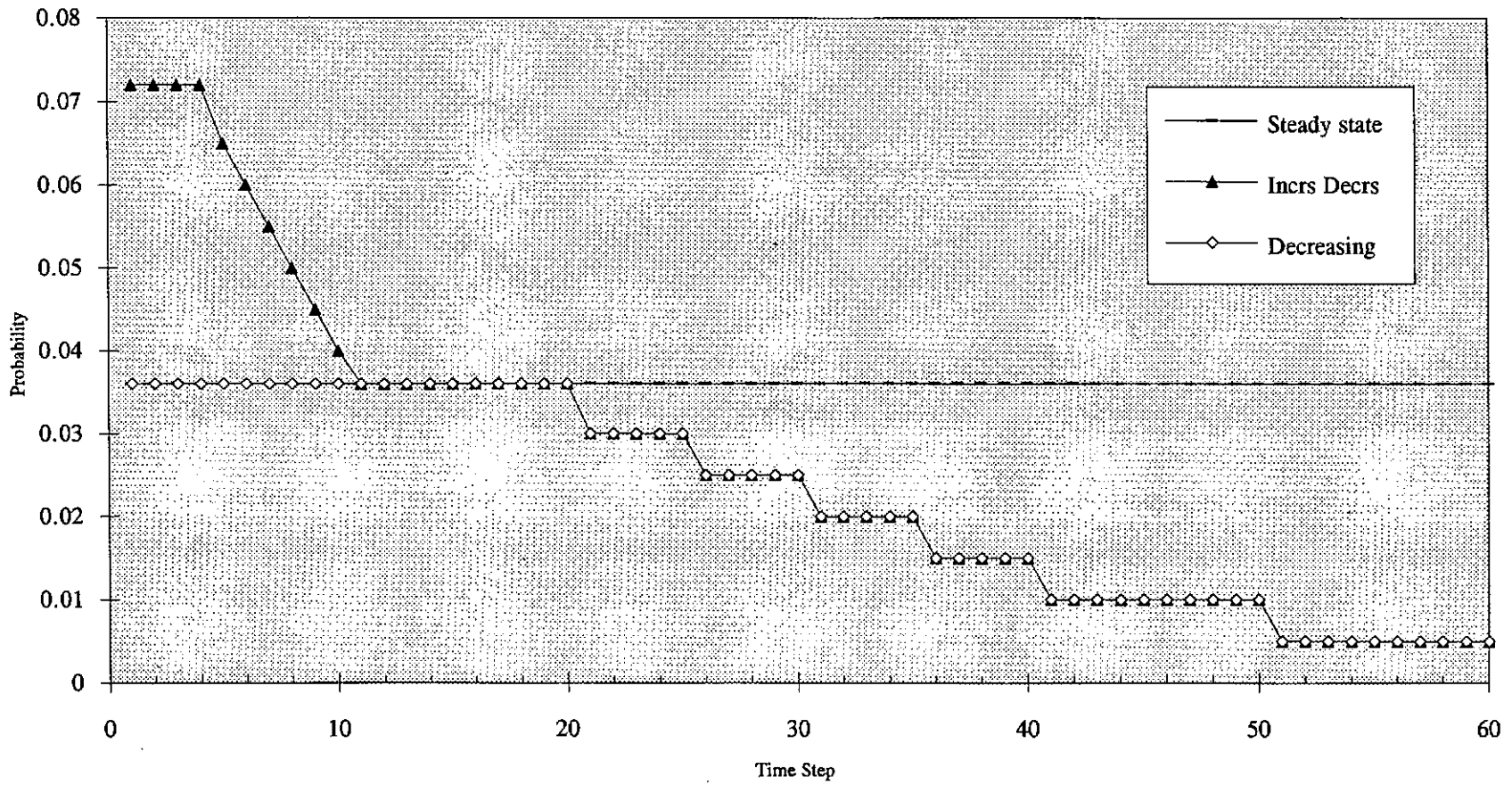


Figure 14: Probability of LOD Dam Formation in Model Scenarios

from second-growth stands are near zero.

The gradually reduced probability of new dam formation and the relatively high probability throughout the first half of the 60-year model cycle reflected two hypothesized characteristics of LOD dams. First, LOD above and near the channel that originated from the harvested stand continue to enter the channel and become incorporated in new LOD dams. Second, LOD from failed dams may become incorporated in new LOD dams. Hence, the probability of forming new LOD dams did not go to zero immediately following harvest and remained greater than or near the steady-state probability of formation for much of the model cycle.

Decreasing Scenario. In the "decreasing" scenario, the probability of new dams forming remains at the nominal probability through year 20, and then declines in the same pattern as in the increasing-decreasing scenario. This scenario models the potential effect of timber harvest wherein care is taken to neither increase nor decrease LOD density in the channel. The intent of the scenario was to isolate the effect of diminished inputs of LOD following timber harvest.

Logical Rules for Sediment Routing. The model was constrained by conservation of mass. Several logical tests required to maintain mass balance are described in detail in the next section. A few other general rules applied. First, sediment entering a model channel from creep or from upstream was placed in the detention reservoir. When a new dam formed, additional retention reservoir capacity was created. When a dam failed, sediment released from the retention reservoir was first used to satisfy residual retention storage capacity from previous time steps; surplus sediment could then be transferred provided that sufficient bedload transport capacity and sufficient detention sediment was available in that time step. Transport of bedload out of a channel segment was allowed only when no unfilled retention reservoir capacity remained. Finally,

transport of bedload out of a channel segment was limited by sediment availability, that is, the volume of sediment in the detention reservoir.

Hence, detention reservoir sediment that was transported had first to meet the demand of the retention reservoir, as limited by transport capacity, and only then could detention reservoir sediment be transferred out of the channel segment. In other words, the necessary conditions for bedload export were retention reservoirs filled to capacity, available sediment in the detention reservoir, and available transport capacity.

#### Computations of the Routing Model

This section describes the details of the spreadsheet computations performed in executing the model. Conceptual elements and quantitative parameters used in the model have been discussed previously.

There were three separate spreadsheets that calculated sediment routing in each of the three modeled channel segments in the network. A "master" macro-spreadsheet performs the iterative loops and sub-routines required to route sediment from one model segment to the next. For each model run, the sediment routing spreadsheets were executed 100 times and summary results were extracted and saved in a summary output spreadsheet.

Supporting spreadsheets were also used. One of these determined the pattern and magnitude of annual bedload transport capacity (i.e. climatic variability) and input this forcing variable to each channel-routing spreadsheet. This spreadsheet was executed as a subroutine of the master macro-spreadsheet. A second supporting spreadsheet served as an intermediate storage location for sediment outputs from each modeled channel segment from which sediment inputs to downstream segments were drawn. The third supporting spreadsheet was a subroutine of the channel-routing spreadsheets that performed the probability-based calculations which determined annual changes in LOD dams.

The following description proceeds spreadsheet-cell-by-spreadsheet-cell, column-by-column, across a spreadsheet row representing one year of sediment routing. Each cell "name" is given and the calculations made in each column across the row is described along with the type of information in each cell.

Time Step. This column contained constant numbers enumerating rows representing annual time steps in the sediment routing model.

Climate. This column contained variables representing the randomly selected annual recurrence interval which served as an index term for annual bedload transport capacity. The value in each row was the same in each of the three sediment routing spreadsheets for each model run. A sub-routine in the master macro-spreadsheet determined the value of this variable for each 60-year model loop and input these values to the routing spreadsheets.

Bedload Capacity. This column contained bedload transport capacity for the time-step. The numerical value was determined by a spreadsheet formula that retrieved the value of bedload transport capacity corresponding to "Climate" from a two-column table located elsewhere in each routing spreadsheet.

Bedload In. This column contained bedload inputs from upstream channel segments. These values were placed in the routing spreadsheets by the master macro-spreadsheet. The value for the upper two segments of the model channel network was zero.

Rand1. This column contained a formula that drew a random number between 0 and 1. A new random number was drawn each time the spreadsheet was calculated.

Rand2. This column contained a formula that drew another random number between 0 and 1. A new random number was drawn each time the spreadsheet was calculated.

Norm1. This column contained a formula that calculated a random number from a standard normal distribution. Two random

numbers, Rand1 and Rand2, were used in the calculation.

Creep Calc. This column calculated the volume of random inputs of sediment from soil creep processes. The volume input per unit length of channel was calculated as the mean creep rate ( $7.5 \text{ m}^3/\text{channel-km/yr}$ ) plus the product of the random normal deviate (Norm1), and the standard deviation of creep rate ( $3.1 \text{ m}^3/\text{channel-km/yr}$ ). The unit volume was then multiplied by reach length.

Creep In. This column calculated inputs of bedload material via soil creep. Sediment sorting, bedload attrition, and bulk density changes were accounted for in this calculation. A logical test was used to set this value equal to zero if the value of Creep Calc was less than zero; Creep Calc was very rarely negative.

Det0. This column contained the volume of sediment in the detention reservoir at the conclusion of the preceding time step.

Det1. This column summed the volume of inputs of bedload sediment from soil creep (Creep In) and from upstream (Bedload In) with the volume of sediment in the detention reservoir in the preceding time step (Det0).

Ret1. This column contained the volume of sediment in the retention reservoir at the conclusion of the preceding time step.

Steady-state. This column contained the probability of new LOD dam formation for the steady-state scenario. In this scenario, the value was the constant 0.036.

Incr-Decr. This column contained the probability of new LOD dam formation for the increasing-decreasing scenario. In this scenario, the value in the first time step was 0.072 and declined to 0.005 in the final time step as depicted in Figure 14.

Decreasing. This column contained the probability of new LOD dam formation for the decreasing scenario. In this scenario, the value in the first time step was 0.036 and declined to 0.005 in the final time step as depicted in Figure 14.

Dams. This column called the sub-routine "Damcalc" to determine the random change in the number of LOD dams. The sub-routine used four values which were exported from the routing spreadsheet: the probability of new dam formation for the particular model scenario (one of the three preceding columns), the number of dams from the preceding time step, the maximum number of dams allowed, and the minimum number of dams allowed.

The sub-routine was a loop executed once for each dam. Two random numbers were drawn. The first was used in a logical test to determine whether the dam failed in that time step. The second random number was used in a logical test to determine whether a new dam was formed. A counter tallied the number of dams resulting from each execution of the loop. The final step of the sub-routine was a logical test that constrained the number of dams between maximum and minimum values.

DeltaR1. This column first calculated the change in the number of dams relative to the preceding time step. Second, the change in the volume of sediment in the retention reservoir was determined as the product of the change in dams and the sediment volume of one LOD dam retention reservoir. The sign convention for the result of this calculation was negative if there was a net reduction in dams and positive if there was a net increase in dams.

Geom Det. This column kept a tally of the potential volume of sediment in the detention reservoir calculated from the hypothetical reservoir geometry shown in Figure 10. This volume remained constant because the mean depth of the detention reservoir was assumed to be uniform throughout the channel, regardless of the presence or absence of LOD dams.

Geom Ret. This column kept a tally of the potential volume of sediment in the retention reservoir calculated from the hypothetical reservoir geometry shown in Figure 10, the product of the number of dams and the retention capacity of one dam.

DeltaR2. This column calculated the sum of DeltaR1 and the unsatisfied retention reservoir demand from the previous time step (see "Resid storage" below). "Resid storage" was always non-negative. When dams formed, DeltaR1 was positive, and DeltaR2 increased. When dams failed, DeltaR1 was negative, and DeltaR2 decreased. In the latter case, the model directly transferred sediment released from failed dams to previously-unfilled retention reservoirs associated with other dams, regardless of bedload transport capacity. This step simplified the computation of sediment routing, but temporarily violated a model rule requiring that sediment transfers be constrained by transport capacity.

The limitation on transport capacity was ultimately enforced with respect to bedload transport out of model channel segments. If sediment from failed dams was not handled as described above, it would have instead been transferred to the detention reservoir. Transfers of sediment in the detention reservoir were subject to transport capacity limitations. When a dam failed and insufficient transport capacity was available, the sediment released would have enlarged the detention reservoir. The storage capacity of the retention reservoir would have remained unfilled; this condition prevented sediment transport out of the channel segment. In a subsequent time step, sufficient or excess transport capacity would have transferred detention reservoir sediment to the retention reservoir, after which sediment export could occur. This more complicated sequence of events is equivalent to the immediate transfer of sediment described in the preceding paragraph.

DeltaR3. This column performed a logical test comparing Bedload Capacity to DeltaR2 in order that subsequent potential transfer of sediment between the detention and the retention reservoir be limited by available transport capacity in that time step. If DeltaR2 was greater than or equal to Bedload Capacity,

DeltaR2 was the result; if not, Bedload Capacity was the result.

DeltaR4. This column performed a logical test constraining transport-capacity-limited sediment transfers (DeltaR3) by the volume of sediment available for transport (Det1). The result of this operation was Det1 if DeltaR3 was greater than or equal to Det1. Otherwise, the result was DeltaR3.

Resid Storage. This column calculated the unfilled capacity for sediment storage in the retention reservoir, that is, "residual storage". A logical test was performed to determine the value of Resid Storage. If DeltaR2, the intermediate residual storage, was greater than or equal to DeltaR4, the detention reservoir transfers to the retention reservoir as limited by detention reservoir sediment supply and bedload transport capacity, then Resid Storage was set equal to DeltaR2-DeltaR4. If DeltaR2 was less than DeltaR4, then Resid Storage was set equal to zero.

Det2. This column calculated an intermediate value of sediment stored in the detention reservoir as determined by transfers with the retention reservoir. A logical test was performed to determine the value of Det2. If DeltaR4, the sediment transferred between the detention reservoir and the retention reservoir, was equal to Det1 (DeltaR4 could not be greater than Det1 by virtue of the computation of DeltaR4), the volume of sediment in the detention reservoir after inputs from creep and from upstream, then Det2 was set equal to zero, leaving no detention sediment available for routing to the next channel segment. If DeltaR4 was less than Det1, then Det2 was set equal to (Det1)-(DeltaR4). Note that if DeltaR4 was negative, the case where sediment was transferred from the retention reservoir to the detention reservoir, Det2 was greater than Det1.

In addition, there were cases where DeltaR4 was negative and the absolute value of DeltaR4 was greater than the bedload transport capacity. In those cases, sediment was transferred

from the retention reservoir to the detention reservoir in excess of transport capacity. It was assumed that any sediment in the retention reservoir that was no longer restrained by an LOD dam was effectively in the detention reservoir.

Ret2. This column calculated the volume of sediment in the retention reservoir at the end of the time step as the sum of Ret1 and DeltaR4.

Det3. This column calculated the volume of sediment in the detention reservoir at the end of the time step. Det3 was calculated from a sequence of three nested logical tests which ensured that transfers of sediment between the detention and retention reservoirs were constrained by conservation of mass, and that transfers from the detention to the retention reservoir were constrained by transport capacity in the time step.

The first logical test was whether Det2 was equal to zero. If true, Det3 was also zero as there was no sediment remaining in the detention reservoir after transfers to the retention reservoir. There was no bedload transport to the next channel segment in this case.

If the prior logical test was false, the next test determined if DeltaR4 was equal to Bedload Capacity. (DeltaR4 could not be greater than Bedload Capacity owing to the definition of DeltaR3.) If true, Det3 was set equal to Det2. Det2 was determined by one of two conditions: either transfers of detention sediment to the retention reservoir accounted for all the available sediment in the detention reservoir (the case where DeltaR4 was greater than or equal to Det1 and Det2 equals zero) or there was sediment remaining in the detention reservoir after transport-capacity-limited transfer of sediment from the detention reservoir. There was no bedload transport to the next channel segment in the case above. Bedload transfer to a downstream channel segment was possible in the following case.

If the prior logical test was false, that is, DeltaR4 was

less than Bedload Capacity, a logical test determined if  $\Delta R_4$  was less than zero (the case where retention reservoir sediment was transferred to the detention reservoir). If true, then  $Det_3$  was equal to  $Det_2$  minus Bedload Capacity. In most such cases, the detention reservoir was diminished by the quantity Bedload Capacity, which was then either added to the retention reservoir, transported to a downstream segment, or divided between the retention reservoir and downstream routing. In a few cases, Bedload Capacity was larger than  $Det_2$ , yielding a negative number in  $Det_3$ --this possibility was addressed in the following column of the spreadsheet. Hence, the quantity of sediment in the detention reservoir transferred was limited by transport capacity.

If the prior logical tests were false, that is, sediment was transferred from the detention reservoir to the retention reservoir ( $\Delta R_4$  was greater than zero), and sediment transport capacity was greater than the quantity of sediment available for transfer from the detention to the retention reservoir ( $\Delta R_4$  was less than Bedload Capacity), then  $Det_3$  was equal to  $Det_2$  minus the difference between Bedload Capacity and  $\Delta R_4$ . (The latter difference had the effect of adding  $\Delta R_4$  back to  $Det_2$ , and then subtracting Bedload Capacity from  $Det_2$ , thus maintaining mass balance.) In other words, the detention reservoir lost sediment to the retention reservoir and, provided  $Det_2$  was greater than zero, additional sediment could be transported to the next channel segment at the expense of the detention reservoir. In some cases, the difference between Bedload Capacity and  $\Delta R_4$  was greater than  $Det_2$ , causing  $Det_3$  to be negative. These cases are addressed in the following column.

Det4. This column performed a simple test: if  $Det_3$  was less than zero,  $Det_4$  was set equal to zero, otherwise  $Det_4$  was equal to  $Det_3$ . This test was necessary because of the infrequent circumstances under which  $Det_3$  was negative. Sediment in the

detention reservoir was not allowed to be less than zero; sediment was either available for transfer to the retention reservoir or for transport out of the channel segment.

Bedload Yield. This column determined the amount of sediment removed from the detention reservoir and transported out of the channel segment. A series of five nested logical tests were used to ensure that mass was conserved.

The first logical test determined if Det2 was equal to zero. If so, no sediment could be transported out of the channel segment because all available detention sediment and/or transport capacity was required to meet the demands of the retention reservoir. If the logical test evaluated to false, the second test was performed.

The second logical test determined if Det3 was less than zero. If so, transport capacity exceeded the supply of sediment in the detention reservoir available after the retention reservoir demand was satisfied, and Bedload Yield was equal to Det2, the available detention-sediment. If the result of the logical test was false, the third test was performed.

The third logical test was whether DeltaR4 was greater than or equal to Bedload Capacity. If so, Bedload Yield was set equal to zero. In order that DeltaR4 be greater than Bedload Capacity, DeltaR4 had to be greater than zero. Consequently, the available transport capacity transferring sediment from the detention reservoir to the retention reservoir could not be greater than the retention reservoir's demand for sediment, and no surplus capacity was available to transport sediment out of the channel segment. If the third logical test evaluated to false, the fourth test was performed.

The fourth logical test required two conditions to be satisfied: DeltaR4 had to be less than zero and Det2 had to be greater than Bedload Capacity. If both these conditions were met, then Bedload Yield was set equal to Bedload Capacity. If

DeltaR4 was negative, the retention reservoir was yielding sediment to the detention reservoir. If Det2 was greater than transport capacity for the time step, then the sediment transported out of the channel segment was constrained to be equal to Bedload Capacity. If both conditions in the fourth logical test were not true, then the fifth logical test was performed.

The fifth logical test also required two conditions to be satisfied to evaluate as true. DeltaR4 had to be negative and Det2 had to be less than Bedload Capacity. If both conditions were true, then Bedload Yield was set equal to Det2. Again, the retention reservoir was yielding sediment to the detention reservoir, but in this case transport capacity exceeded the volume of sediment available, so all the sediment available was transported out of the channel segment. If the fifth logical test evaluated false, then DeltaR4 was necessarily positive. In addition, because the third test evaluated false (otherwise the fifth test would never have been performed), DeltaR4 was less than Bedload Capacity. Finally, because the second test evaluated false (Det3 was not less than zero), Det2 had to be greater than Bedload Capacity. Hence, Bedload Yield was equal to Bedload Capacity less DeltaR4.

Suspended Load. This column calculated the suspended load transported out of the channel segment. In the routing model of upper channel segments, there was no suspended load transported from upstream. In that case, suspended load output was equal to the portion of creep input that was fine enough to be transported in suspension (the product of Creep Calc and 0.3) plus suspended load generated by bedload attrition, which was equal to 0.07 times the product of Creep Calc and 0.7. In the middle and lower channel segments in the model, an additional term added suspended load outputs from the upstream channel segment.

Mass Balance. This column performed a simple check to confirm that the routing model conserves bedload mass. The calculation was: Creep In plus Bedload In (equal to zero in the upper channel segments), plus Det0 minus Det4 (the change in storage in the detention reservoir), plus Ret1 minus Ret2 (the change in storage in the retention reservoir), minus Bedload Yield. This column should always equal zero. It was used to debug early versions of the routing model. In subsequent model runs, mass was conserved.

## RESULTS

### Bedload Model

The predicted annual transport capacities of bedload generated by the bedload transport model were derived from 5000 years of simulated 24-hour precipitation totals greater than or equal to 2.6 inches. For purposes of the bedload transport model, it was assumed that there was unlimited sediment available in the model channels. The resulting cumulative frequency distributions are shown in Figure 15. The magnitude of bedload transport capacity for various recurrence intervals and the maximum transport capacity predicted by the model is shown in Table 9.

These cumulative frequency distributions were used in the sediment routing model. The frequency distributions were transferred to a tabular format for use in the sediment routing model. The intervals used to sort the data into a tabular format were chosen such that the cumulative frequency distributions were smoothed (Figure 15).

The probability of bedload transport capacities less than  $0.01 \text{ m}^3$  in any year decreased with the contributing drainage area of the three model channels. Bedload transport capacity less than  $0.01 \text{ m}^3$  may be considered to be effectively zero. In the modelled upper second-order channel, based on monitoring data from Eight-ten Creek, the probability of negligible bedload transport capacity was 0.19. For the lower second-order channel, based on monitoring data from Sister Creek, the probability was 0.15. For the third-order channel, based on Ramp Creek, the probability was 0.14.

The characteristic differences in transport capacity among these channels can best be described by using an arbitrary magnitude of transport capacity to describe "significant" transport. The probability of transport capacity of at least  $1 \text{ m}^3$  for the smallest channel is about 0.36, or slightly greater

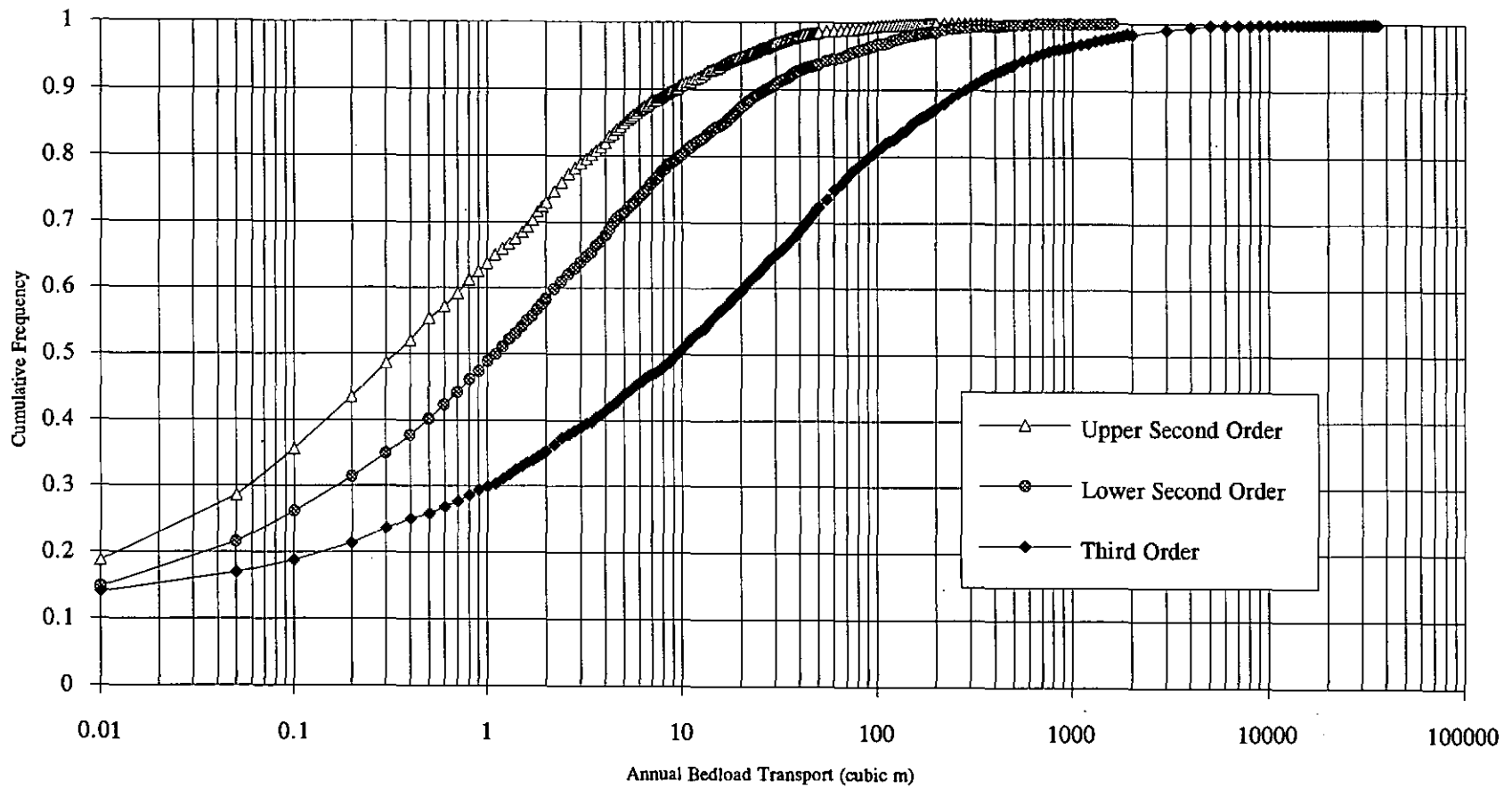


Figure 15: Cumulative Frequency Distribution of Bedload Transport Capacity

**Table 9: Predicted Bedload Transport Capacity for Selected Recurrence Intervals**

Annual Recurrence Interval	Annual Bedload Transport Upper 2nd Order (0.31 sq. km)		Annual Bedload Transport Lower 2nd Order (0.53 sq. km)		Annual Bedload Transport 3rd Order (1.12 sq. km)	
	Cubic m	Tonnes	Cubic m	Tonnes	Cubic m	Tonnes
2	0.35	0.9	1.1	2.9	9.3	24
5	3.4	8.8	10	26	92	240
10	9.4	24	27	70	280	730
20	20.5	53	70	182	625	1630
50	39	101	145	377	1600	4160
100	75	195	220	570	3000	7800
<hr style="border-top: 1px dashed black;"/>						
Maximum	380	988	1600	4160	37000	96200

than one chance in three. For the next larger and largest channels, the probability of at least 1 m<sup>3</sup> of bedload transport capacity were 0.51 (one chance in two) and 0.70 (slightly greater than two chances in three), respectively.

#### Routing Model

Bedload yield was modeled for six scenarios, including either high or average initial density of debris dams and three scenarios for debris dam dynamics: steady-state, increasing-decreasing, and decreasing. The steady-state case was the best estimate of the sediment routing process in a natural or unmanaged channel. We used the steady-state case as a baseline against which the other two cases could be compared. The model was run for 500 60-year cycles for the steady-state case in order to establish baseline values over a wider range of variation. Predictions for the other two scenarios for dynamics of debris dams were based on 100 60-year model cycles.

Initial model runs used the two-dimensional geometry of the channel (Figure 11) to define initial sediment storage. The initial runs revealed that in most cases sediment in the detention reservoir was exhausted during the 60-year model cycle. This suggested that in the modelled channels, the sediment transport capacity was consistently greater than sediment supply, that is, these channels were supply-limited.

The modelled initial detention reservoir storage was likely to be too large and bias the model. Therefore, an alternate method to determine initial detention reservoir volume was used. Model runs using the geometrically-determined initial storage were used to estimate the distribution of the initial volume of sediment in the detention reservoir volume for each channel from the distribution of the volume of sediment in the detention reservoir at the end of the 60-year model cycle. These distributions were used in the routing model to randomly-determine initial volume of sediment in the detention reservoir.

Comparison of Scenarios. The workings of the routing model may be seen in plots of the number of LOD dams, sediment reservoir volumes, and bedload yield as a function of time. Figures 16a, 16b and 16c are individual examples drawn from at least 100 simulations. These figures demonstrate the relationship between the dynamics of LOD dams and bedload storage and transport in the scenario for average initial dam density in the third-order channel under each of the three scenarios for dynamics of LOD dams.

In the example model run for steady-state dynamics (Figure 16a), the number of LOD dams increased for about 35 years, expanding the volume of sediment in the retention reservoir. During this time, the detention reservoir was virtually empty and there was very little bedload transported downstream. Thereafter, LOD dams begin to decline, releasing sediment from the retention reservoir. This sediment then either accumulated in the detention reservoir or was transported downstream.

The example for increasing-decreasing dynamics (Figure 16b), showed a pattern typical for this scenario. During the initial decade or so, the number of LOD dams and the volume of sediment in the retention reservoir increase. During the second decade, LOD dams begin a steady decline, releasing sediment from the retention reservoir. The volume of sediment in the detention reservoir periodically increases, and is then routed downstream in years when transport capacity is high. In this example, LOD dams reached the minimum number allowed during the final decade. No change in retention storage occurs; the retention reservoir is full. Consequently, small quantities of bedload are transported downstream in most years. These small quantities are comparable in magnitude to sediment inputs via creep processes, but may include sediment routed from the tributary channels.

In the example for the decreasing dynamics of LOD dams (Figure 16c), LOD dams decline during the first 20 years. During

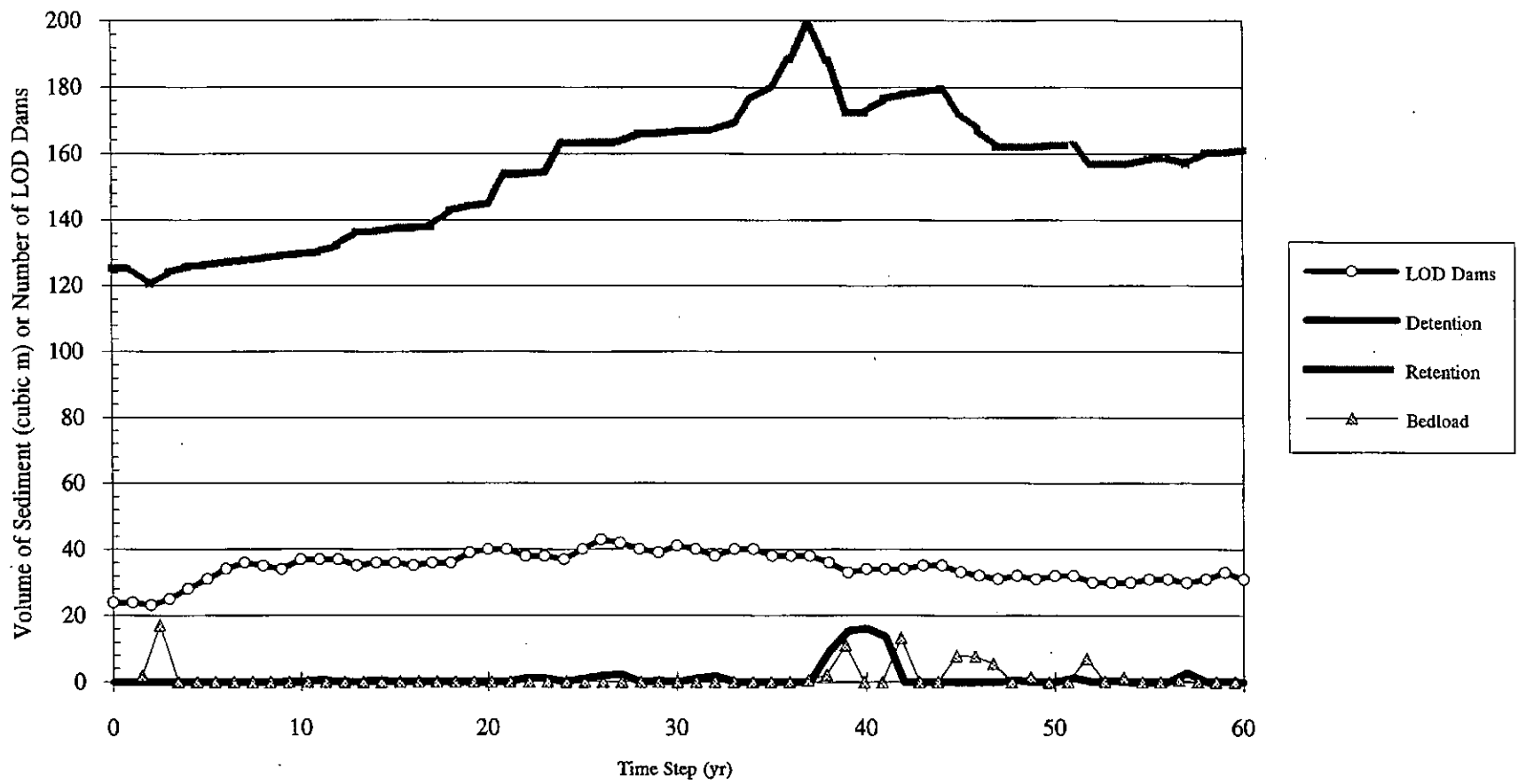


Figure 16a: Reservoir Change and Bedload, Steady-State Scenario

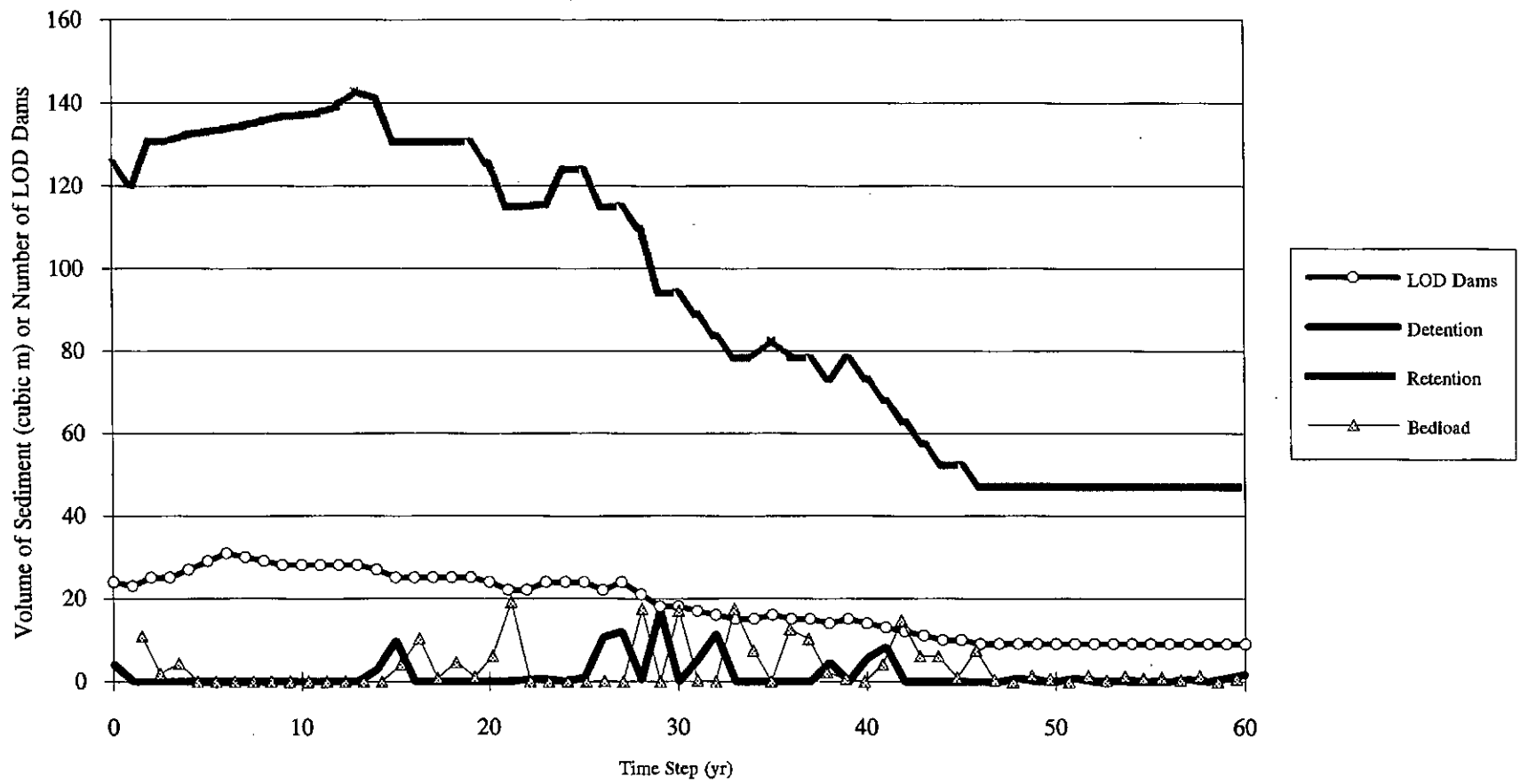


Figure 16b: Reservoir Change and Bedload, Increasing-Decreasing Scenario

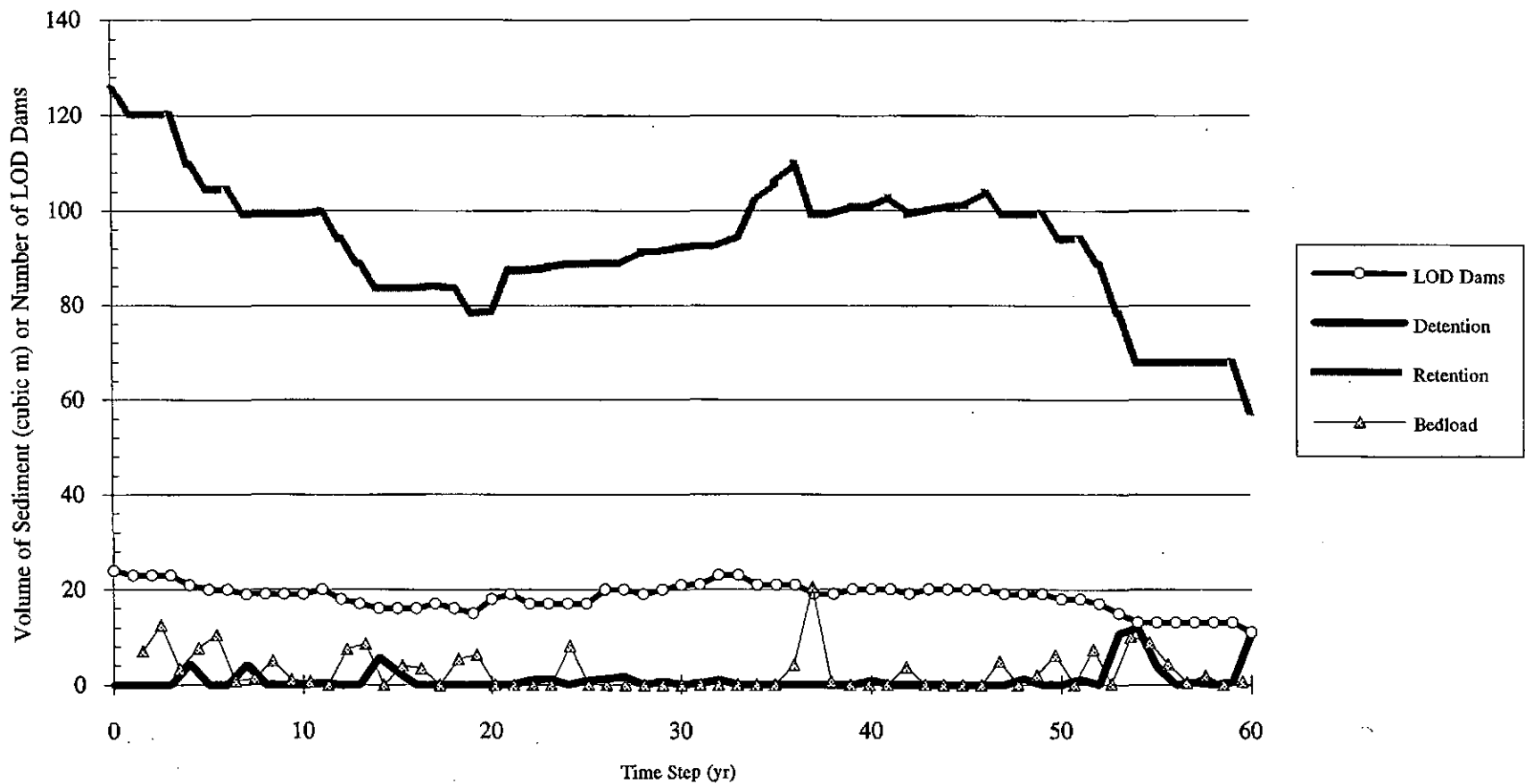


Figure 16c: Reservoir Change and Bedload, Decreasing Scenario

the next 30 years, LOD dams happen to increase with occasional small declines. In the final decade, LOD dams again decline steadily. This demonstrates the variation in the number of LOD dams possible under the stochastic structure of the routing model. Collectively, these examples show the tight coupling between changes in retention reservoir storage and bedload yield. In addition, it is evident that bedload yield is often zero, and that much of the total yield of bedload during a 60-year period comes in a few individual years.

Mean annual bedload yield for all six scenarios and each of the three channels is shown in Figure 17. The model results from the third order channel, which drains an area of 1.1 km<sup>2</sup>, are of most interest because the bedload yield from this channel would, presumably, be routed to the upper reaches of fish bearing streams.

In the high initial dam density case, mean annual bedload yield for the third order channel increased from 3.34 m<sup>3</sup> (8.7 tonnes) in the steady-state case to 6.55 m<sup>3</sup> (17 tonnes) and 7.69 m<sup>3</sup> (20 tonnes) in the increasing-decreasing and decreasing scenarios, respectively. In the average initial dam density case, the mean annual bedload in the steady-state case was 3.00 m<sup>3</sup> (7.8 tonnes). Increases in mean annual bedload in the increasing-decreasing and decreasing scenarios were proportionately smaller than in the high initial density scenario. In the increasing-decreasing scenario, mean annual bedload was 4.69 m<sup>3</sup> (12 tonnes), and in the decreasing scenario it was 5.15 m<sup>3</sup> (13 tonnes).

The routing model was designed to assess the sensitivity of bedload yield to the dynamics of LOD dams. Therefore, bedload yield was interpreted in the context of changes in LOD dams. The number of debris dams declined by about one-half in both the increasing-decreasing and decreasing scenarios. The range of net change in debris dams was -40 to -58 percent (Figure 18).

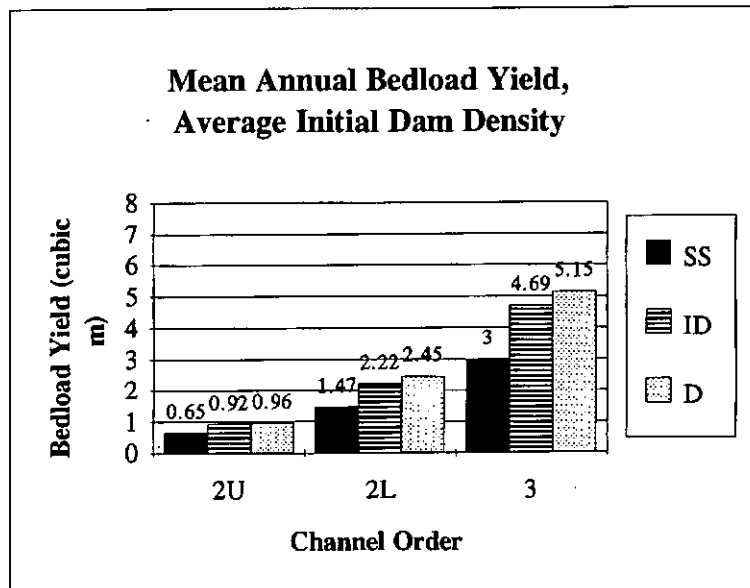
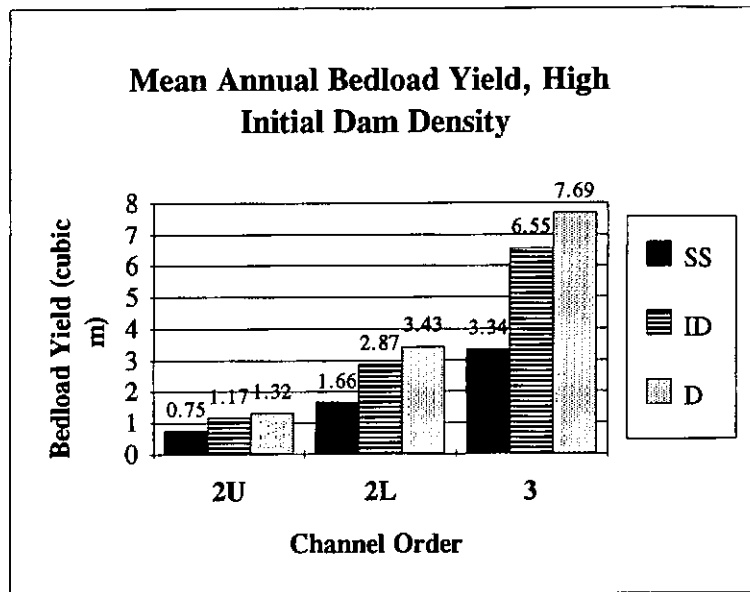


Figure 17. Predicted annual bedload yield for each channel segment and each model scenario; SS refers to the steady-state scenario for LOD dam dynamics, ID refers to the increasing-decreasing scenario and D refers to the decreasing scenario.

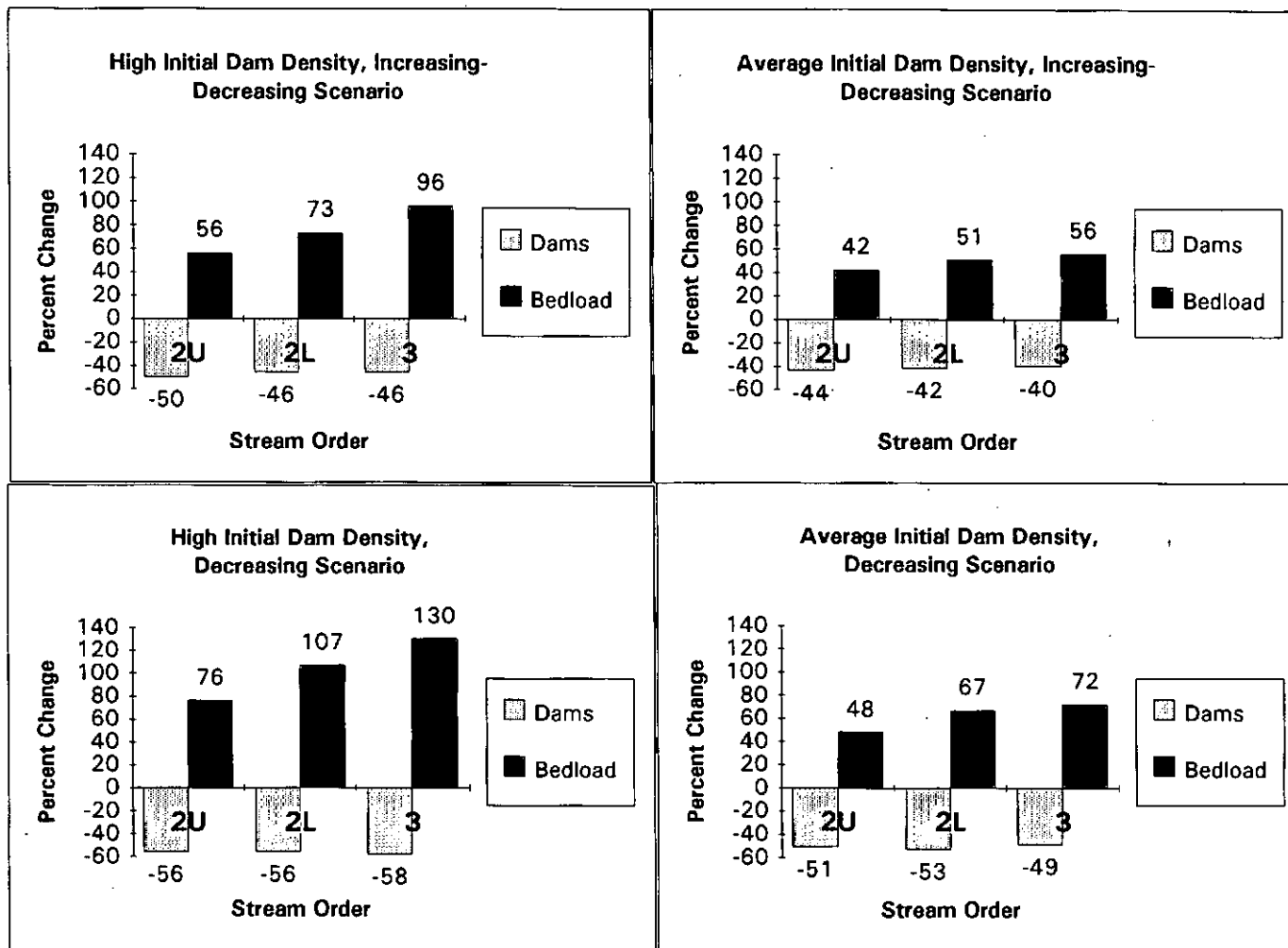


Figure 18. Percent change in average bedload yield and LOD dams relative to steady-state scenario for 60-year model cycles. Scenarios for initial density of LOD dams and dynamics of LOD dams are compared for each modeled channel segment. "2U" refers to upper second-order channel segments, "2L" refers to lower second-order channel segments, and "3" refers to third-order channel segments.

Consequently, transfers of sediment from the retention reservoir to the detention reservoir enlarged the supply of sediment available for transport. Bedload yield subsequently increased relative to the steady-state case owing to a greater supply of transportable sediment and the excess bedload transport capacity characteristic of the modelled channels. Despite the foregoing general result, which was not surprising given the model's assumptions about the routing process, there were substantial differences between scenarios and channels (Figure 18).

The change in bedload yield relative to the steady-state case was always positive and ranged from 42 to 130 percent. In any given scenario, the change in yield was least for the smallest channel and greatest in the largest channel. Increases in bedload yield were greater in the case of high initial density of dams than in the case of average initial density of dams. Increases in bedload yield were greater in the decreasing scenario than the increasing-decreasing scenario.

The scenario that generated the greatest change in bedload yield was high initial dam density and decreasing dams. In the upper second order, lower second order, and third order channels the increase was 76, 107 and 130 percent, respectively. The smallest changes in bedload yield were from the average initial density of dams, increasing-decreasing scenario. From smallest channel to largest, the increases were 42, 51, and 56 percent. With respect to delivery of bedload downstream, the bedload yield from the third order channel is most important; this increased at least 56 percent and as much as 130 percent.

The foregoing described the model results in terms of overall average changes. Because of the stochastic nature of the model, however, the results may also be described as probability distributions. Two types of probability distributions are presented below.

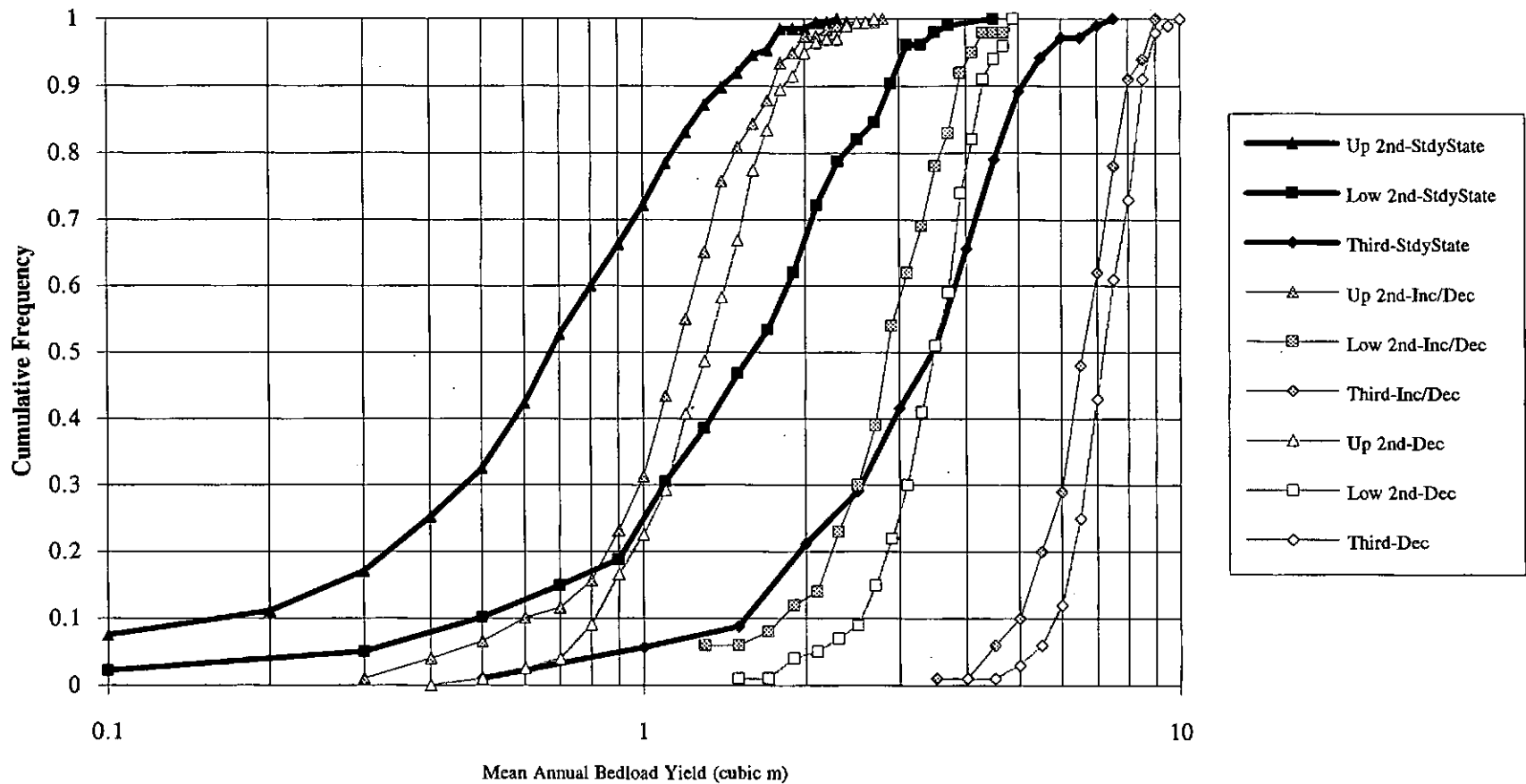


Figure 19a: Cumulative Frequency Distribution of Mean Annual Bedload Yield, High Initial Debris Dam Density

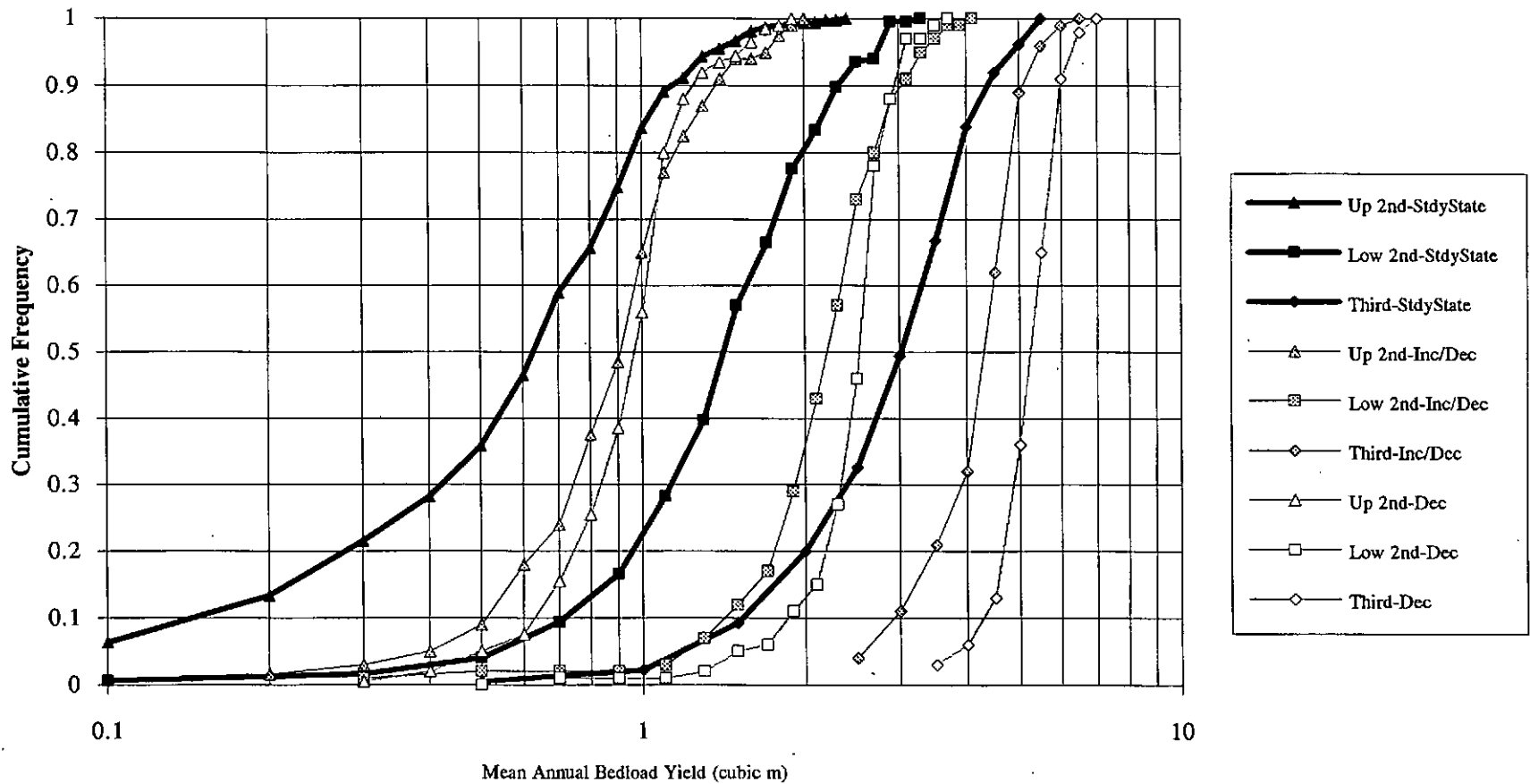


Figure 19b: Cumulative Frequency Distribution of Mean Annual Bedload Yield, Average Initial Dam Density

The first type is a cumulative frequency distribution of mean annual bedload yield (Figures 19 a & b). Cumulative frequency is plotted as a function of bedload yield. Distributions for each channel and each scenario of debris-dam-dynamics are shown. The frequency distributions for the high initial debris dam case are shown in Figure 19a and for the average initial debris dams case in Figure 19b. Median values (cumulative frequency of 0.5) of these distributions are similar to the mean values shown in Figure 17.

These plots show the shifts in the probability distributions that occur under different scenarios. The lower portions of the frequency distributions (e.g. below 0.5) are shifted to a greater degree than the upper portions of the distributions. In the scenario for high initial density of dams, the increasing-decreasing and decreasing scenarios shift the distribution of the lower second-order channel into bedload yields of magnitudes comparable to the third-order channel in the steady-state scenario.

Relationship Between Dam Changes and Bedload Yield. The yield of bedload sediment from the routing model is quite sensitive to declining density of LOD dams. Total bedload yield from third-order channels, which includes bedload routed from the second-order channel segments, is compared to bedload yield from retention reservoirs summed over all three channel segments in Figure 20. When density of LOD dams declines substantially, the proportion of the total bedload yield that was released from storage in the retention reservoir is large.

In the scenario for high initial density of debris dams and steady-state dynamics of debris dams, 18 percent of the total bedload was released from retention reservoirs throughout the model channel network. In the increasing-decreasing scenario, 61 percent of total bedload came from the retention reservoir. In the decreasing scenario 63 percent of the total bedload

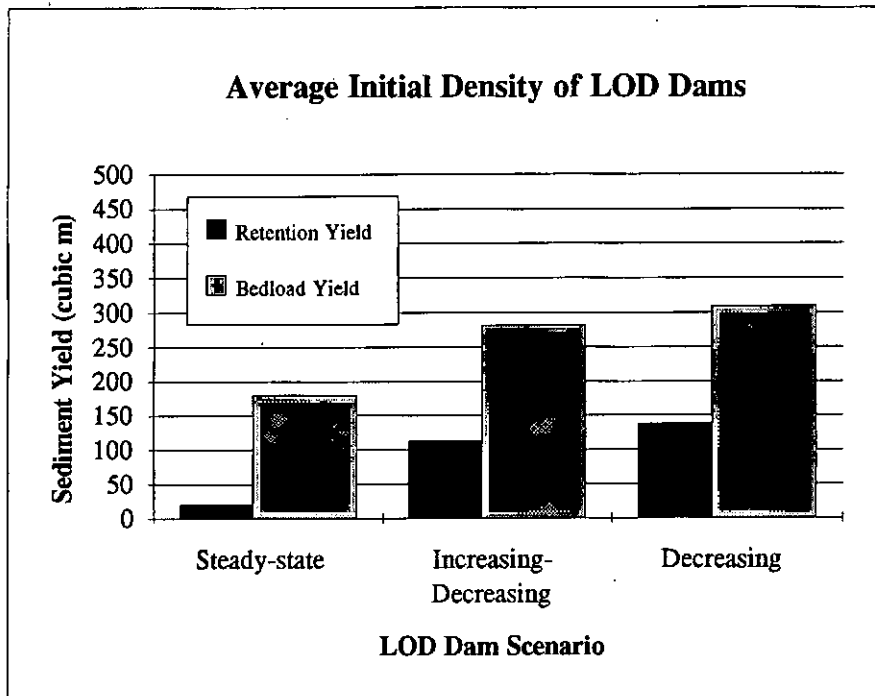
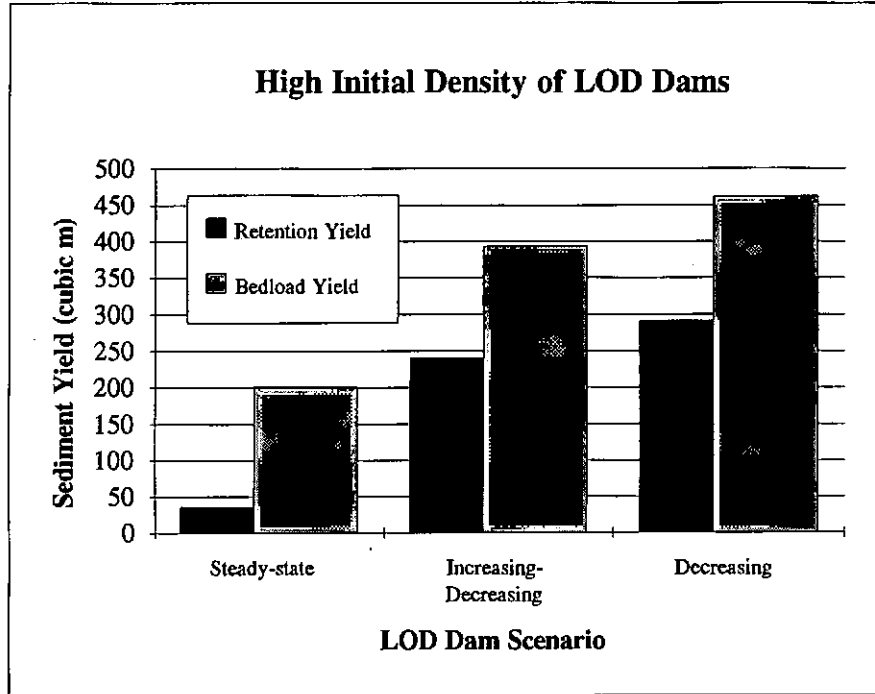


**Figure 20: Yield of Bedload From Retention Storage Reservoirs in Modelled Channel Network In Comparison With Total Bedload Yield From Modelled Third-Order Channels**

originated in the retention reservoir. In the scenario for average initial density of debris dams, the percentage of total bedload released from the retention reservoirs was 11, 40 and 45 percent for the steady-state, increasing-decreasing, and decreasing scenarios, respectively.

The mean yield of bedload is shown in scatter plots (Figures 21 a-f) as a function of the net change in debris dams in individual model runs for each of the three channel type in each of the six model scenarios. The influence of failure of LOD dams is evident in these plots. As the net loss of LOD dams increases, the yield of bedload increases. Failed LOD dams release sediment from the retention reservoir to the detention reservoir, increasing the volume of sediment in the detention reservoir. Bedload transport capacity typically exceeded sediment volume available in the detention reservoir, so the yield of bedload generally increased with the decline in LOD dams.

The effect of random variation of climatic patterns and the patterns of establishment and failure of LOD dams can also be seen in the scatter plots (Figures 21 a-f). Random variation is expressed by the range of bedload yield for a given net change in the number of LOD dams.

In general, the data clouds shown in Figures 21 a-f for different channels in the steady-state cases are close together. In the decreasing and increasing-decreasing cases, the data clouds for different channels separate and become more distinct.

In the scenario for average initial density of LOD dams with either increasing-decreasing or decreasing LOD dams, data points tend to be clumped near the maximum decrease. This reflects the fact that the model required a minimum number of debris dams in the channel, and that within the 60 year model cycle, this limit was frequently reached. The effects of imposed limits on the number of debris dams can also be seen in the steady-state

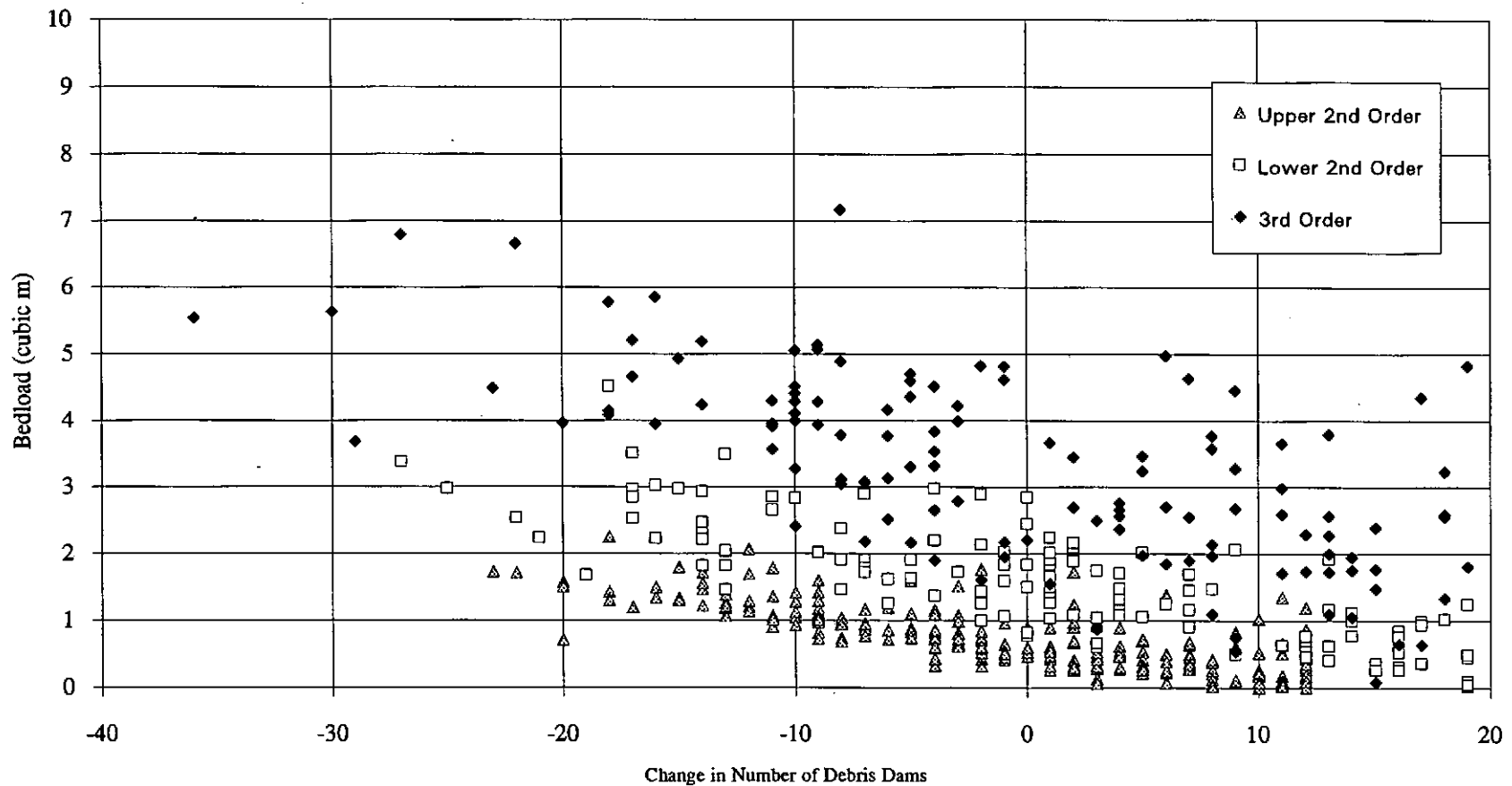


**Figure 21a: Mean Annual Bedload vs. Number of Debris Dams, High Initial Density, Steady-State Scenario**

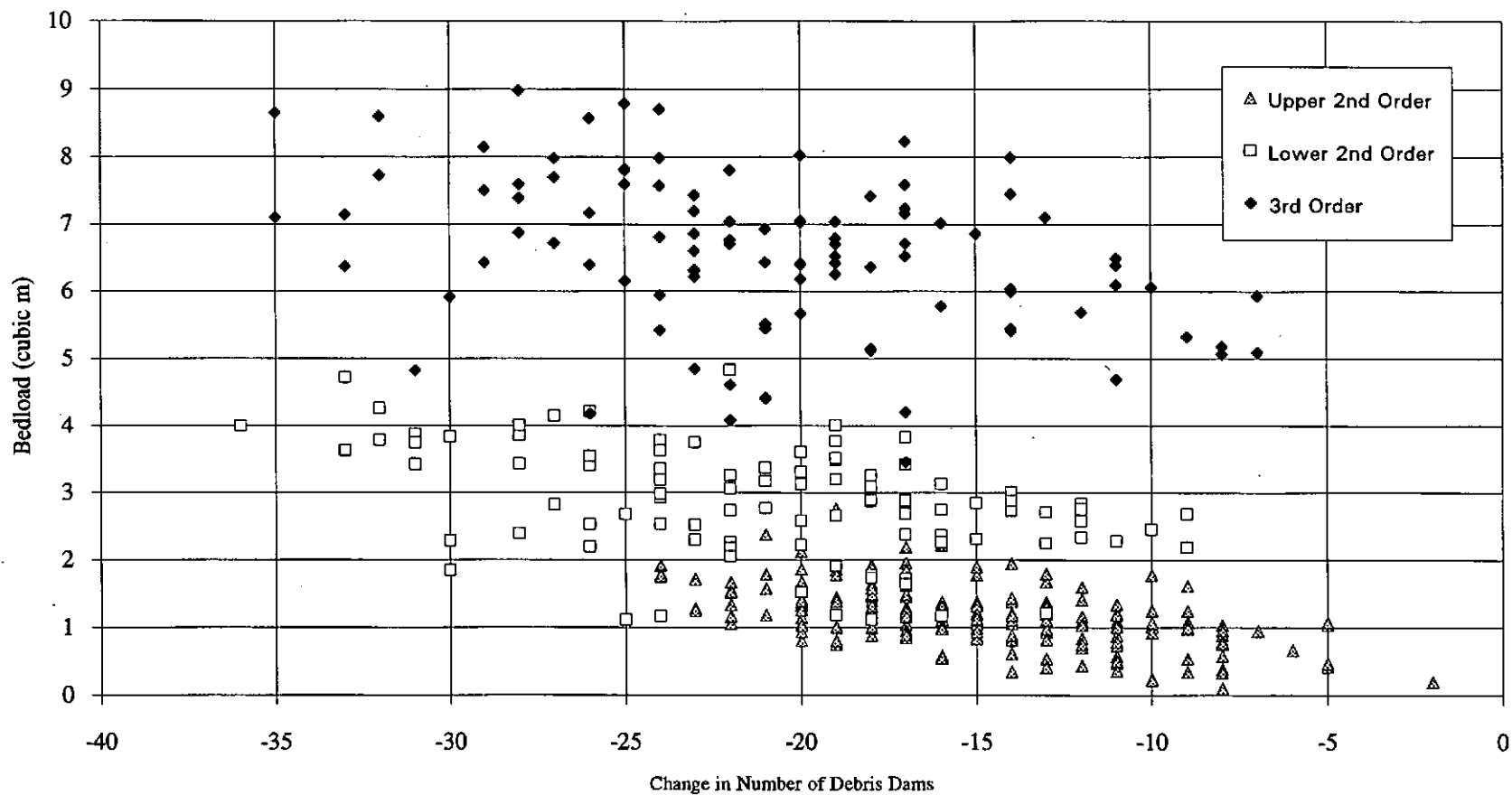
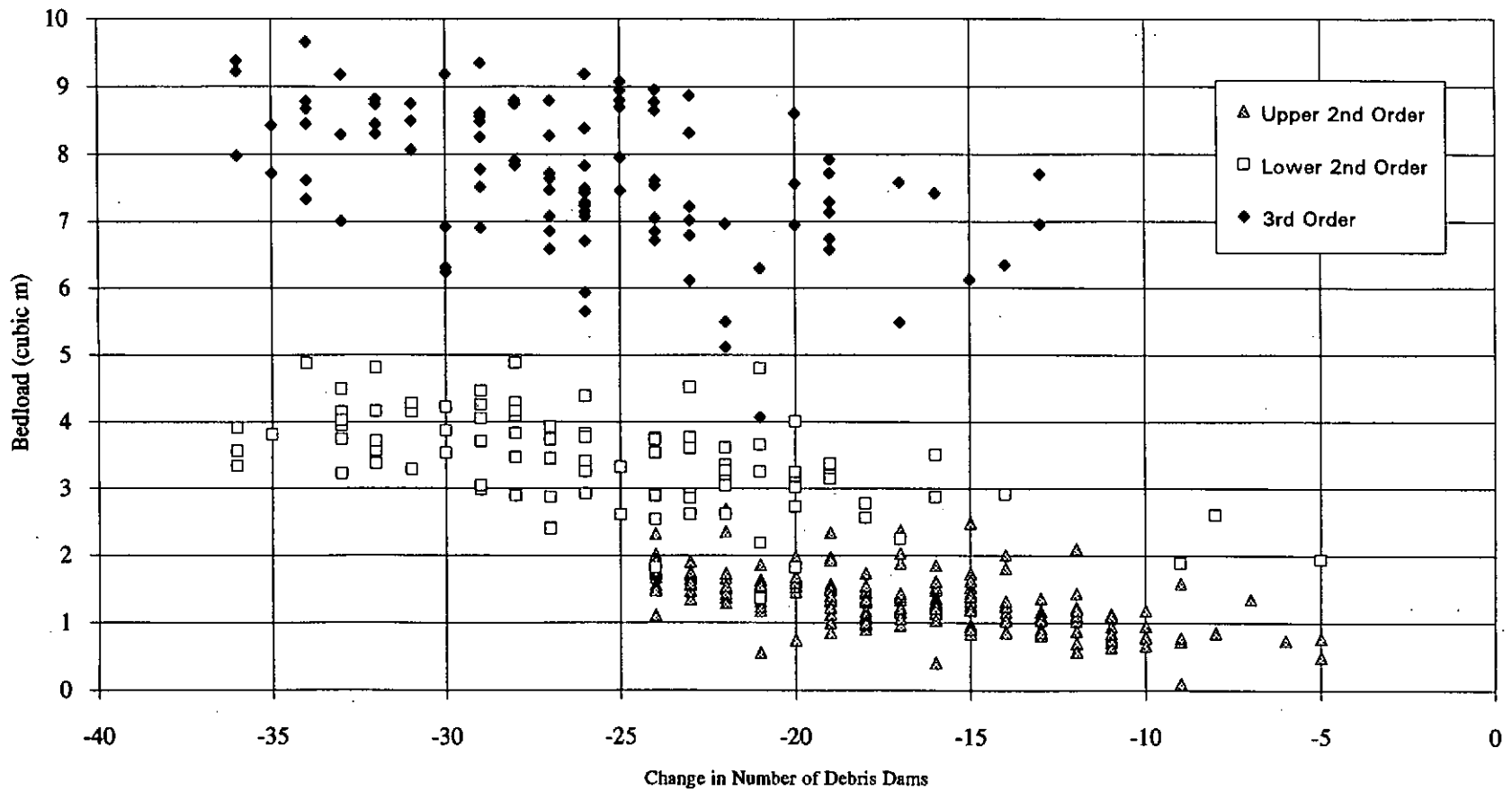


Figure 21b: Mean Annual Bedload vs. Change in Number of Debris Dams, High Initial Density, Inc.-Dec. Scenario



**Figure 21c: Mean Annual Bedload vs. Number of Debris Dams, High Initial Density, Decreasing Scenario**

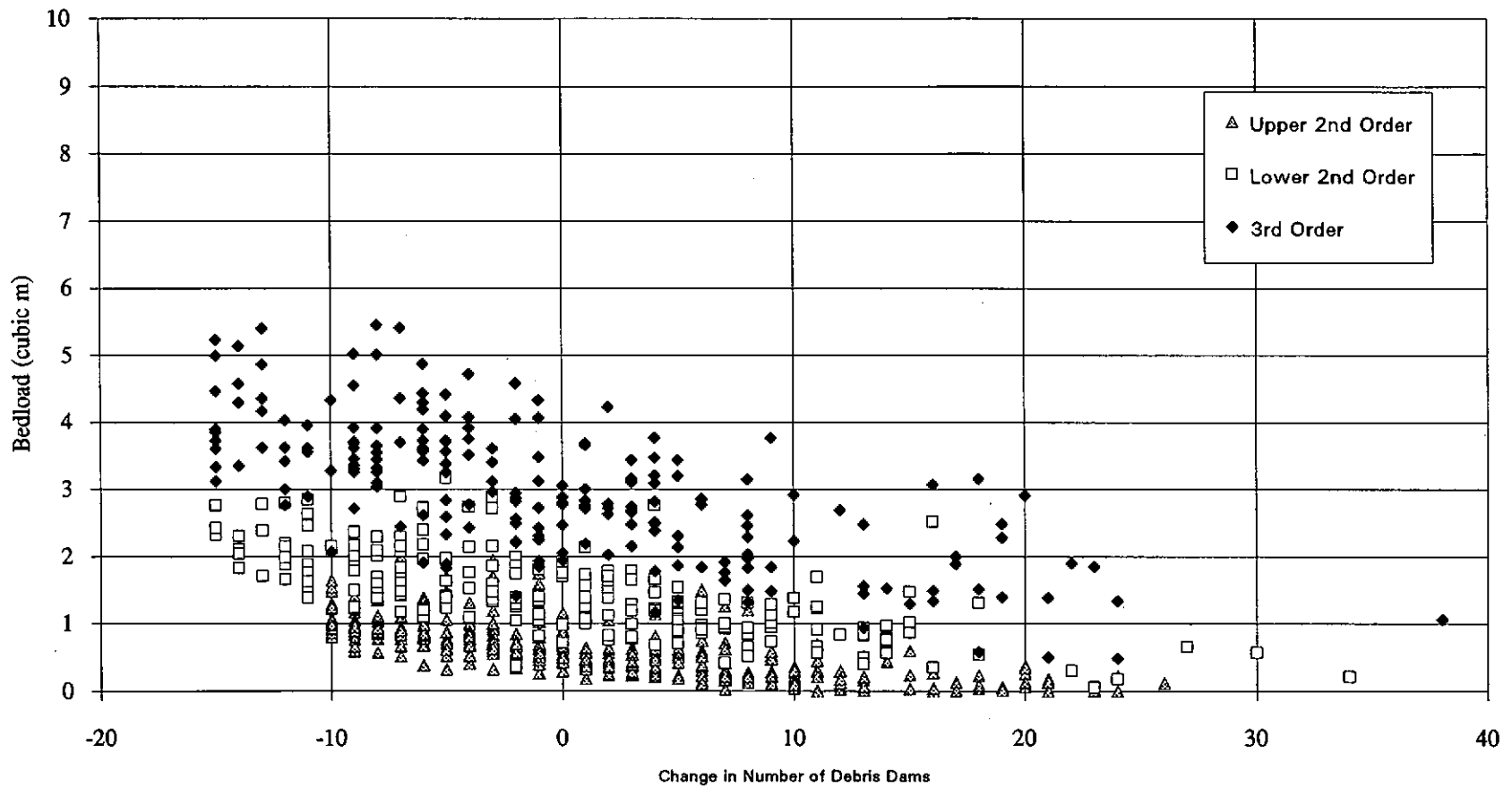


Figure 21d: Mean Annual Bedload vs. Number of Debris Dams, Average Initial Density, Steady-State Scenario





scenario.

As shown in Table 10, the number of dams tended to decrease by a small amount in the steady-state scenario with high initial density of dams. On the other hand, dams tended to increase slightly in the steady-state scenario with average initial density. In the former case, because the initial density was near the maximum density, the upper limit was frequently encountered in the routing model and the mean of random changes tended to be negative. In the latter case, when initial dam density was substantially smaller than the maximum dam density, the upper limit on dams was not frequently reached, and the number of dams was allowed to vary more freely, resulting in a slight tendency for dams to increase.

Residence Time. Residence time is defined as the mass or volume of a reservoir divided by the flux rate through the reservoir. This ratio has units of years, and indicates the average duration of sediment residence in the channel. We calculated reservoir volume as the average volume of sediment storage (the sum of initial and final sediment storage in both the detention and retention reservoirs, divided by two). Residence time was calculated as the reservoir volume divided by the average bedload yield. These calculations for each scenario and each channel type are summarized in Table 11. Both the mean and median values of residence time are given.

The median value of residence time was a better measure of central tendency of these distributions than the mean. Mean values were inflated by the few instances when bedload yield was very small, leading to a very large residence time and skewing the mean. The median residence times are shown graphically in Figure 22.

In the upper second-order channels, median residence times ranged from 40 to 115 years. In the lower second-order channels, median residence time ranged from 29 to 109 years. In the third-

### Table 10: Changes in LOD Dams

Scenario	Upper Second Order			Lower Second Order			Third Order		
	Initial	Final	% Change	Initial	Final	% Change	Initial	Final	% Change
<b>High Initial Density</b>									
SS	30	29.4	-2	45	44.7	-1	45	44.5	-1
ID	30	15.0	-50	45	24.2	-46	45	24.1	-46
D	30	13.3	-56	45	19.7	-56	45	18.8	-58
<b>Average Initial Density</b>									
SS	16	16.8	5	24	24.6	3	24	23.5	-2
ID	16	9.0	-44	24	14.0	-42	24	14.5	-40
D	16	7.9	-51	24	11.4	-53	24	12.2	-49

---

Note: Final values are means of distributions.

**Table 11: Bedload Residence Time**

SCENARIO			Upper	Lower	Third
Initial	Dam		Second	Second	Order
Dams	Dynamics		Order	Order	
High	Steady State	Median	155	109	68
		Mean	1370	278	125
High	Incrsng.- Decrsng.	Median	74	52	28
		Mean	108	60	29
High	Decrsng.	Median	59	40	22
		Mean	78	44	23
Average	Steady State	Median	81	66	40
		Mean	1020	99	52
Average	Incrsng.- Decrsng.	Median	47	35	21
		Mean	68	45	23
Average	Decrsng.	Median	40	29	18
		Mean	47	34	19

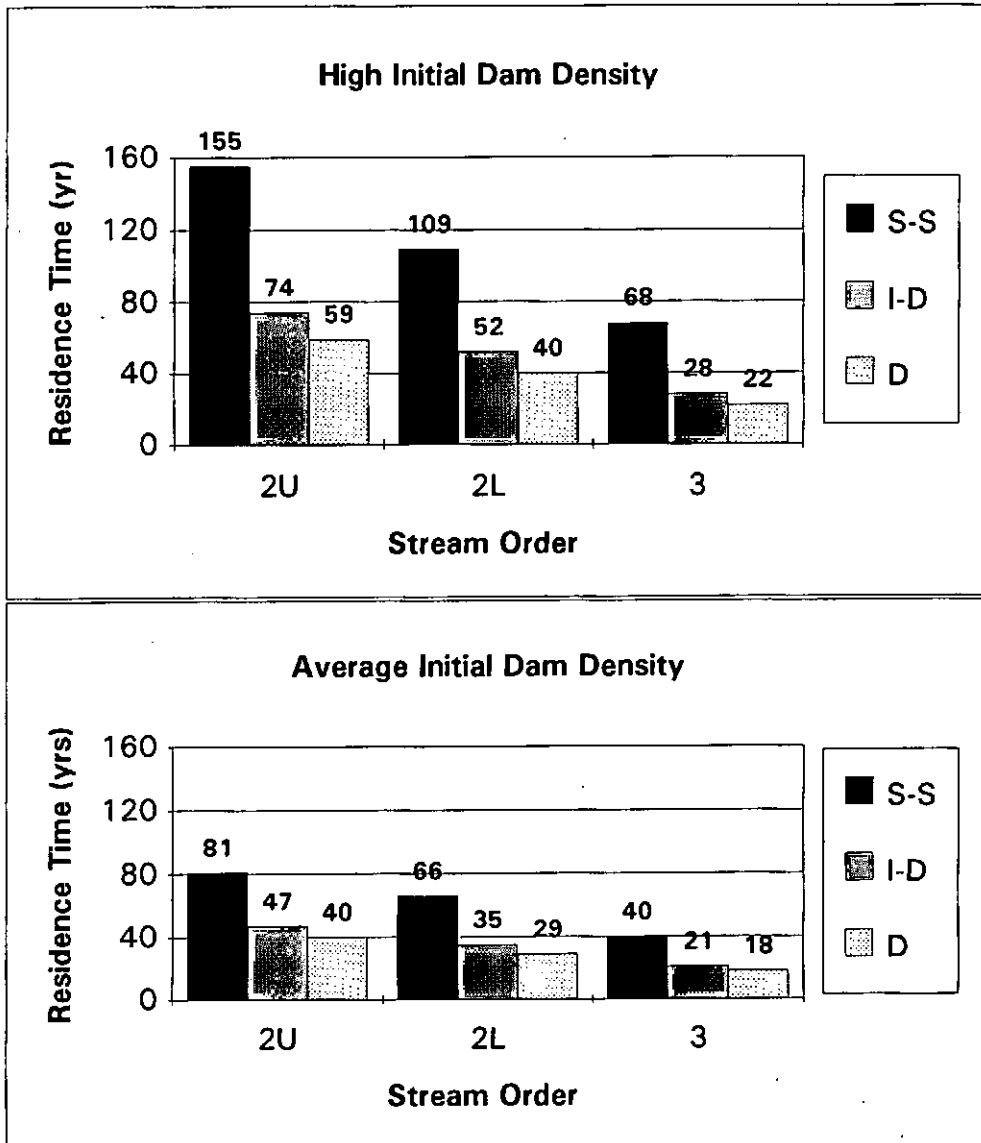


Figure 22: Average ~~Residence~~ Bedload Residence Time

order channel the range was 18 to 68 years. The behavior of residence time under different scenarios mirrored bedload yields shown in Figure 17 because residence time is inversely-proportional to bedload yield.

Using the steady-state case as a baseline for comparison, median residence time for bedload in the third-order channels declined as much as 55 percent under the scenario for average initial density of LOD dams. Under the scenario for high initial density of LOD dams, residence time declines as much as 68 percent. Decreases in the residence time in the lower second-order channels were similar to those in the third-order channels, ranging from 56 to 63 percent. Decreases in residence time in the upper second order channel tended to be greater, ranging from 62 to 103 percent.

Residence times for bedload were typically on the order of decades. In most scenarios, the residence time was less than or equal to the 60-year cycle of model runs. Residence time for bedload was never more than 2.5 times greater than the 60-year cycle.

Suspended Sediment Yield. Suspended load in our model was immediately routed downstream and was equal to the input of sediment finer than 1 mm by creep processes, plus seven percent of the bedload material (coarser than 1 mm) input by creep processes, which represents bedload attrition. Because our model did not store suspended sediment in the channel, there were no differences in sediment output among the different scenarios. Mean annual suspended sediment yield was equal to 2.6 t/yr. This rate was based on creep inputs to 1 km of channel in a 1.1 km<sup>2</sup> watershed.

## DISCUSSION

In order to establish confidence in our model, we compared the magnitude of bedload transport calculated in our model to observed values elsewhere. Bedload transport data for small streams are scarce, so only a few such comparisons were possible.

One exceptional data set for sediment transport from three small (0.60 to 1.01 km<sup>2</sup>) forested watersheds in the H.J. Andrews Experimental Forest in the western Cascade Mountains of Oregon spans a 30-year period (Grant and Wolff 1991). The channels in these streams have gradients of 27 to 36 percent, roughly twice those in the streams monitored for this study.

Two of the three Oregon watersheds had substantial periods of record under unmanaged conditions (no timber harvest or road construction). Watershed 1 (0.96 km<sup>2</sup>) had nine years of pre-treatment monitoring and Watershed 2 (0.60 km<sup>2</sup>) had a 30-year record for undisturbed conditions. Mean annual bedload yield for these watersheds were 3 and 9 t/km<sup>2</sup>, respectively.

In our model channel network, the drainage area of the third-order channel was about 1.1 km<sup>2</sup>. The median value of the distribution of mean annual bedload (Figures 19 a & b) for the third-order channel in the steady-state scenario was 7.8 t/km<sup>2</sup> under the scenario for average initial density of dams and 9.1 t/km<sup>2</sup> under the scenario for high initial density of dams. These results are in reasonable agreement with the data from the watersheds in the H.J. Andrews Experimental Forest.

The data for bedload reported by Grant and Wolff (1991) may tend to overestimate actual yield of bedload. Bedload was determined by measuring the volume of material accumulated in sedimentation basins. It is likely that some of the accumulated material was suspended load sediment that was deposited in the low-velocity water column of the sedimentation basin.

Bedload transport was monitored in the central Oregon Coast Range at Flynn Creek, a 2.2 km<sup>2</sup> watershed with a stream gradient

of 2.5 percent (Beschta et al. 1981). Although this channel drains a larger watershed and has a significantly lower gradient than the streams monitored in this study, it is among the few reasonably comparable systems for which data are available. The channels one stream order upstream from the monitored channel are similar to the channels monitored in our study.

A bedload flow-duration curve was constructed for Flynn Creek from the bedload rating curves developed over 5 years and extended using 15 years of streamflow records (Beschta et al. 1981). The 99th percentile of streamflow, which occurs approximately 3.5 days per year, corresponds to a bedload transport rate of 100 kg/hr. The transport rate corresponding to the 96th percentile of streamflow was 10 kg/hr and occurred 14 days per year. Extrapolating these durations and rates yields an estimate for annual bedload yield of about 7 t/km<sup>2</sup>. Smaller streamflow magnitudes were not considered for the purpose of estimating annual bedload transport. This crude estimate of annual bedload, made for a system only roughly comparable to the monitoring sites in this study, is in reasonable agreement with the median values of routing model predictions for annual bedload yield.

A third data set for bedload transport from southwestern Oregon (Coyote Creek) was summarized by Reid (1981). Annual bedload transport in four experimental watersheds with drainage areas of 0.49 to 0.70 km<sup>2</sup> ranged from 0.2 to 13.6 t/km<sup>2</sup>. The mean annual bedload, weighted by the number of annual observations, was 7.5 t/km<sup>2</sup>. In the only watershed where more than one year of data was collected, mean annual bedload was 13.6 t/km<sup>2</sup> over a 10-year monitoring period. These data were based on measurements of accumulated sediment in settling basins and may therefore overestimate bedload. The Coyote Creek data are in reasonable agreement with the routing model.

Suspended Sediment. The routing model estimate for suspended sediment was 2.6 t/km<sup>2</sup>. This estimate represents creep inputs from only one kilometer of channel. Drainage density in the study area was estimated to be about 7 km/km<sup>2</sup>. Assuming that the processes governing suspended sediment transport are the same in the tributaries of our model channel network, suspended sediment yield for the entire 1.1 km<sup>2</sup> model drainage can be estimated as the product of drainage density and the model suspended load yield of 2.6 t/km of stream channel. This calculation produces a mean annual suspended sediment yield of 18 t/km<sup>2</sup>.

Watersheds 1 and 2 in the H.J. Andrews Experimental Forest had mean annual suspended sediment yields under undisturbed conditions of 14 and 16 t/km<sup>2</sup>. The close agreement of our crude estimate and the measured suspended sediment yield suggests that our model produced and routed suspended load in a reasonable fashion.

The average annual suspended load yield under undisturbed conditions in Flynn Creek was 98 t/km<sup>2</sup> over a 15-year monitoring period (Reneau and Dietrich 1991). A tributary to Flynn Creek, Needle Branch (0.7 km<sup>2</sup>), had average annual suspended load of 53 t/km<sup>2</sup> under undisturbed conditions over an 8-year monitoring period. These suspended load data are substantially greater than suspended load estimated by the routing model (18 t/km<sup>2</sup>); however, they are of the same order of magnitude.

The average annual suspended load in Coyote Creek as reported by Reid (1981), weighted by the number of annual observations, was 37.3 t/km<sup>2</sup>. This is about two times greater than the estimate made from the routing model results.

Reid (1981) also reported annual suspended load data from one year of monitoring in two small watersheds (about 2.5 km<sup>2</sup>) on the western Olympic Peninsula having geology and climate similar to the three monitoring sites in this study. The mean for these

two watersheds was 21.4 t/km<sup>2</sup>/yr. This is in good agreement with the routing model estimate of 18 t/km<sup>2</sup>.

Ratio of Bedload to Total Sediment Load. At the two watersheds in the H.J. Andrews Forest, bedload was 17 and 36 percent of the total sediment yield (Grant and Wolff 1991). The average for these two watersheds was 27 percent. For Flynn Creek, using the annual bedload estimated from the flow-duration curve and suspended yield as reported by Reneau and Dietrich (1991), bedload was 7 percent of the total load. Benda (1994) reported that bedload was 3 percent of the total load for Flynn Creek. In Coyote Creek, as reported by Reid (1981), bedload averaged 20 percent of the total load.

Using the median average annual bedload yield predicted by our model (about 8 t/km<sup>2</sup>) and the estimate of mean annual suspended load (18 t/km<sup>2</sup>), our model predicted bedload yield to be 31 percent of total sediment yield. This is in reasonable agreement with most of the available data. Data from Flynn Creek indicate a substantially lower proportion of bedload in the total sediment load.

One tentative conclusion that may be drawn from comparison of bedload to total load is that bedload is a larger portion of the sediment load in small, steep streams than in larger, low-gradient streams. In low-gradient rivers in western Washington where both bedload and suspended load have been monitored, suspended load was about 20 to 25 times greater than bedload (Nelson 1984). In this simulation and in other monitoring studies, suspended load was roughly three to five times greater than bedload. Headwater streams appear to have a greater capacity to transport the bedload material supplied to them compared to large, low gradient streams. In either type of stream, however, the caliber and hardness of bedload material entering the channels will have a strong influence on the ratio of bedload to total load. This ratio may, therefore, be expected

to vary locally or regionally in relation to bedrock geology and geomorphic history.

Sediment-Supply Limitations on Yield of Bedload. Previous monitoring studies have focused on sediment yield with little or no attention paid to in-channel sediment storage. Consequently, it has not been possible to conclude whether sediment yields from small, steep streams are limited by sediment supply or transport capacity. Preliminary model runs with initial sediment storage defined by the geometry of Figure 11 produced insights regarding this issue.

In the modelled channels, the supply of sediment in the detention reservoir was reduced nearly to zero in all model runs. In the upper second-order channels, however, sediment storage in the detention reservoir tended to be somewhat greater than in the larger channels. By definition, the detention reservoirs contained bedload that was available for transport when sufficient transport capacity existed. The depletion of sediment in the detention reservoirs suggested that the bedload transport capacity in these channels routinely exceeded the supply of sediment entering the channels as the result of creep processes.

The routing model predicted bedload transport capacity substantially in excess of the yield of bedload when summed over the 60-year duration of the simulation model (Table 12). In the second-order channel segments, bedload transport capacity was about three to nine times greater than bedload yield. In the third-order channel segments, transport capacity was 20 to 50 times greater than bedload yield. The comparison between bedload yield and transport capacity under the scenario for high initial density of dams and steady-state dynamics of dams is shown graphically in Figure 23. Excess bedload transport capacity predicted by the routing model suggests that additional bedload sediment entering the channels would be routed downstream.

**Table 12: Ratio of Bedload Transport Capacity to Bedload Yield**

<u>SCENARIO</u>	<u>Upper Second-Order</u>	<u>Lower Second-Order</u>	<u>Third-Order</u>
<b>High Initial Density of LOD Dams</b>			
Steady-State	5.3	7.7	46
Increasing-Decreasing	3.7	4.8	20
Decreasing	3.3	4.1	21
<b>Average Initial Density of LOD Dams</b>			
Steady-State	6.3	9.0	50
Increasing-Decreasing	4.7	6.2	34
Decreasing	4.5	5.7	31

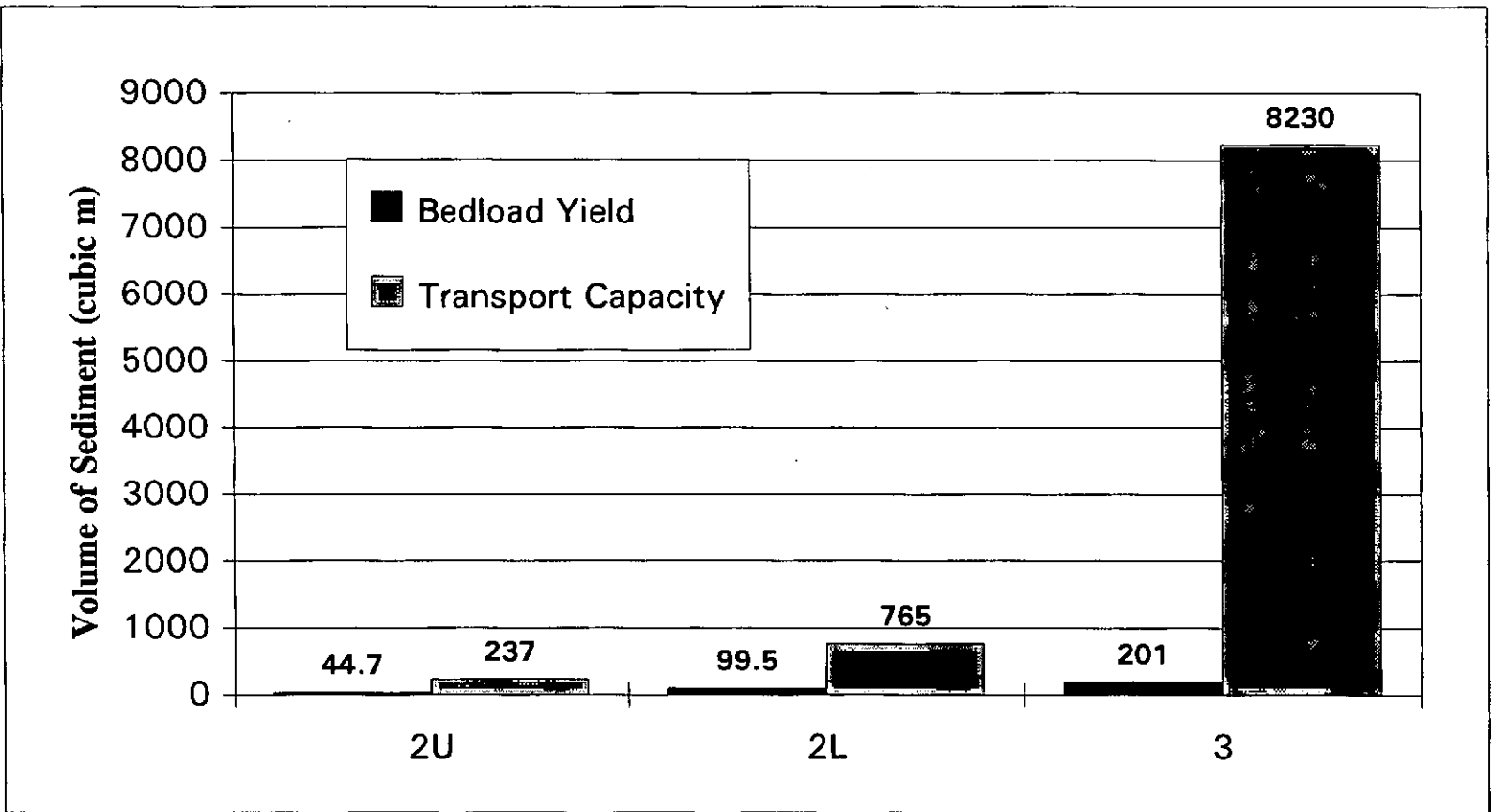


Figure 23: Average bedload yield and transport capacity for a 60-year model cycle, high initial density of LOD dams, steady-state scenario.

Potential Transport of Bedload in First-Order Channels. The quantity of excess bedload transport capacity, at least three times bedload yield in the upper second-order channels, suggests that first-order channels may also be supply-limited. If first-order channels were also supply-limited, they would be expected to transport quantities of bedload that are significant in the context of the routing model. The routing model implicitly assumes that bedload transport in first-order channels is negligible. No field data for bedload transport were collected in first-order channels. Further examination of two aspects of the bedload monitoring data suggests the potential magnitude of bedload transport in first-order channels.

First, plots of mean tracer travel distance (Figure 15) show that data points for each of the three streams are clustered together. Data from Eight-ten Creek, the upper second-order channel, are grouped at the lower end of the range of mean tracer travel distance. Data from Sister Creek, the lower second-order channel, fall in the middle of the range, and data from Ramp Creek, the third-order channel, are placed in the upper portion of the range. The clustering of these data by stream order (or drainage area) suggests that mean tracer travel distance in first-order streams would not be greater than a few meters. This interpretation does not suggest that bedload velocity in first-order channels is zero; rather, it merely suggests that bedload velocity would be substantially smaller than that observed in the upper second-order channel. Bedload velocity is a multiplicative factor in the equation for estimated bedload transport rate, therefore a low bedload velocity would result in a low transport rate.

Second, an estimate of bedload transport rates in first-order channels can be made from the empirical relationship between modelled bedload yield and transport capacity as a function of drainage area (Figure 24). Assuming that there are

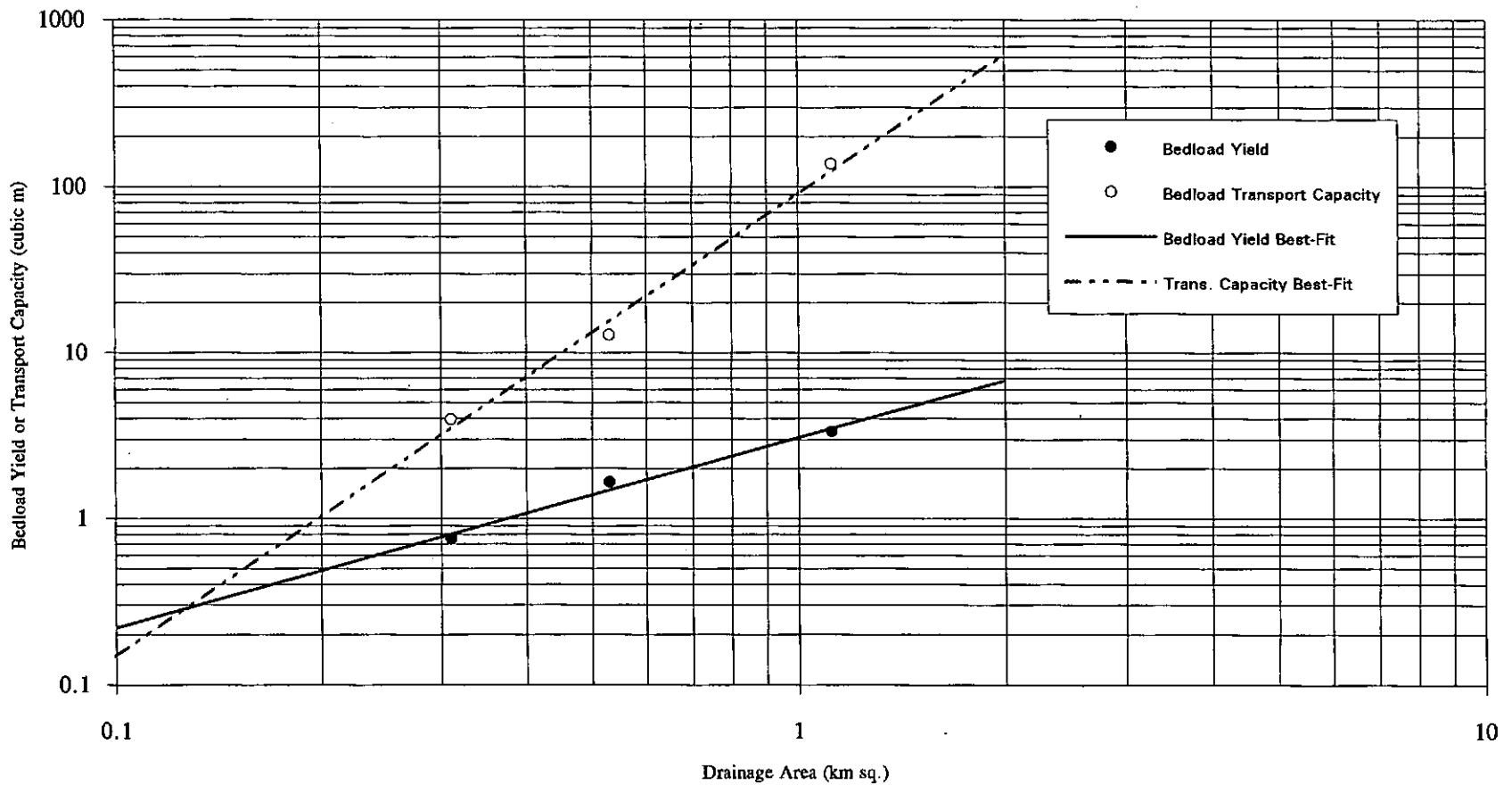


Figure 24: Bedload Transport Capacity and Bedload Yield as a Function of Drainage Area

three first-order channels linked to the upper second-order channel with a drainage area of  $0.3 \text{ km}^2$ , and assuming that the drainage area for each channel is evenly divided among three channels, the drainage area for a first-order channel would be  $0.1 \text{ km}^2$ . Least-squares fits to the mean annual bedload yield and mean annual bedload transport capacity as a function of drainage area are plotted (Figure 24) and extrapolated to a drainage area of  $0.1 \text{ km}^2$ .

Figure 24 indicates that in a first-order channel, bedload yield and bedload transport capacity are approximately equal. This suggests that first-order channels may be transport-limited. If first-order channels are in fact transport-limited, then they would tend to be accumulating sediment. The magnitude of sediment yields from an aggrading system would be expected to be substantially less than that from a degrading (supply-limited) channel.

Mean annual bedload yield from first-order channels, whether supply-limited or transport-limited, would be about one-quarter of that routed through second-order channels. Figure 24 also suggests that mean annual bedload yield from first-order channels would be about  $0.2 \text{ m}^3$ . Assuming that there are eight first-order links in the model channel network, then a total of  $1.6 \text{ m}^3$  of bedload would be routed from first-order channels. This bedload would presumably be routed through the (supply-limited) second- and third-order channels, and represents about 20 to 50 percent of the total bedload yield from the third-order channels. Thus, even if bedload transport rates in first-order channels are small, their greater total length in the channel network could make their overall contribution of bedload relatively large.

Sediment Routing by Debris Flow. Benda's (1990) suggestion that low-order channels are transport-limited with respect to transport of sediment by fluvial processes is contradicted in some respects by the bedload routing model. The routing model

predicts that bedload sediment entering second- and third-order channels via creep processes is routed downstream, provided that sediment storage reservoirs associated with LOD dams are filled. The model predicts that these reservoirs are, on average, filled to capacity when the density of LOD dams is in a steady-state condition. In this scenario there is little change in sediment storage. Consequently, sediment inputs to the channel are roughly equal to sediment outputs from the channel in the steady-state scenario.

The routing model does not evaluate a scenario for increasing density of LOD dams. Such a scenario could simulate the accumulation of LOD dams and sediment in a channel that had been scoured by a debris flow. Data on the rate of formation of LOD dams in scoured channels would be required to develop a simulation of dynamics of LOD dams under this scenario.

Perspective on the potential effect of LOD dams on bedload routing in scoured channels can be gained by comparing mean creep rates to the potential volume of sediment storage associated with LOD dams. The mean creep rate for bedload material, adjusted for density and attrition, is about  $2.3 \text{ m}^3/\text{channel-km/yr}$ . In a 3 m-wide channel, a 0.7 m-high LOD dam could store about  $4 \text{ m}^3$  of bedload sediment.

In the modelled channel network, which contained one kilometer of channel, the formation of one LOD dam every two years would be sufficient to store the quantity of bedload entering the channel via creep processes. Given this crude quantitative assessment, it is not difficult to imagine that the quantity of bedload routed through scoured channels could be quite small. This interpretation is dependent on the rate of formation of LOD dams. In the context of a sediment routing model based on transport by debris flow such as Benda's (1990, 1994), the long-term rate of accumulation of LOD dams and changes in the rate of accumulation would determine the proportion of

bedload stored in LOD dams and the proportion of bedload routed downstream.

It is likely that formation of LOD dams occurs at a faster rate in channels bordered by mature forest than in channels flowing through clearcuts. This implies that post-debris flow bedload delivery would be higher in logged watersheds than in watersheds with mature forests in riparian zones.

The fluvial bedload routing model suggests that a greater proportion of sediment inputs to channels may be routed downstream than was assumed in Benda's (1990, 1994) models of sediment routing by debris flow. Substantial quantities of sediment that would have accumulated in channels and ultimately transported downstream by debris flow may instead be transported downstream by fluvial processes. This implies that the magnitude of sediment routing by debris flow could be overestimated.

The sediment routing model for fluvial processes explicitly excluded debris flow processes. Implications that the fluvial model may have regarding long-term sediment routing, which includes debris flow, should be tempered by the fact that the model's primary purpose was to assess the potential significance of LOD dams in fluvial sediment routing. The fact that the fluvial routing model predicted excess transport capacity in the channels in our model network suggests that sediment deposited in these channels by debris flow may be routed downstream relatively quickly.

Table 9 lists the predicted bedload transport capacities for the modelled channels. Benda (1994) predicted debris flow deposits on the order of 1000 m<sup>3</sup> in low-order channels. In a lower second-order channel, bedload transport capacity at the 100-year recurrence interval is 220 m<sup>3</sup>. In a third-order channel, 625 m<sup>3</sup> of transport capacity exists at the 20-year recurrence interval. This suggests that fluvial transport of debris flow deposits are significant, particularly in the modelled

third-order channel.

The fluvial routing model could be modified to simulate the erosion of debris flow deposits. This would require a function simulating the armoring process by which the concentration of erosion-resistant grains on the bed surface increases, thereby limiting subsequent erosion of debris-flow deposits. The fluvial routing model might also require a component simulating lateral channel migration, which is likely to be important in modeling fluvial erosion of debris flow deposits. Neither the armoring process nor the channel migration process are simulated in the fluvial routing model.

Influence of Timber Harvest on Creep Rates. In the modelled channel network, transport of sediment by fluvial processes is likely to be at least as great as the long-term creep rate of sediment into channels, LOD dams notwithstanding. It is likely that timber harvest operations near stream channels would cause increased creep rates, primarily in the form of bank erosion and small-scale streamside landslides. The routing model assesses only the influence of decreased sediment storage in the channels. Sediment inputs were not adjusted to reflect potential increases in sediment delivery to channels. The supply-limited character of bedload transport suggests that any additional inputs of bedload sediment caused by timber harvest would be routed downstream.

In addition, the channels in the model had bedrock bottoms with overlying sediment no deeper than 0.7 m. This constraint does not allow for the possibility of valleys with thicker sediment deposits that could be eroded by an incising channel. In such a setting, declining density of LOD dams might allow channel incision to occur. The definition of the detention reservoir in the model would have to be modified to provide for this scenario.

Residence Time. Dietrich and Dunne (1978) estimated residence time of sediment within the channel deposits of similar drainage networks in coastal Oregon. In their study, bedload discharge was estimated as a function of drainage area and was based on the difference between textures of hillslope sediment and fluvial sediment. They calculated residence times of 19, 114 and 231 years in the first, second and third order channels, respectively. The fluvial routing model in this study predicted residence times of the same order of magnitude, however, residence time decreased with increasing stream order, just opposite to the pattern predicted by Dietrich and Dunne (1978).

The discrepancy in the pattern of residence time as a function of stream order can be explained. In Dietrich and Dunne's study, the sediment reservoirs comprised of all sediment stored in the valleys, not just that sediment in channels. In their model, the quantity of sediment in storage increases more rapidly in the downstream direction than does sediment transport. Consequently, residence time increases downstream. In the fluvial routing model presented in this study, sediment transport increases more rapidly than sediment storage in the downstream direction.

Dietrich and Dunne's (1978) model of sediment reservoirs assumes extensive interaction between active channel sediment and other floodplain or terrace deposits. The fluvial routing model in this study implicitly assumed that there was no interaction between terrace/floodplain sediment reservoirs, aside from sediment inputs to the channels from bank erosion. Dietrich and Dunne's model pertained to a long-term sediment budget whereas this study focused on a shorter time interval in the context of forest management issues.

The residence time of sediment in a channel indicates the approximate average time required to route sediment through a channel, beginning with the incorporation of sediment in the

sediment storage reservoirs of the channel. The residence time also suggests the time scale over which changes in sediment inputs could be expected to affect downstream systems.

Management Implications. Analysis of residence time could help managers of forest and aquatic ecosystem managers to assess the effects of alternate land management plans on sediment delivery to stream channels of interest, such as those containing spawning and rearing habitat for sensitive fish species. For instance, if managers were evaluating alternative timber harvest plans, and the relationship between harvest technique and sediment routing were known, the temporal and spatial sequence of harvesting that had the most advantageous consequences for sediment delivery to the channel reach of interest could be chosen.

With respect to the negative impacts of sediment on fish habitat, the predictions made by our model frame the following question: Are increases of 40 to 130 percent in fluvial transport of bedload from third-order channel networks over a 60 year period significant? Considering that the magnitude of change appears to be of the same order as the "background" (that is, steady-state) bedload yield, a strong argument can be made that the potential change is significant. This implies that management practices should avoid this outcome.

There are, however, many perspectives that may be worth considering, and not all perspectives necessarily suggest the same management response. For instance, in a stream system that has already been severely impacted by debris flow sedimentation, are changes in delivery rates from headwaters of 40 to 130 percent of any consequence? This would depend on the extent of sedimentation and the sediment transport capacity of the larger streams in the basin, and the desired conditions in the larger streams. If the larger system already contains far greater sediment than its transport capacity, then "recovery" of the

larger system may already be a remote prospect and the increment of inputs from the headwaters may be deemed insignificant. On the other hand, if the larger stream system is near recovery from previous sedimentation or is thought to be delicately balanced, then the additional increment of sediment from regions upstream may be considered threatening.

In the absence of specific known circumstances, and given that the present understanding of the effects of sediment routing on fish habitats, it could be argued that maintaining the function of a stream system at levels found in pristine systems is the most reasonable goal. Specifically, based on the results of the routing model, this approach suggests that in stream channels draining watersheds of 0.3 km<sup>2</sup> or smaller (for example, Type 4 streams in Washington), inputs of LOD should be maintained at levels equivalent to those found in unlogged forests. The primary function of this LOD is creation of quasi-stable reservoirs for sediment storage. Failure to maintain a steady, long-term supply of LOD to such channels would allow the quantity of stable storage reservoirs to diminish. Failed LOD dams would release sediment from storage; new storage reservoirs would not be numerous enough to replace the lost storage, resulting in a net loss of storage and an increase in sediment export. In supply-limited stream systems, the sediment released from storage is likely to be routed downstream over a period ranging from a few to several years.

The geographic area over which this management response is appropriate is difficult to determine with certainty. It probably includes steep, dissected headwater drainages in Washington in and west of the Cascades, where soils are shallow and debris flow is the dominant mass-wasting process. Average hydrologic and creep processes in these types of stream systems probably do not vary a great deal. In terrain that is less dissected and is mantled by deeper soils, such as the Sister

Creek watershed among our monitoring sites, it was apparent that runoff processes may be significantly different. (This difference necessitated the synthesis of a rainfall-runoff relationship for Sister Creek for application to the routing model.) In locales with such hydrologic characteristics, this management strategy may not be appropriate. In any case, the model suggests that LOD dams are an important control on sediment routing.

Regardless of geographic area, the model implies that sediment storage by LOD dams becomes less important as bedload transport capacity diminishes. In other words, in streams where sediment yield is limited by transport capacity, LOD dams would be expected to be less significant. In supply-limited streams, the presence of LOD dams is highly influential because sediment stored by these features would otherwise be transported downstream.

In a stream system where LOD dams persist in a relative steady-state, sediment storage reservoirs would typically be filled to capacity most of the time, so sediment outputs would tend to be very nearly equal to sediment inputs. In systems where LOD dams are persistent and in which LOD dams may become superimposed, effectively causing the stream valley to aggrade, relatively little bedload would be expected to be transported downstream. Disruption of LOD in these systems would obviously have a dramatic effect on bedload yield. The chief concerns regarding LOD in Type 4 streams are the potential loss of LOD dams, the consequent release of stored sediment and the diminished opportunities to retain in storage sediment that enters the channel.

Owing to the fact that LOD enters headwater streams gradually over time from the stream banks, the most effective means to preserve LOD function for sediment storage is to maintain a riparian forest stand sufficient to provide a steady supply of LOD to the channel. If the processes by which LOD

enters stream channels and functions can be quantified, then more specific goals and more flexible riparian forest management alternatives might be possible.

The simulation model was not used to predict sediment yield or the density of LOD dams in streams during the period beyond 60 years following initial timber harvest. Provided that there is no timber harvest in the second-growth forest adjacent to channels after 60 years, it is likely that recruitment of coniferous LOD to streams channels would begin to increase. Assuming that LOD dams are formed in proportion to total LOD load in stream channels, the density of LOD dams per unit stream length would also begin to increase. Consequently, the sediment storage capacity per unit stream length would increase, causing a decrease in bedload yield.

Had the simulation model been extended beyond 60 years, it is conceivable that bedload yield could have decreased to near zero when the rate of increase of sediment storage exceeded the rate of sediment delivery to the channels. Assuming that the rate of creation of sediment-storage capacity does not increase indefinitely (i.e. that there is an upper limit to the number of LOD dams formed per unit channel length), there would be a point in time when sediment storage associated with LOD dams reaches a steady-state condition. At that time, sediment reservoirs would be effectively full, and an approximate balance between sediment entering the channels and sediment exiting the channels would again be achieved.

If forests are harvested in a manner that prevents recruitment of LOD to these streams, and the channels do in fact lose most of the sediment storage capacity associated with LOD, then a significant change in channel morphology and bedload routing could be expected. These channels would be expected to be dominated by bedrock and cobble-boulder beds. Local channel slopes would tend to be nearly equal to the average valley slope.

Storage of bedload would be limited to areas of low slope induced by geologic and geomorphic factors and to pockets between and in the lee of cobble and boulder clasts. Bedload residence times would be short, and sediment eroded from hillslopes, whether induced by management or not, would quickly be routed to low-gradient, fish-bearing channels immediately downstream.

In areas where low-order channels flow over unconsolidated materials such as glacial deposits, it is possible that the loss of LOD could lead to channel incision. Lateral migration of channels might also occur, creating the potential for erosion of terraces and other deposits in narrow valley bottoms.

Either of these scenarios could have severe consequences. Channel incision would greatly increase sediment yield, and could propagate into hillslopes, generating even larger quantities of sediment. The potential for incision is most likely determined by the proportion of cobbles and boulders in the unconsolidated material. When the concentration of relatively-immobile cobbles and boulders on the channel bed and banks reaches an as-yet unidentified threshold, incision and/or lateral migration will cease.

Another likely, but unproven, consequence of logging old growth forests adjacent to low-order channels is that the average diameter of LOD recruited to channels in the future would decrease. Assuming that dam height is correlated with diameter of LOD in the stream, streams draining watersheds with second-growth stands would have dam heights substantially less than that in streams draining unlogged areas. This would have a significant effect on potential sediment storage because the volume of the retention reservoirs are proportional to the square of dam height. For example, if dam height is reduced from 1.0 m to 0.7 m, the sediment storage capacity of the retention reservoir is reduced by about half.

In summary, the foregoing analysis suggests that fluvial sediment transport processes in steep, low-order channels are significant. Bedload transport occurs with magnitudes and frequencies great enough to make the bedload storage function of LOD a significant control on bedload yield from low-order drainages. This suggests that efforts should be made to maintain the sediment storage function of LOD in these streams. The risk of losing the sediment-storage function of LOD in steep, low-order streams is inducing long-term change in the delivery of fluvial sediment to streams containing spawning and rearing habitat of several salmonids species. Some of these fish species are presently being considered for designation as threatened or endangered under provisions of Federal law.

## REFERENCES

- Andrus, C.W., Long, B.A., and Froehlich, H.A. (1988) Woody debris and its contribution to pool formation in a coastal stream 50 years after logging. *Canadian Journal of Fisheries and Aquatic Sciences*, Vol. 45, No. 12, pp. 2080-2086.
- Benda, L. (1990) The influence of debris flow on channels and valley floors of the Oregon Coast Range, U.S.A. *Earth Surface Processes and Landforms*, Vol. 15, pp. 457-466.
- Benda, L. (1994). Stochastic geomorphology in a humid mountain landscape. Unpublished Ph.D. Thesis, University of Washington, Seattle, Washington. 356 p.
- Beschta, R.L., O'Leary, S.J., Edwards, R.E., and Knoop, K.D. (1981) Sediment and organic matter transport in Oregon Coast Range streams. Water Resources Research Institute, Oregon State University, Corvallis, Oregon. WRRRI-70, 67 p.
- Bilby, R.E. (1981) Role of organic debris dams in regulating the export of dissolved and particulate matter from a forested watershed. *Ecology*, Vol. 62, No. 5, pp. 1234-1243.
- Bryant, M.D. (1980) Evolution of large organic debris after timber harvest: Maybeso Creek, 1949 to 1978. U.S.D.A. Forest Service, Pacific Northwest Forest and Range Experiment Station, Portland, Oregon. General Technical Report PNW-101, 30 p.
- Collins, B.D. and Dunne, T. (1989) Gravel transport, gravel harvesting and channel-bed degradation in rivers draining the southern Olympic Mountains, Washington, U.S.A. *Environ. Geol. Water Sci.*, Vol. 13, No. 3, pp. 213-224.
- Dietrich, W.E. and Dunne, T. (1987) Sediment budget for a small catchment in mountainous terrain. *Zeitschrift fur Geomorphologie, Suppl. Bd.*, Vol. 29, pp. 191-206.
- Froehlich, H.A. (1973) Natural and man-caused slash in headwater streams. IN Proc. Pacific Logging Congress, Vancouver, British Columbia, Loggers Handbook Vol. 33.
- Grant and Wolfe (1991) Long-term patterns of sediment transport after timber harvest, western Cascade Mountains, Oregon, USA. IN Sediment and Stream Water Quality in a Changing Environment: Trends and Explanation, Proceedings of the Vienna Symposium, August, 1991. International Association for Hydrological Sciences, Publ. No. 203, pp. 31-40.

Grette, G.B. (1985) The abundance and role of large organic debris in juvenile salmonid habitat in streams in second growth and unlogged forests. Unpublished Masters Thesis, University of Washington, Seattle, Washington, 105 pp.

Hassan and Church (1992) The movement of individual grains on the streambed. IN Billi, P., Hey, R.D., Thorne, C.R., and Tacconi, P. (eds.) Dynamics of Gravel-bed Rivers, John Wiley & Sons Ltd., pp. 159-175.

Hassan, M.A., and Church, M. (1994) Vertical mixing of coarse particles in gravel bed rivers: a kinematic model. Water Resources Research, Vol. 30, No. 4, pp. 1173-1185.

Hassan, M.A., Church, M., and Ashworth, P.J. (1992) Virtual rate and mean distance of travel of individual clasts in gravel-bed channels. Earth Surface Processes and Landforms, Vol. 17, pp. 617-627.

Hedin, L.O., Mayer, M.S., and Likens, G.E. (1988) The effect of deforestation on organic debris dams. Verh. Internat. Verein. Limnol. Vol 23, pp. 1135-1141.

Lienkaemper, G.W. and Swanson, F.J. (1987). Dynamics of large woody debris in streams in old-growth Douglas-fir forests. Canadian Journal of Forest Resources, Vol. 17, pp. 150-156.

MacDonald, A. and Ritland, K.W. (1989) Sediment dynamics in Type 4 and 5 waters. Draft final report for SHAMW Steering Committee and Washington Dept. of Natural Resources, Olympia, Washington. 87 pp.

Mosely, M.P. (1981) The influence of organic debris on channel morphology and bedload transport in a New Zealand forest stream. Earth Surface Processes and Landforms, Vol. 6, pp. 571-579.

Nelson, L.M. (1982) Streamflow and sediment transport in the Quillayute River basin, Washington. U.S. Geological Survey, Open File Report 82-627, 29 pp.

O'Connor, M.D. (1986) Effects of logging on organic debris dams in first order streams in northern California. Unpublished Masters Thesis, University of California, Berkeley. 90 p.

O'Connor, M.D. (1993) Bedload transport processes in steep tributary streams, Olympic Peninsula, Washington, U.S.A. IN Wang, S.Y. (ed.) Advances in Hydro-science and Engineering, The Mississippi State University, Oxford, Mississippi. Vol. 1, pp. 243-251

O'Connor, M.D. and Harr, R.D. (1991) Sediment transport processes in steep mountain streams in forested watersheds on the Olympic Peninsula, Washington: Interim Final Report. Unpublished report to Timber/Fish/Wildlife and State of Washington Department of Natural Resources, 50 p.

Perkins, S.J. (1988) Interactions of landslide-supplied sediment with channel morphology in forested watersheds. Unpublished Masters Thesis, University of Washington, Seattle. 100 pp.

Reid, L.E. (1981) Sediment production from gravel-surfaced forest roads, Clearwater Basin, Washington. Unpublished Masters Thesis, University of Washington, Seattle, Washington, 350 p.

Reneau, S.L. and Dietrich, W.E. (1991) Erosion rates in the southern Oregon Coast Range: evidence for an equilibrium between hillslope erosion and sediment yield. *Earth Surface Processes and Landforms*, Vol. 16, pp. 307-322.

Sidle, R.C. (1988) Bed load transport regime of a small forest stream. *Water Resources Research*, Vol. 24, No. 2, pp. 207-218.

Swanson, F.J., Bryant, M.D., Lienkaemper, G.W., and Sedell, J.R. (1984) Organic debris in small streams, Prince of Wales Island, southeast Alaska. U.S.D.A. Forest Service, Pacific Northwest Forest and Range Experiment Station, Portland, Oregon. General Technical Report PNW-166, 12 p.

Tally, T. (1980) The effects of geology and large organic debris on stream channel morphology and process for streams flowing through old growth redwood forest in northern California. Unpublished Ph.D. Thesis, University of California, Santa Barbara, 273 p.

Toews, D.A. and Moore, M.K. (1982) The effects of three streamside logging treatments on organic debris and channel morphology of Carnation Creek. IN Hartman, G. (ed.) Proc. of the Carnation Creek Workshop: A 10-Year Review. February 24-26, 1982, Nanaimo, British Columbia, pp. 129-153.

U.S.D.A. Soil Conservation Service (1987) Soil survey of Clallam County area, Washington.